DEUTSCHES ELEKTRONEN-SYNCHROTRON DESY

DESY 84-108
November 1984

EXPERIMENTAL TESTS OF GAUGE THEORIES

by

D. Haidt

Deutsches Elektronen-Synchrotron DESY, Hamburg

ISSN 0418-9833

NOTKESTRASSE 85 · 2 HAMBURG 52

To be sure that your preprints are promptly included in the
HIGH ENERGY PHYSICS INDEX ,
send them to the following address (if possible by air mail) :

DESY
Bibliothek
Notkestrasse 85
2 Hamburg 52
Germany

DESY 84-108
November 1984

ISSN 0418-9833

EXPERIMENTAL TESTS OF GAUGE THEORIES

D. Haidt, DESY

Lectures presented at the CERN 1984 Summer School at Lofthus, Norway,
11 - 24 June 1984

Lecture 1: Phenomenology

1. INTRODUCTION

The experimental and theoretical efforts of the last two decades merged into a comprehensive picture of elementary particle physics. A central rôle played the theoretical concept of local gauge theories. The forces acting between the elementary particles are then arising through the exchange of spin 1 gauge bosons. It became gradually clear that the leptons and quarks constitute the elementary building blocks of all matter and that they appear systematically ordered in families. The concepts 'flavor' and 'color' proved particularly useful. The experimental observation of weak neutral currents - just a decade ago - was the discovery giving substance to the idea that weak and electromagnetic phenomena have a common origin. It was one of the driving forces in the research program highlighted by the observation of interference effects between the weak and electromagnetic currents and finally the observation of the weak gauge bosons with the predicted mass. The other main research line centered on the investigation of the strong force. This field progressed considerably since , also a decade ago, the rôle of the exact local color gauge group was recognized.

This series of five lectures is intended to provide the experimental basis to the theoretical courses on gauge symmetries delivered by C. Jarlskog[1] and R. Petronzio[2]. The framework will be the standard model. The experimental material is taken mainly from lepton-hadron and e^+e^--experiments. Results from the CERN $\bar{p}p$-collider are presented in the lectures by J. Dowell[3]. The same subject "Test of Gauge Symmetries" was also treated in previous CERN schools[4] and other schools[5]. There is necessarily substantial overlap. Choosing the Standard Model as framework offers the possibility of a simple and organized presentation of the rich material. But it should not be forgotten that the present picture grew up step by step and remarks here and there shall illustrate this. The other advantage of the present form of the standard model concerns the formulation of the critical questions leading beyond the tested ground, for instance why are weak interactions lefthanded or is the multitude of quarks and leptons hinting at yet another substructure.

2. THE STANDARD MODEL

The standard model is characterized by the

- group structure SU(2) x U(1) x SU(3)
- fermion representations
- spontaneous symmetry breaking and HIGGS representation

a) THE BUILDING BLOCKS

On a distance scale of $10^{-15\pm1}$cm the fundamental building blocks of matter are the spin 1/2 fermions. There are many of them. They can be ordered in a periodic system, as shown in table 1. All known particles are classified vertically in families or generations, of which the first one is explained in more detail

Table 1: Periodic System of the Spin 1/2 Fermions

PARTICLES			FORCES
ν_e	ν_μ	ν_τ	only weak
e	μ	τ	weak and electromagnetic
u	c	(t)	weak, electromagnetic and strong
d	s	b	

in table 3, and horizontally in groups of equal electric charge. Most striking are the symmetry between the leptons and quarks and the regular mass pattern[6]. Neutrinos are the particles of lowest mass in each family, in fact it is still an open question whether they are exactly massless, as will be assumed in these lectures. The properties of the ν_τ are inferred from decays. Sofar no reaction induced by a ν_τ has been observed[7,10].

The first fundamental fermion was the electron discovered at the end of the last century. In order to explain the nuclear β-decay experiments PAULI postulated 1929 the neutrino. It took some time to recognize that nucleons and mesons were in fact composite particles. Only in the 70ies the periodic structure of leptons and quarks became evident. As a consequence of the periodicity a new quark was anticipated at the marked place in the third family with predicted properties - except for its mass. The postulated top-quark was announced to exist[8] just at the beginning of this School. It is amusing to think of the historical parallel, when 1871 an element, called eka-Silicinum, was predicted to occupy a yet empty place in the periodic table of MENDELEYEV and the subsequent discovery 15 years later of this element called then Germanium.

Sofar there are no experimental indications of fermions beyond the ones in the three families. The Standard Model does not tell how many families exist.

b) THE FORCES

As indicated in table 1 three types of forces between the pointlike, spin 1/2 fermions are distinguished according to their strength. Within the Standard Model all three forces are assumed to arise from a local gauge symmetry. The forces are then mediated by vector gauge bosons. The crucial feature is the locality of the gauge symmetry fulfilled by the Lagrangian.

Table 2: The types of forces

Local Gauge Symmetry	Force	Intermediate Vector Boson
SU(2)	weak	W^+ W^- Z^0
U(1)	electro-magnetic	γ
SU(3)	strong	g_1, g_2, ... g_8

Contrary to U(1) the algebrae SU(2) and SU(3) are nonabelian, i.e. not commutative . Therefore, the 3 respectively 8 intermediate spin 1 bosons have the property of coupling to themselves. The electromagnetic force is of inifinite range, because the photon is massless. The weak force, on the other hand, has short range requiring massive mediators and thus a broken symmetry. The situation is again different in the case of the strong force which is assumed to be mediated by massless gluons and nevertheless of finite range (confinement).

c) THE FERMION REPRESENTATION

The three generations are replicas of each other regarding their symmetry properties. It is therefore sufficient to show the multiplet structure of the first generation under the gauge groups SU(2) and SU(3).

Table 3: MULTIPLET STRUCTURE UNDER SU(2) AND SU(3)

$\begin{pmatrix}\nu_e\\ e\end{pmatrix}_L$	$\begin{pmatrix}u\\ d\end{pmatrix}^r_L$ $\begin{pmatrix}u\\ d\end{pmatrix}^w_L$ $\begin{pmatrix}u\\ d\end{pmatrix}^b_L$	SU(2) doublet
e_R	u^r_R u^w_R u^b_R d^r_R d^w_R d^b_R	SU(2) singlet SU(2) singlet
SU(3) singlet	SU(3) triplet	

Left- and righthanded fermions behave differently under SU(2). Each fermion can be decomposed uniquely into a left- and a righthanded spinor:

$$\psi_L \equiv \frac{1}{2}(1 + \gamma_5)\psi \quad \text{and} \quad \psi_R \equiv \frac{1}{2}(1 - \gamma_5)\psi$$

with

$$\psi = \psi_L + \psi_R \quad ; \text{ note: } (1 + \gamma_5)(1 - \gamma_5) = 0$$

Should experiments prove the neutrino to be massive, then there would be also a ν_R.

3. THE ELECTROWEAK LAGRANGIAN

In the Standard Model weak and electromagnetic phenomena are treated on the same footing. Both phenomena exhibit a local gauge structure. However, a new principle had to be introduced: spontaneous symmetry breaking and the HIGGS mechanism. The Lagrangian can be decomposed into a kinetic term, into a term responsible for electromagnetic interactions (γ) and three terms for weak interactions (W^+, W^-, Z), and finally into a term containing the HIGGS sector:

$$L^{GSW} = L_o + L_{em} + L_{CC} + L_{NC} + L_H$$

free γ $W^\pm$ Z HIGGS

with

$$L_{em} = g \sin\theta \; J^{em}_\lambda A^\lambda$$

$$L_{CC} = \frac{g}{2\sqrt{2}} (J^{CC}_\lambda W^\lambda + h.c.)$$

$$L_{NC} = \frac{g}{4\cos\theta} J^{NC}_\lambda Z^\lambda$$

All three interaction Lagrangians have the same structure:

COUPLING CONSTANT x CURRENT x GAUGE BOSON FIELD

One identifies $g\sin\theta$ with the electromagnetic coupling e:

$$e \equiv g\sin\theta$$

This may be called the unification equation. It is evident, that weak and electromagnetic phenomena are not truly unified, since then only a single coupling constant would appear. Nevertheless, it is justified to talk about "electroweak" phenomena, since the three coupling constants can be expressed in terms of two, e.g. the electromagnetic coupling constant e, which is precisely measured, and the weak angle θ, which is not yet pre-

cisely measured.

Two terms of the Lagrangian appearing in the simplest, nontrivial HIGGS sector

$$L_H = (\frac{gv}{2})^2 \; W^+_\lambda \; W^\lambda + \frac{1}{2} (\frac{gv}{2\cos\theta})^2 \; Z_\lambda \; Z^\lambda + \ldots$$

are given explicitely. They show which quantities are to be identified with the masses of the weak gauge bosons:

$$m_W \equiv \frac{gv}{2} \qquad \text{and} \qquad m_Z = \frac{m_W}{\cos\theta}$$

The constant v is the vacuum expectation value of the HIGGS field Φ defined as $v \equiv \frac{1}{\sqrt{2}} (0|\Phi|0)$. All the other terms appearing in L_H describe the HIGGS couplings to itself, to Z, $W^\pm$ and to the fundamental fermions.

4. THE CURRENTS

The explicite structure of the three currents is summarized in the following three equations:

$$J^{em}_\lambda = \sum_f Q_f \, \bar{\psi}_f \, \gamma_\lambda \, \psi_f$$

$$J^{CC}_\lambda = \sum_\ell \bar{\psi}_{\nu_\ell} \, \gamma_\lambda \, (1 + \gamma_5) \, \psi_\ell + \sum_{q,q'} \bar{\psi}_q \, \gamma_\lambda \, (1 + \gamma_5) \, U_{qq'} \, \psi_{q'}$$

$$J^{NC}_\lambda = \sum_f \bar{\psi}_f \, \gamma_\lambda \, (g^f_V + g^f_A \, \gamma_5) \psi_f$$

To the notation:

f is the flavor index, i.e. runs over ν_e, e, ν_μ, μ, ν_τ, τ, u, d, c, s, t, b

$\ell = (e, \mu, \tau)$ $q = (u, c, t)$ $q' = (d, s, b)$

Q_f is the electric charge in units of $e > 0$

U = flavor mixing quark matrix (KOBAYASHI - MASKAWA matrix)
U is unitary, i.e. $UU^+ = 1$

$g^f_{V,A}$ = vector and axialvector coupling constants of fermion f to the neutral weak gauge boson Z, which depends only upon $\sin^2\theta$ (c.f. appendice)

The electromagnetic current is a pure vector current (V), whereas the weak charged current is of pure V - A type (the minus sign is conventional), i.e. only the lefthanded component of ψ_f is active in interactions due to $W^{\pm}$ (c.f. p. 6). The weak neutral current is in general neither pure V nor pure A.

5. THE CURRENT x CURRENT FORM

Low energy weak phenomena are known to be well described by the following effective Lagrangian:

$$L^{eff} = \frac{G}{\sqrt{2}} \left(J_\lambda^{CC} (J_\lambda^{CC})^+ + \frac{\rho}{2} J_\lambda^{NC} J_\lambda^{NC} \right)$$

where G is the FERMI coupling constant and ρ[9] a parameter measuring the overall strength of the weak neutral current with respect to the weak charged current. This effective form can be derived in the Standard Model in the limit $|q^2| << m^2$ (m is the relevant gauge boson mass). Consider the 2nd order process $\nu_\mu e \to \mu \nu_e$:

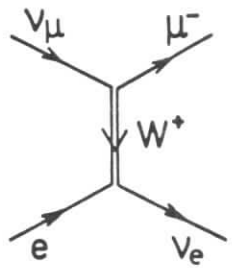

The amplitude of this process contains besides the weak currents the W-propagator:

$$-i \frac{\delta_{\lambda\kappa} + \frac{q_\lambda q_\kappa}{m_W^2}}{q^2 + m_W^2 - i\varepsilon} \xrightarrow{|q^2| << m_W^2} -i \frac{\delta_{\lambda\kappa}}{m_W^2}$$

Thus one obtains:

$$L^{CC} \xrightarrow[|q^2|<<m^2]{} \left(\frac{g}{2\sqrt{2}}\right)^2 \frac{1}{m_W^2} J_\lambda^{CC} (J_\lambda^{CC})^+$$

$$L^{NC} \longrightarrow \left(\frac{g}{4\cos\theta}\right)^2 \frac{1}{m_Z^2} J_\lambda^{NC} J_\lambda^{NC}$$

As a consequence, one reads off

$$\frac{G}{\sqrt{2}} \equiv \frac{g^2}{8m_W^2} \quad \text{and} \quad \frac{\rho}{2} \frac{G}{\sqrt{2}} \equiv \frac{g^2}{16\cos^2\theta\, m_Z^2}$$

thus $\rho \equiv \frac{m_W^2}{m_Z^2 \cos^2\theta}$

This consideration makes clear what the terms "low energy" and "weak" really mean. The masses of the weak gauge bosons set the scale for weak phenomena. So, all previous neutrino experiments are to be considered low energy experiments, since e.g. for a wide band neutrino experiment at the CERN SPS $\langle q^2 \rangle \approx (7\ \text{GeV})^2$ which is small compared to $m_W^2 \approx (80\ \text{GeV})^2$. Furthermore, it becomes clear, that weak interactions get "weak" due to the suppression factor $1/m^2$, which is the remainder of the W or Z propagator. At sufficiently high energies weak and electromagnetic phenomena occur at comparable rate. In the Standard Model the parameter ρ equals 1 in lowest order as a consequence of the simplest choice or the HIGGS representation. This parameter is experimentally accessible.

6. TESTS OF THE ELECTROWEAK STANDARD MODEL

For practical purposes the most important claim is the renormalizability of the theory. In recent years processes have been predicted in next to leading order. The radiative effects turn out to be finite, but for the time being too small to be detected. However, a promising test seems to be possible, provided a precision measurement of $\sin^2\theta$ can be performed. This has been discussed in the context of the SPS Fixed Target Workshop[11]. The test consists in comparing the mass of the weak gauge bosons predicted

in terms of $\sin^2\theta$ (including 1-loop corrections) with the value measured directly in experiments at the CERN $S\bar{p}pS$ collider (see sect. 9 below).

The tests of the Standard Model fall under two heads:

a) the gauge sector
- existence of 4 gauge bosons with masses predicted
- gauge couplings to fermions
- gauge self couplings
- fermion representations, existence of t-quark, ℓ-q symmetry, universality

b) the HIGGS sector
- existence of a neutral spin 0 boson
- ρ-parameter
- H couplings to fermions, W, Z and itself.

All tests described in lectures 2, 3 and 4 are based on "low" energy experiments ("low" in the sense mentioned above). This implies that many aspects listed here remain untested. Nevertheless, precisely the low energy experiments played the crucial rôle in establishing the current form of the standard model. The recent tests performed at the $\bar{p}p$ collider, in particular those related to the discovery of the intermediate vector bosons $W^\pm$, Z, are discussed in J. Dowell's lectures[3].
Before entering into the description of the experimental tests it may be worthwhile to sketch the starting-point of the Standard Model and in particular the discovery of the weak neutral currents in the GARGAMELLE neutrino experiment.

7. THE FIRST TEST

The situation of weak interaction physics in the 1960ies can be summarized as follows:
- sussessful description of low energy ($\sqrt{s} < 4$ GeV) weak phenomena (V-A theory, CABIBBO theory)
- calculations of higher order processes are divergent

Thus, the outstanding theoretical problem was to investigate solutions to such divergences, i.e. to understand the high energy behaviour of weak processes. The first step consisted in postulating - in analogy to the photon in QED - intermediate vector bosons W^+, W^-. They would mediate the weak force as the photon mediates the electromagnetic force. However, the $W^\pm$ should be massive, contrary to the photon, in order to agree with the short range behavour of weak forces. The postulated $W^\pm$, indeed, led to some taming of the divergences. As a further step, other new particles were proposed, which give rise to new phenomena such that their contributions cancel the dangerous infinities, as for instance in $\nu\bar{\nu} \to W^+W^-$. One such proposal was the introduction of weak neutral currents, another one new heavy leptons.
Since these speculations involved genuinely new weak phenomena, available experimental data were scrutinized to get evidence for at least upper limits. Around 1970 upper limits on the existence of weak neutral currents came from two sources:

a) decays: strangeness changing transitions ($\Delta S \neq 0$) and $\Delta Q = 0$ are strongly suppressed, e.g.

$$K^\pm \to \begin{cases} \pi^\pm e^+e^- & < 0.26 \cdot 10^{-6} \\ \pi^\pm \mu^+\mu^- & < 2.4 \cdot 10^{-6} \\ \pi^\pm \nu \bar{\nu} & < 0.6 \cdot 10^{-6} \end{cases}$$

$$K_L^0 \not\to \begin{cases} e^+e^- \\ \mu^+\mu^- & < 1.6 \cdot 10^{-9} \\ e^\pm\mu^\mp \end{cases}$$

$$K_S^0 \to \begin{cases} e^+e^- & < 35 \cdot 10^{-5} \\ \mu^+\mu^- & < 0.3 \cdot 10^{-5} \end{cases}$$

b) neutrino experiments:

$$\left.\begin{array}{ll} \dfrac{\#\ \nu p \to \nu p}{\#\ \nu n \to \mu^- p} & < 0.12 \pm 0.06 \\[2ex] \dfrac{\#\ \nu p \to \nu n \pi^+}{\#\ \nu p \to \mu^- p \pi^+} & < 0.08 \pm 0.04 \end{array}\right\} \text{ from CERN HLBC}[12]$$

$$\frac{\#\nu_\mu e \rightarrow \nu_\mu e}{\#\nu_e e \rightarrow \nu_e e} < 0.4 \qquad \text{from CERN SC}^{13)}$$

The main experimental problem in the neutrino experiments using the CERN heavy liquid bubble chamber was the treatment of the neutron background. Elastic νp and np interactions appear in a bubble chamber as a short track due to the recoil proton and nothing else. Therefore, only upper limits could be quoted (actually in agreement with measurements[14)] performed later).

These upper limits were quite discouraging. One of the highlights at that time was the observation of BJORKEN scaling in ep-experiments at SLAC and, indeed, the investigation of this new phenomenon got highest priority in the first neutrino proposal[15)] for the new heavy liquid bubble chamber GARGAMELLE, whereas the search for neutral currents ranged lowest in priority.

At first sight the observed strong suppression of strangeness changing neutral currents appeared desastrous for models based precisely on weak neutral currents. This shortcoming is related to the particular structure of the hadronic weak charged current as determined from experimental studies of semileptonic weak interactions. In the CABIBBO theory the u-quark couples weakly to d- and s-quarks only in the combination:

$$d_c \equiv d\cos\theta_c + s\sin\theta_s$$

where θ_c is the CABIBBO angle. Recent measurements[16)] gave

$$\sin\theta_c = 0.231 \pm 0.003$$

Thus, two types of weak neutral currents are expected

$$u \rightarrow u \quad \text{and} \quad d_c \rightarrow d_c$$

With the shorthand notation $(d_c d_c)$ for the amplitude

$$\bar{\psi}_{d_c} \gamma_\lambda (g_V + g_A \gamma_5) \psi_{d_c}$$

one gets $(d_c d_c) = (d\cos\theta_c + s\sin\theta_c \;\; d\cos\theta_c + s\sin\theta_c)$

$$= (dd)\underbrace{\cos^2\theta}_{\Delta S = 0} + (ss)\sin^2\theta_c + ((sd)+\underbrace{(ds)}_{\Delta S \neq 0})\cos\theta_c \sin\theta_c$$

It is now evident that the neutral current $d_c \rightarrow d_c$ would give rise to notsuppressed strangeness changing processes $d \rightarrow s$ or $s \rightarrow d$ in eclatant contradiction to the experiment. A way out of this dilemma has been put forward 1970 by GLASHOW, ILIOPOULOS, MAIANI[17)]. They postulated in addition to the three known quarks u, d, s a forth quark c (called u' at that time) with electric charge 2/3 like the u-quark. Then, a new charged current

$$(cs_c) = \bar{\psi}_c \;\; \gamma_\lambda (1 + \gamma_5) \psi_{s_c} \quad \text{with} \quad s_c \equiv -d\sin\theta_c + s\cos\theta_c$$

could be introduced relating the charmed quark c to the combination s_c being orthogonal to d_c. It then follows, that $(d_c d_c) + (s_c s_c) = (dd) + (ss)$, i.e. the dangerous strangeness changing currents drop out.

1971 the model of GLASHOW, SALAM, WEINBERG[18)] received a decisive theoretical support by t'HOOFT proving its renormalizability[19)]. Since no further experimental information, except for the known upper limits, became available the subject "neutral currents" played a rather minor rôle at the Tirrenia workshop 1972, where the phyiscs prospects of the forthcoming CERN SPS were discussed[20)].

The situation changed dramatically, when the GARGAMELLE neutrino collaboration found in december 1972[21)] a candidate for the reaction

$$\bar{\nu}_\mu e^- \rightarrow \bar{\nu}_\mu e^-$$

and had collected by spring 1973 a sizeable sample of muonless hadronic events in their neutrino and antineutrino runs (see table 4).

Table 4: Event rates in the GARGAMELLE experiment[22)]

Event type	ν-Expt.	$\bar{\nu}$-Expt.
# Events without μ	102	64
# Events with μ	428	148

The vertex distribution of events with and without muons is displayed in fig. 1 as a function of the position along the chamber axis. They look similar. It was very tempting to conclude that the muonless events are neutrino induced and not dominated by neutron interactions, since the neutron interaction length in the bubble chamber liquid is only 70 cm and an exponentially decaying distribution at the beginning of the chamber volume would have to be seen. One of the specific features of GARGAMELLE was its longitudinal extention of almost 5 m. Unfortunately, the above argument proved to be fallacious, since neutrons do not only enter at the front but also along the side of the cylindrical chamber with the consequence that also neutron induced events would have a rather flat vertex distribution along the beam direction. Therefore, it was crucial to perform an absolute calculation of the neutron background in order to find out whether the observed muonless events are evidence for a new phenomenon or simply neutron (or more generally neutral hadron)induced background.

The bubble chamber GARGAMELLE came into operation 1970, it was filled with the heavy liquid CF_3Br and was exposed to the CERN PS neutrino and antineutrino beams. The average neutrino energy was 2 GeV, useful event rates could be obtained up to 10 GeV. The fiducial volume of a bit more than 3 m^3 was sufficient to have typically 1.5 m potential path for each track such that a good distinction of muons from charged hadrons and a good efficiency for neutron interactions were ensured. Since muons could not be identified the search for the new process

$$\nu N \rightarrow \nu + \text{hadrons}$$

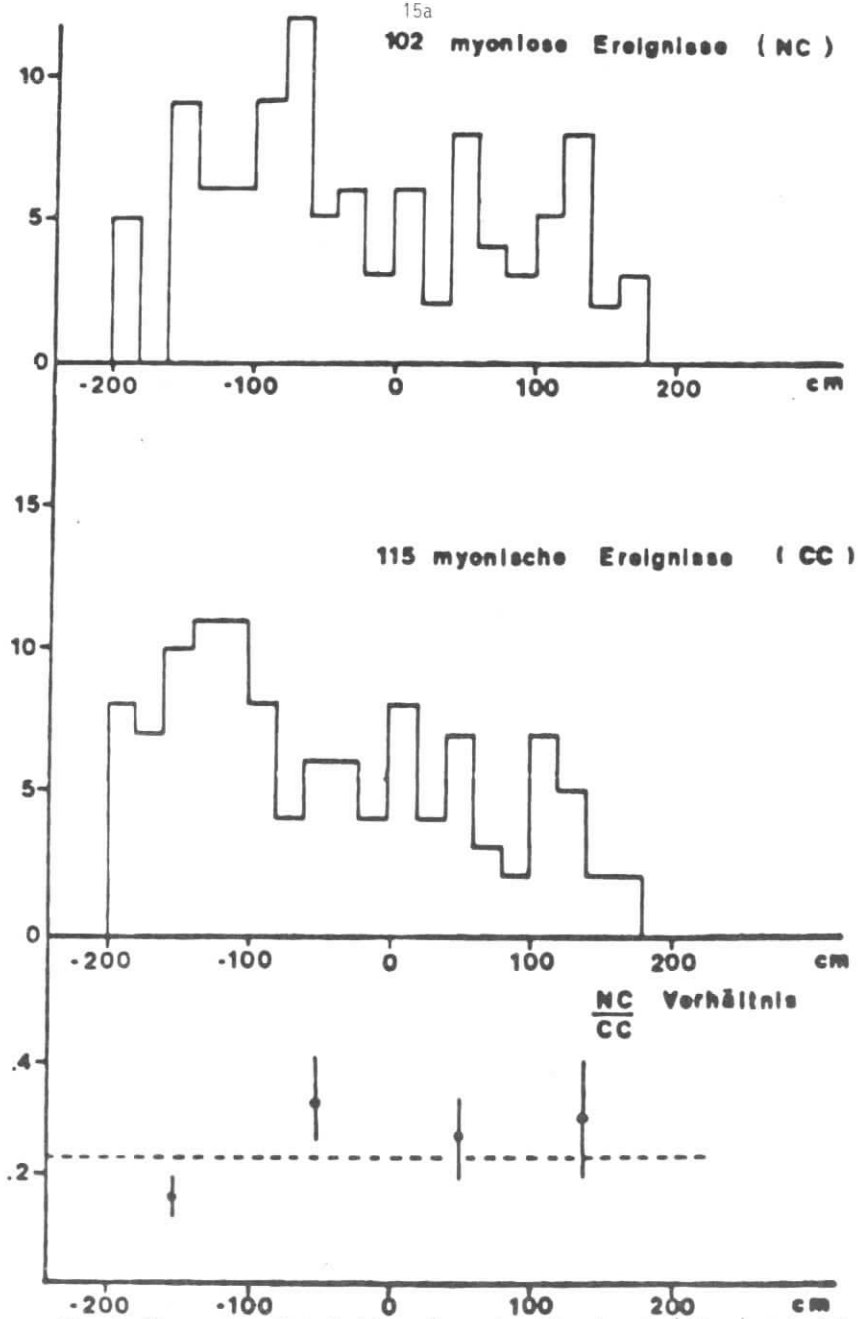

Fig. 1: The vertex distribution of events without muon (above) and with muon candidate (middle) along the chamber. The fiducial volume starts at -200 cm. Below is the raw NC/CC ratio (ref. 23).

was restricted to those events which consisted only of final state particles identified as hadrons, with total visible event energy in excess of 1 GeV. These events, called NC, were compared to a corresponding charged current event sample, called CC, where apart from the presence of a muon candidate with the appropriate charge the hadrons satisfied the same selection criteria as in the NC sample. Early 1973 the analysed NC sample consisted of about 100 events (cf table 4). Without going into the details of the analysis the essential features of the neutron, or more generally the neutral hadron, background calculation is sketched next[23,24]. The origin of neutrons having enough (namely more than 1 GeV) energy to simulate a NC event are neutrino interactions themselves. As indicated by the two sketches in fig. 2 the neutron source, i.e. upstream neutrino interaction, can occur in two configurations. The neutral hadron interaction (n*) is consequently said to be associated (AS) or not associated (B). It was the aim of the background calculation to get the number of B-events and to compare it with the observed number of NC-events. This was done in the following way:

$$\#B = \frac{B}{AS} \quad \#AS$$

i.e. the number of background events (#B) is obtained from the number of observed associated events (#AS) by means of the calculated ratio B/AS. With this trick only a ratio had to be calculated. The great worry in attempting such a calculation was how to treat the neutron cascade. Obviously, AS events are trivial, as they represent just the first cascade step. But in the case of B events, the source is in the heavy shielding material and the cascade can consist of many steps before finally a neutral hadron enters the chamber to produce a star simulating a NC candidate. Furthermore, the density of the shielding material was about 5 times higher than the density of the chamber liquid, thus the neutrino induced neutral hadron flux was potentially high. Obviously,

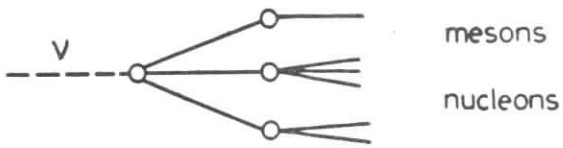

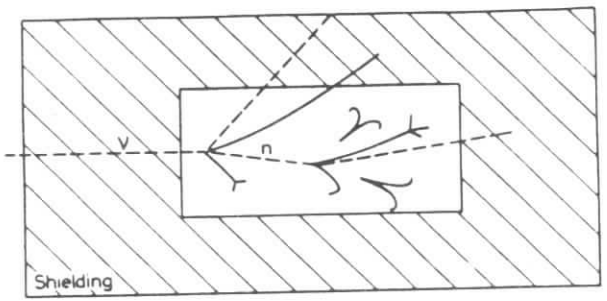

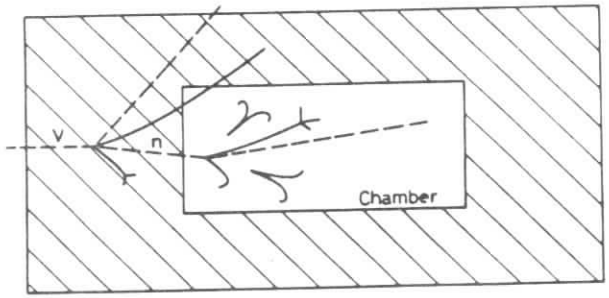

Fig. 2: Sketch of the simplified, but realistic setup. The chamber filled with the liquid freon (ρ=1.5 g/cm³) is imbedded in a dense medium (chamber well, magnet coils, iron shielding etc.). The neutrino beam enters from left and has a broad energy dependent radial distribution. A neutrino event with a subsequent neutron star is shown in two topologies: case above is an associated neutron star (AS), case below a nonassociated neutron star (B)(ref. 24.).

the understanding of the cascade was the crucial part for the evaluation of the neutral hadron background and thus for the interpretation of the whole experiment. The basic ideas of the cascade calculation were:

i) the meson component is inactive
ii) at each step at most one nucleon carries the cascade further

In other words, the cascade is linear. This reflects the dynamics of neutrino reactions as well as the dynamics of nucleon and meson interaction in the few GeV region together with the 1 GeV requirement mentioned above. The initially complex structure of the cascade has been reduced to the extent that a single quantity, the elasticity, can characterize it. This quantity could be extracted from published data. In conclusion, the ratio B/AS could be safely calculated with the result (for the neutrino experiment):

$$\left.\begin{array}{l} \frac{B}{AS} = 0.6 \pm 0.3 \\ \#AS = 15 \end{array}\right\} \rightarrow \#B = 9 \pm 4.5$$

to be compared with #NC = 102

showing that really a new effect has been observed. A similar conclusion could be drawn for the antineutrino data. By spring 1974 - after some turbulent months - the new effect, interpreted as weak neutral currents, has been observed in three experiments[25]. The GARGAMELLE experiment itself corroborated its first results by three further investigations[26]

- BARTLETT analyses of the spatial distribution of the events in the NC and CC samples confirm that the neutron contamination of the NC sample is small
- the charge distributions of pions in NC-events and in neutron induced events are different
- in a separate run protons of 4, 7, 12 and 19 GeV/c have been sent into GARGAMELLE thus allowing a direct check of the cascade calculation[24]. Fig. 3 shows an example. In fig. 4 the measured and the calculated - following the method described above - cascade length is displayed. The agreement is good.

Once established, the weak neutral currents initiated a new and rich activity in physics and even astrophysics. The aim of the experiments was to measure

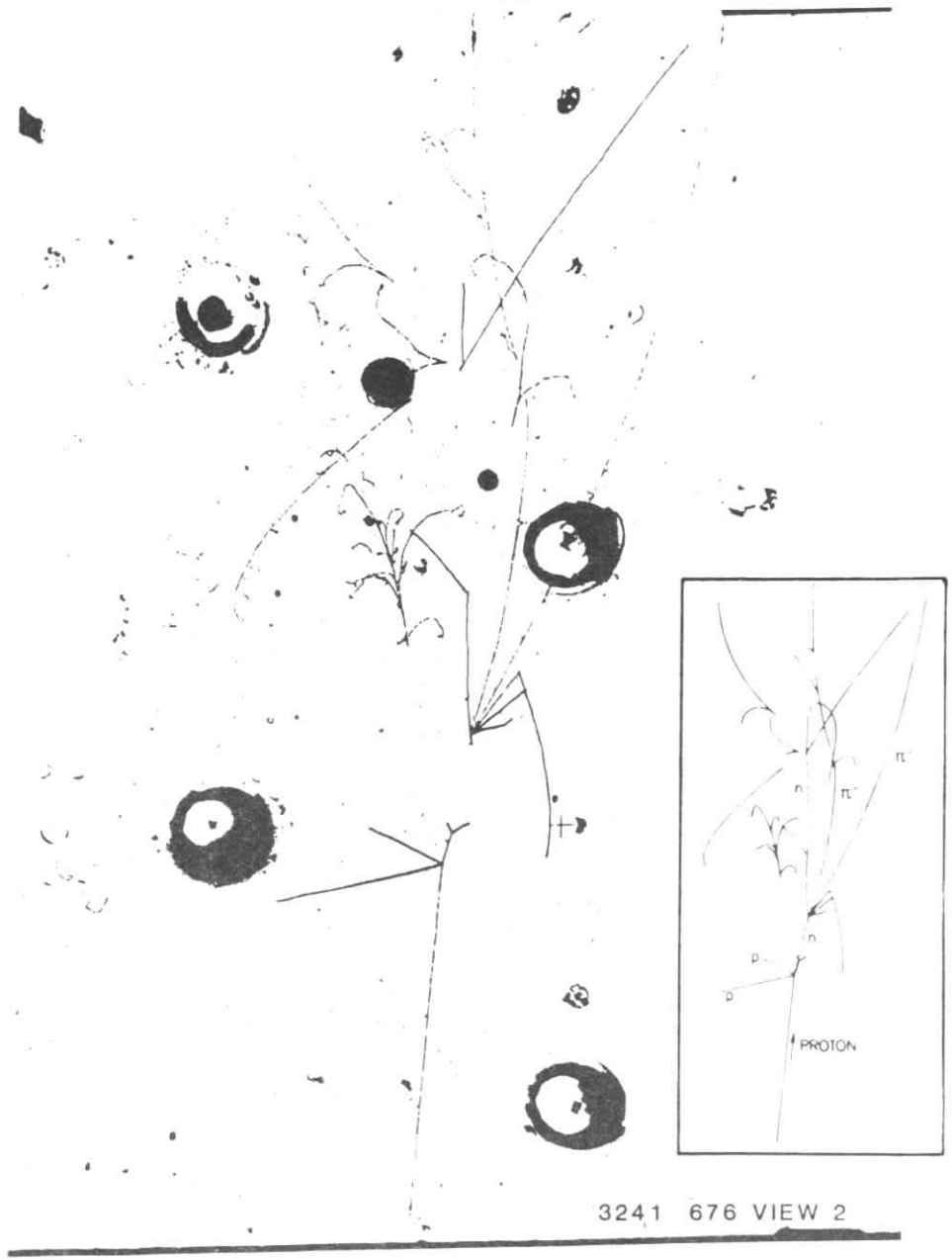

Fig. 3: Photo of a 6.1 GeV proton entering GARGAMELLE from below. The insert sketches the cascade (ref. 24).

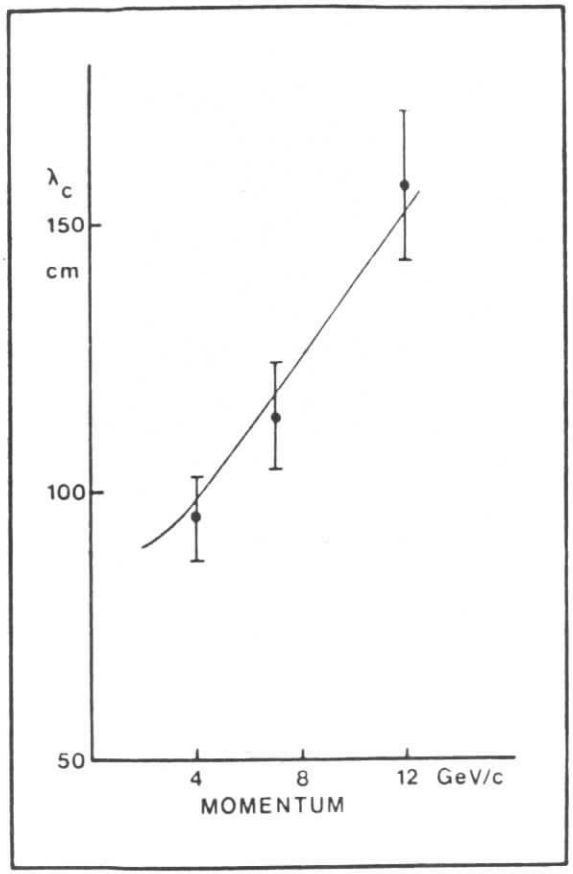

Fig. 4: Comparison of the measured and calculated cascade length as a function of the incoming proton momentum (ref. 24).

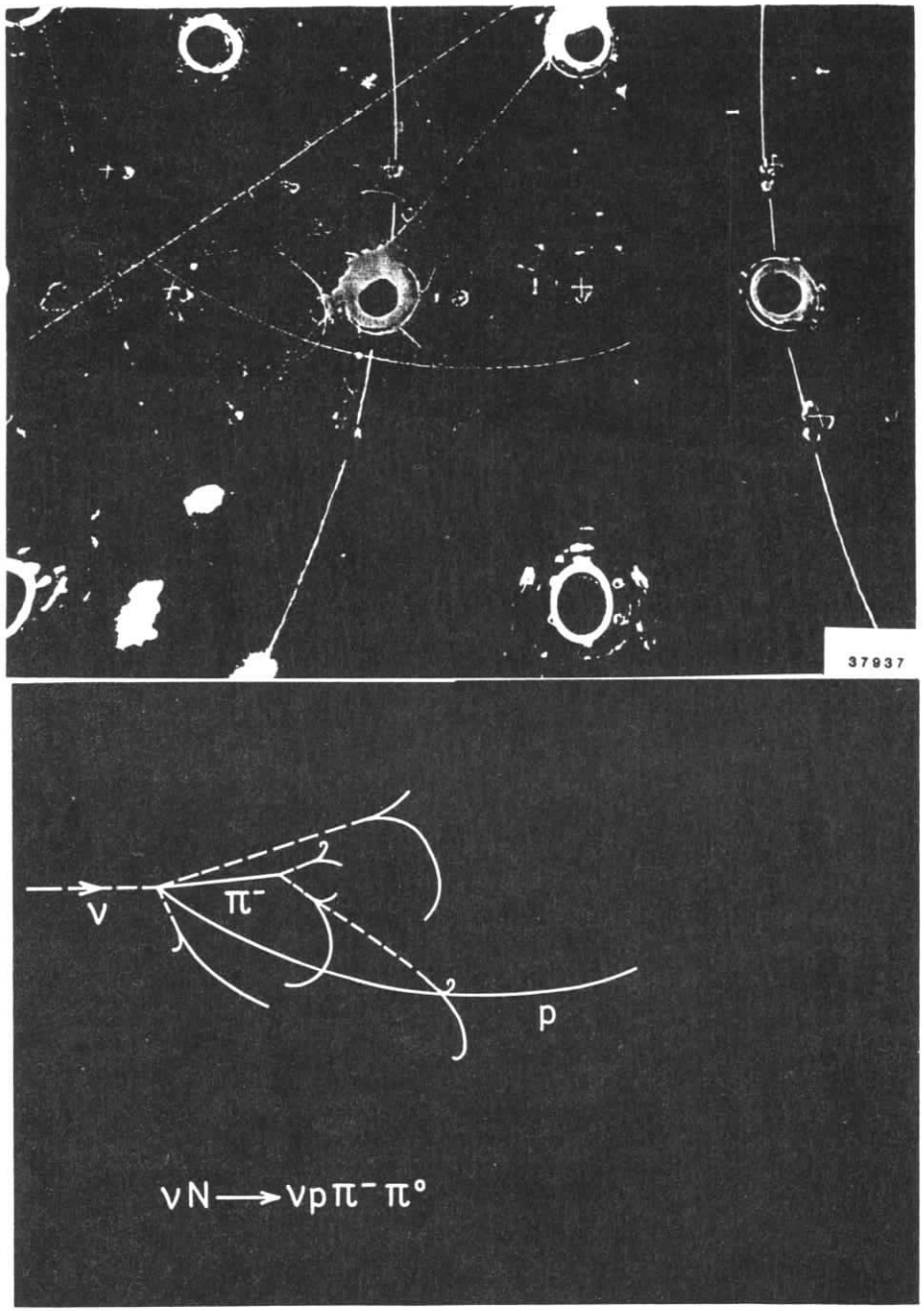

Fig. 5: Neutrino induced neutral current event observed in GARGAMELLE. All final state hadrons are indentified. Note the charge exchange reactions of the π^-.

the properties of the weak neutral current and to compare them with the variety of theoretical models. One of these models, the GSW model, received particular popularity, because only one unknown parameter, the weak angle, θ, was involved and because of its success. Very soon, this model was simply called the Standard Model.

8. FREE PARAMETERS IN THE STANDARD MODEL

Here and in the next three lectures only the electroweak part is dealt with. The above discussion has shown that there are three groups of free parameters:

couplings	g, $\sin^2\theta$, v
KM-matrix	3 angles, 1 phase
masses	Higgs and all fermions

All these free parameters must be determined from experiment. Once this is done, all electroweak phenomena can be predicted and consistency with measurements can be checked. For instance, all measured Zff couplings must be shown to agree with a universal value of $\sin^2\theta$ (cf. lecture 3 sect. 2).

9. CHOICE OF BASIC COUPLINGS

The outstanding property of a renormalizable theory, as for instance the Standard Model, is that any observable can be calculated in any order in terms of a finite set of parameters. Each such parameter must be defined by a suitable experimental procedure.
In the literature various choices are adopted. For the purpose of these lectures dealing with low energy electroweak phenomena the following choice is appropriate: e, G, $\sin^2\theta$.

1. The fine structure constant: The positron charge is defined as the electromagnetic coupling at very low energies.
   Using the JOSEPHSON effect

$$\frac{1}{\alpha} \equiv \left(\frac{e^2}{4\pi}\right)^{-1} = 137.035963\ (\pm 15)$$

   has been obtained[27].

2. The FERMI coupling constant G: The lifetime of positive muons can be measured very accurately. G is by definition obtained from:

$$\tau_\mu^{-1} = \frac{G^2 m_\mu^5}{192\pi^3}\left(1 - 8\frac{m_e^2}{m_\mu^2}\right)\left(1 + \frac{\alpha}{2\pi}\left(\frac{25}{4} - \pi^2\right)\right)$$

$$\rightarrow G = 1.166365\ (\pm 16)\ 10^{-5}\ \text{GeV}^{-2} \qquad 28)$$

   The term proportional to α represents the electromagnetic radiative correction.

3. The weak angle θ: At low energies:

$$\frac{\sigma(\bar{\nu}_\mu e \rightarrow \bar{\nu}_\mu e)}{\sigma(\nu_\mu e \rightarrow \nu_\mu e)} = \frac{1 - \xi + \xi^2}{1 + \xi + \xi^2} \quad \text{with} \quad \xi = 1 - 4\sin^2\theta$$

   This definition involves only leptons. The CHARM collaboration obtained sofar $\sin^2\theta = 0.24 \pm 0.04 \pm 0.015$[29]. An improved measurement with the anticipated precision of ± 0.005 is underway. In the meantime the more precise value coming from measurements of the NC/CC ratio in neutrino nucleon experiments is used.

Electroweak observables can be expressed as functions of e, G, $\sin^2\theta$. For illustration, the prediction of the $W^\pm$-mass may be considered. In terms of e (or α) G, $\sin^2\theta$ - the renormalized quantities - one derives from the Standard Model

$$m_W^{BORN} = \left(\frac{\pi\alpha}{\sqrt{2}\ G \sin^2\theta}\right)^{1/2} \qquad \text{prediction in lowest order (BORN approximation)}$$

$$m_W^{CORR} = m_W^{BORN}\ (1 + \delta) \qquad \text{prediction including next to leading order}$$

The shift δ, predicted by corrections due to 1-loop graphs, has recently been calculated and amounts to about 3.5%[30], i.e. about 3 GeV. The presence and size of this correction tests the renormalization aspect of the Standard Model. In order to make this test significant the measurement precision of $\sin^2\theta$ must be increased to $\pm$ 2%, i.e. $\Delta\sin^2\theta \quad \pm 0.005$. Among other choices of 3 basic couplings the one of MARCIANO and SIRLIN[30] may be mentioned. With the operation of the CERN $S\bar{p}pS$ collider the energy regime beyond the W, Z-masses is accessible and thus a natural choice are the physical masses

m_W, m_Z of the weak bosons together with the fine structure constant α. In this scheme $\sin^2\theta$ is a derived quantity, which can be related to $\sin^2\theta_M \equiv 1 - (\frac{m_W}{m_Z})^2$. Note that: $\sin^2\theta \neq \sin^2\theta_M$.

Lecture 2: Purely Leptonic Interactions

1. Introduction
2. Elastic neutrino-electron scattering
3. The processes $e^+e^- \to \ell^+\ell^-$
4. Muon decay
5. Inverse muon decay
6. The tau lepton
7. Higher order QED processes
8. Search for new heavy leptons

1. INTRODUCTION

Conceptually, but not necessarily experimentally, the simplest interactions are those involving only leptons. Their interpretation is theoretically clean. Leptons are pointlike and interact only weakly, like neutrinos, or electroweakly, like charged leptons. No complications due to strong interactions occur.
Table 5 shows some reactions, the currents involved and the couplings they are sensitive to. A prominent rôle play $\nu_\mu e$ and $\bar{\nu}_\mu e$ elastic reactions. Their occurrence proves weak neutral current interactions, since ν_μ and e belong to different generations. Charged lepton interactions, as observed at e^+e^- colliders for instance, were for a long time prototypes of electromagnetic processes. Recently, with the advent of high energy colliders like PETRA and PEP it could be demonstrated that charged leptons interact also weakly.

Table 5: Some purely leptonic reactions

Reaction	Currents	Sensitive to
$\nu_\mu e \to \nu_\mu e$	$(\nu_\mu\nu_\mu)(ee)$	$g_V^e,\ g_A^e$
$\bar{\nu}_\mu e \to \bar{\nu}_\mu e$	$(\bar{\nu}_\mu\bar{\nu}_\mu)(ee)$	
$\bar{\nu}_e e \to \bar{\nu}_e e$	$(\nu_e\nu_e)(ee)$	
	$(\nu_e e)(e\nu_e)$	
$\ell^- \to \nu_\ell e \bar{\nu}_e (\ell=\tau,\mu)$	$(\nu_\ell\ell)(e\,\nu_e)$	V - A
$\nu_\mu e \to \mu^- \nu_e$	$(\mu\nu_\mu)(\nu_e e)$	
$e^+e^- \to \ell^+\ell^-$	$(ee)(\ell\ell)$	$g_A^\mu,\ g_A^\tau$

2. ELASTIC NEUTRINO-ELECTRON SCATTERING

Neutrino beams at accelerators are derived from $\pi^\pm$ and $K^\pm$ decays and are thus basically ν_μ beams with small contaminations of ν_e, $\bar{\nu}_e$, $\bar{\nu}_\mu$. The use of magnetic horns ensures a good separation of particles from antiparticles. Since the early GARGAMELLE runs at the PS up to the recent CHARM runs at the SPS a tremendous development has taken place from 1 event/run to about 50 - 100/run. This gain comes from better and more intense neutrino beams, higher neutrino energies ($\sigma \sim E$!) and the use of very massive target calorimeters.
The kinematics and dynamics of neutrino and antineutrino interactions off electrons is easy to work out:

$$d\sigma(\nu_\mu e) = \sigma_o(e_L^2 + (1-y)^2\, e_R^2)\, dy$$

$$d\sigma(\bar{\nu}_\mu e) = \sigma_o(e_R^2 + (1-y)^2\, e_L^2)\, dy$$

where y measures the final state electron energy in terms of the initial neutrino energy and $\sigma_o = \frac{G^2 \rho^2 s}{\pi} = 1.72 \cdot 10^{-41}\ cm^2\ \frac{E}{GeV}$.
Neutrinos, which are lefthanders, interacting with a lefthanded electron, lead to an isotropic distibution, whereas those interacting with a right-handed electron to a distribution $\sim(1-\cos\theta^*)^2$ in the νe rest frame or $(1-y)^2$ in the laboratory frame. The two contributions are proportional to the square of the respective weak couplings e_L and e_R (cf. appendice).
For antineutrino interactions e_L and e_R are to be exchanged. In the presently accessible energy regime is $|q^2| \ll m_Z^2$; therefore, the total elastic cross section rises linearly with neutrino energy. Since $\sigma \sim m_e$ the expected rates are very small.
Fig. 6 shows all the experimental results so far. The CHARM collaboration[29] has investigated in the same apparatus ν_μ and $\bar{\nu}_\mu$ interactions and noted that the cross section ratio

$$R = \frac{\sigma(\nu_\mu e)}{\sigma(\bar{\nu}_\mu e)} = \frac{1 + \xi + \xi^2}{1 - \xi + \xi^2} \quad \text{with } \sin^2\theta = \frac{1}{4}(1-\xi)$$

can be obtained with small systematic error. The sensitivity of R to $\sin^2\theta$ is high due to the fact that $\sin^2\theta$ is around 0.22 (and not e.g. 0.5), as

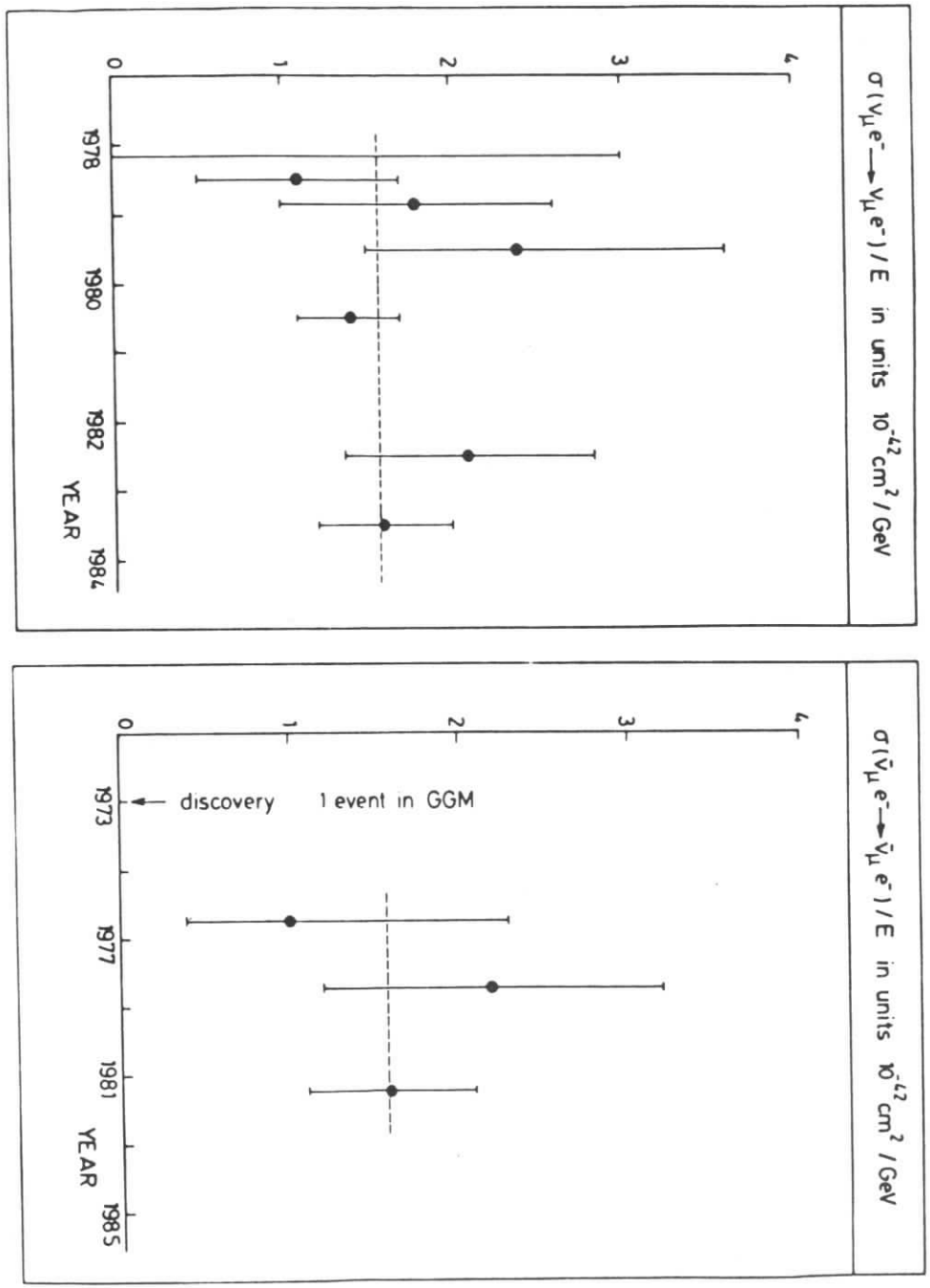

Fig. 6: Compilation of $\nu_\mu e$ - and $\bar{\nu}_\mu e$ scattering experiments (ref. 32 and 33).

seen in fig. 7. From $\sigma(\bar{\nu}_\mu e)$ the couplings e_L, e_R or v_e, a_e can be deduced. Fig. 9 shows the two ellipses of all data combined[31]:

a) Assume $\rho = 1$: $\quad a_e = -0.521 \pm 0.034$

$\qquad\qquad\qquad\qquad\quad v_e = 0.002 \pm 0.058$

This solution is in agreement with the Standard Model. The constraint equations contain the coupling constants squared, thus there is another solution which can however be excluded on the basis of other experiments (e.g. $e^+e^- \to \mu^+\mu^-$).

b) Assume $a_e = -0.5 \quad v_e = -\frac{1}{2}(1-4\sin^2\theta)$

get $\quad \sin^2\theta = 0.251 \pm 0.029 \quad \rho = 1.04 \pm 0.07$

c) Assume a_e, v_e and $\rho = 1$, then $\sin^2\theta = 0.244 \pm 0.029$

d) Use R (CHARM) alone[29]

$\qquad \sin^2\theta = 0.215 \pm 0.040 \pm 0.015 \qquad$ (independent of ρ)

Results on $\bar{\nu}_e e$ scattering are also indicated in fig. 9. They get contributions both from Z^0 and W^- exchange. The interference reduces the sign ambiguities by a factor 2. Data on $\nu_e e$ scattering are expected from LAMPF. In a dedicated experiment the CHARM Collaboration[34] is aiming at more than 1000 $\nu_\mu e$ and 1000 $\bar{\nu}_\mu e$ elastic events. Compared to their previous set-up the fiducial mass will be increased from 70 to 436 tons. The background rejection (see fig. 8) will be improved by reducing the angular resolution from 32 mr/$\sqrt{E}$ to 16 mr/$\sqrt{E}$. The relative ν, $\bar{\nu}$ flux monitoring should be controlled to ± 2%. Measuring then $\sigma(\nu_\mu e)/\sigma(\bar{\nu}_\mu e)$ to an accuracy of ±0.05 translates into $\Delta\sin^2\theta = \pm 0.005$. This precision is enough to test whether the difference

$$m_Z^{PHYS} - m_Z^{TREE} = m_Z^{PHYS} - \frac{e}{2\sqrt{\sqrt{2}G}} \frac{1}{\sin\theta\cos\theta} = m_Z^{PHYS} - \frac{37.2810(\pm 3)\ \text{GeV}}{\sin\theta\cos\theta}$$

is equal to the 1-loop weak correction calculated to be about 3 GeV within the renormalizable Standard Model. m_Z^{PHYS} is the physical mass of the Z as measured at the $S\bar{p}pS$ collider. This test on the presence and predicted size

of higher order weak corrections is crucial to the Standard Model.

4. THE PROCESSES $e^+e^- \to \ell^+\ell^-$

Consider the Lagrangian for $e^+e^- \to \mu^+\mu^-$:

$$L = -g \sin\theta(\bar{\psi}_e \gamma_\lambda \psi_e + \bar{\psi}_\mu \gamma_\lambda \psi_\mu) A^\lambda$$

$$+ \frac{g}{4\cos\theta} (\bar{\psi}_e \gamma_\lambda (g_v^e + g_A^e \gamma_5) \psi_e + \bar{\psi}_\mu \gamma_\lambda (g_v^\mu + g_A^\mu \gamma_5)\psi_\mu) Z^\lambda$$

In tree or BORN approximation the two relevant graphs are:

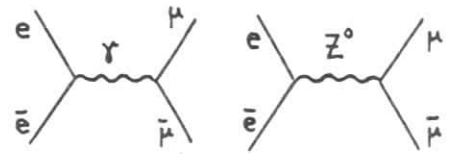

The electromagnetic contribution is of order $\frac{(g\sin\theta)^2}{s} = \frac{4\pi\alpha}{s}$ and dominates the weak contributions of order $(\frac{g}{4\cos\theta})^2 \frac{1}{m_Z^2} = \frac{G\rho}{2\sqrt{2}}$ as long as $s \ll m_Z^2$. In the standard model $\rho^2 = 1$ in tree approximation and gets slightly reduced by 1-loop corrections. For most of the following discussion it is sufficient to consider only the leading order.

The angular distribution is:

$$\frac{4s}{\alpha^2} \frac{d\sigma}{d\Omega} = R_\mu \left| (1 + \cos^2\theta) + \frac{8}{3} A_\mu \cos\theta \right|$$

with $R_\mu = Q_\mu^2 - 2Q_\mu g_V^e g_V^\mu \kappa + ((g_V^e)^2 + (g_A^e)^2)((g_V^\mu)^2 + (g_A^\mu)^2)\kappa^2$

$$A_\mu = -\frac{3}{2} \frac{Q_\mu g_A^e g_A^\mu + 2 g_V^e g_A^e g_V^\mu g_A^\mu \kappa^2}{R_\mu}$$

$$= \frac{1}{(2\sin 2\theta)^2} \frac{s}{s - m_Z^2} = \frac{G m_Z^2}{8\sqrt{2}\pi\alpha} \frac{s}{s - m_Z^2} = -0.45 \cdot 10^{-4} \frac{s}{1 - \frac{s}{m_Z^2}}$$

These formulae apply equally well to $e^+e^- \to f\bar{f}$ provided $f \neq e$ and $g_{V,A}^\mu$, Q_μ replaced by $g_{V,A}^f$, Q_f. The existence of Z^0-exchange in addition to photon exchange entails a significant modification of the differential cross section of $e^+e^- \to \mu^+\mu^-$ (fig. 10).

- Angular asymmetry A_μ: Right- and lefthanded contributions are no longer equally strong, the angular distribution gets a term proportional to $\cos\theta$. The γ - Z^0 interference (V,A type) gives rise to a forward-backward angular asymmetry:

$$A_\mu = \frac{F - B}{F + B} = -\frac{3}{2} \frac{g_A^e g_A^\mu}{Q_\mu} \kappa + O(\kappa^2) \approx \begin{cases} -10\% \text{ PETRA } (\sqrt{s} = 35 \text{ GeV}) \\ -6\% \text{ PEP } (\sqrt{s} = 29 \text{ GeV}) \end{cases}$$

For small s/m_Z^2 A_μ decreases with increasing s. In the adopted scheme with α, G, $\sin^2\theta$ as basic couplings A_μ depends only upon G/α, which is accurately known, and weakly upon m_Z, which is calculable using α, G, $\sin^2\theta$ up to a few GeV (due to uncertainty in $\sin^2\theta$). The Z-mass enters through the propagator term and has little influence, since $s/m_Z^2 < 0.2$ in the PETRA energy range. The measurement of A and its s-dependence is a crucial test of the standard model. The results (excluding the results at the Leipzig 1984 conference) are summarized in table 6[35]:

Table 6: Results from asymmetry measurements

	PETRA	PEP
$g_A^e g_A^\mu$	1.16 ± 0.10	1.03 ± 0.14
$g_A^e g_A^\tau$	0.88 ± 0.20	0.98 ± 0.18
g_A^τ / g_A^μ	0.76 ± 0.19	0.95 ± 0.21

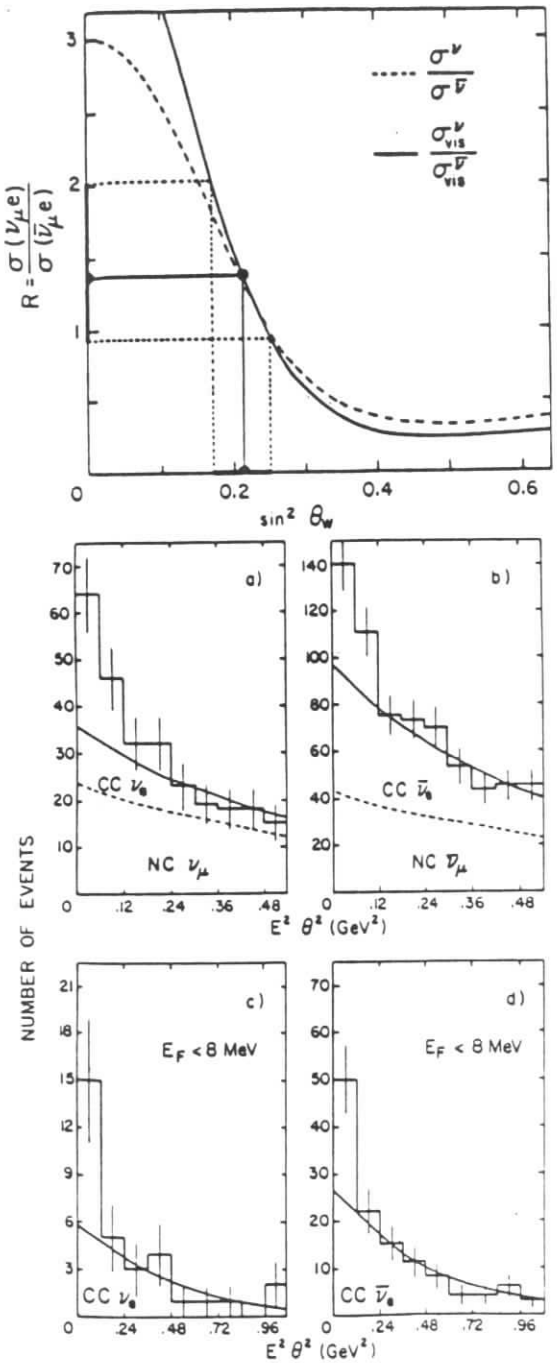

Fig. 7: The CHARM analysis (ref. 29).

Fig. 8: The background subtraction in the CHARM experiment.

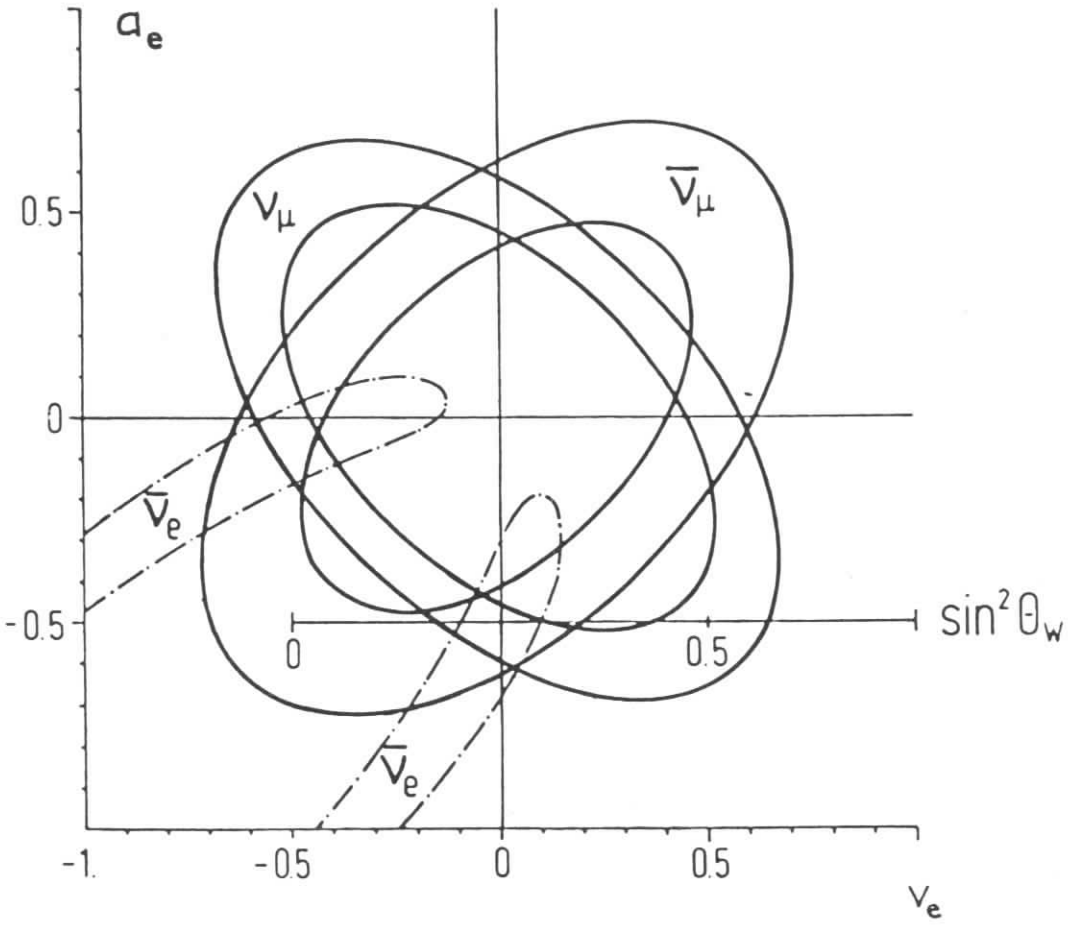

Fig. 9: Fit of all νe and $\bar{\nu}$e data (ref. 31).

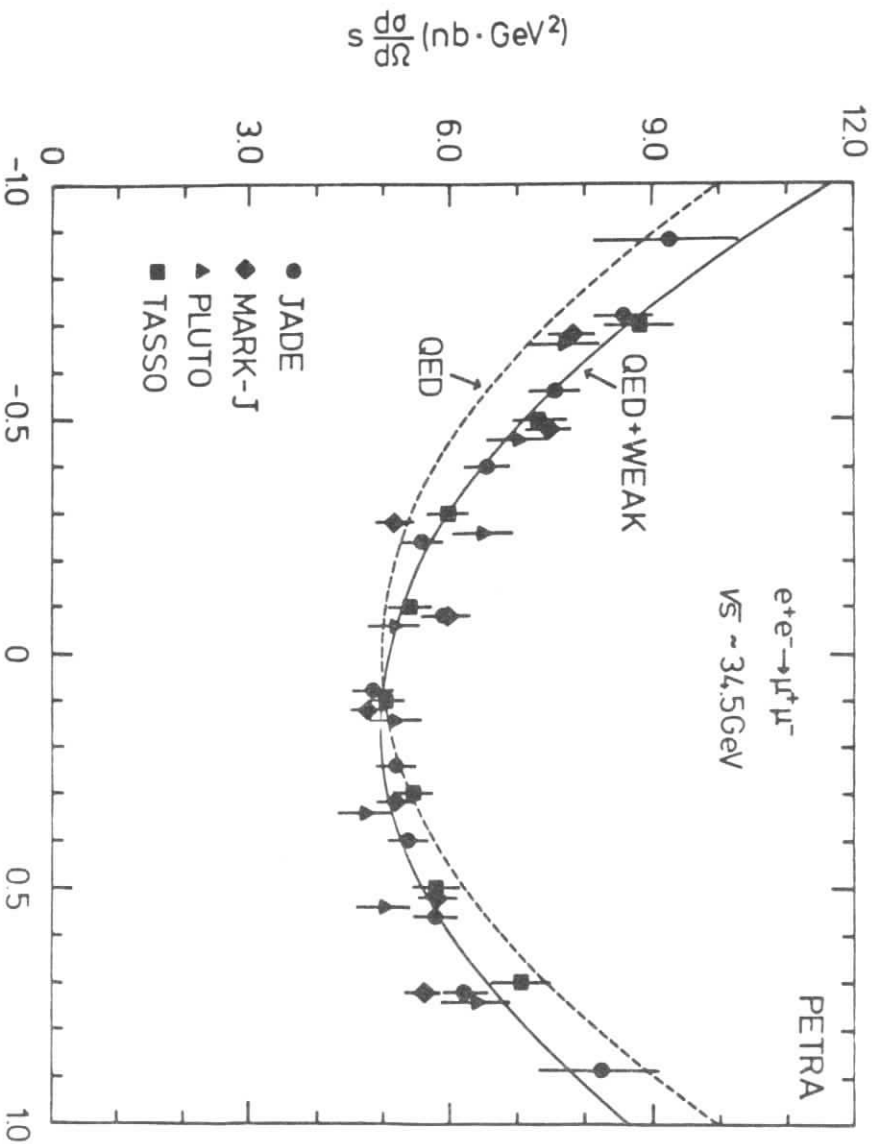

Fig. 10: Angular asymmetry in $e^+e^- \to \mu^+\mu^-$ (ref. 35).

The measurements agree with the predictions of the Standard Model ($g_A^e g_A^\mu = 1$ and $g_A^e g_A^\tau = 1$) within 1 to 2 standard deviations. This is a remarkable achievement, extending its validity up to $Q^2 = s = 2000\ \text{GeV}^2$ (time like). The ratio of the axial couplings of μ and τ confirms lepton universality within 20%.

Also the process $e^+e^- \to e^+e^-$ gets modified through the Z-graph. However, the angular distribution is already strongly asymmetric due to the γ-exchange in the t-channel. No group succeeded yet in demonstrating a significant deviation from the QED-prediction of the measured angular distribution.

- Ratio $R_\mu = \sigma(e^+e^- \to \mu^+\mu^-)/\sigma_{QED}$ is predicted to deviate from 1, the more so the higher the energy. Putting in the weak couplings $g_A^e = g_A^\mu = -1$ and $g_V^e = g_V^\mu = -1 + 4\sin^2\theta$ $|R_\mu - 1| \lesssim 0.02$ up to highest PETRA energies. The data, both for $e^+e^- \to \mu^+\mu^-$ (fig. 11) and $e^+e^- \to \tau^+\tau^-$ (fig. 12), agree well with 1. Since there is a normalisation error of about 5%, these measurements provide a poor limit on the weak vector couplings. Electromagnetic radiative corrections at $\sqrt{s} = 35$ GeV are about 30%, in other words the effective fine structure constant is $\alpha_{eff}^{-1} \approx 120$ compared to $\alpha^{-1} = 137$.

  R_μ can also be used to set limits on the pointlikeness of charged leptons by interpreting the deviation from 1 in terms of a formfactor:

$$F_\pm(q^2) = 1 \mp \frac{q^2}{q^2 - \Lambda_\pm^2}$$

  Present data constrain $\Lambda_\pm \gtrsim 200$ GeV, which means that leptons are structureless on the distance scale 10^{-16} cm.

- Z-propagator: It is intriguing to find out whether the existing data on the muon angular asymmetry A_μ exhibit the Z^0-propagator. A_μ is proportional to the ratio of the Z- and γ-couplings and to the ratio of the Z- and γ-propagators. Since the photon propagator contributes a term $1/s$, the quantity $\frac{A_\mu(s)}{s}$ is proporitonal to $\frac{1}{s - m_Z^2}$. The most general test consists in just looking at the slope of $(\frac{A_\mu}{s})^{-1}$. This slope is independent of the Z- and γ-couplings and is finite ($\neq 0$) for a massive propagator. Fig. 13 shows all data on $A(e^+e^- \to \mu^+\mu^-)$. The uncertainties are still too big to

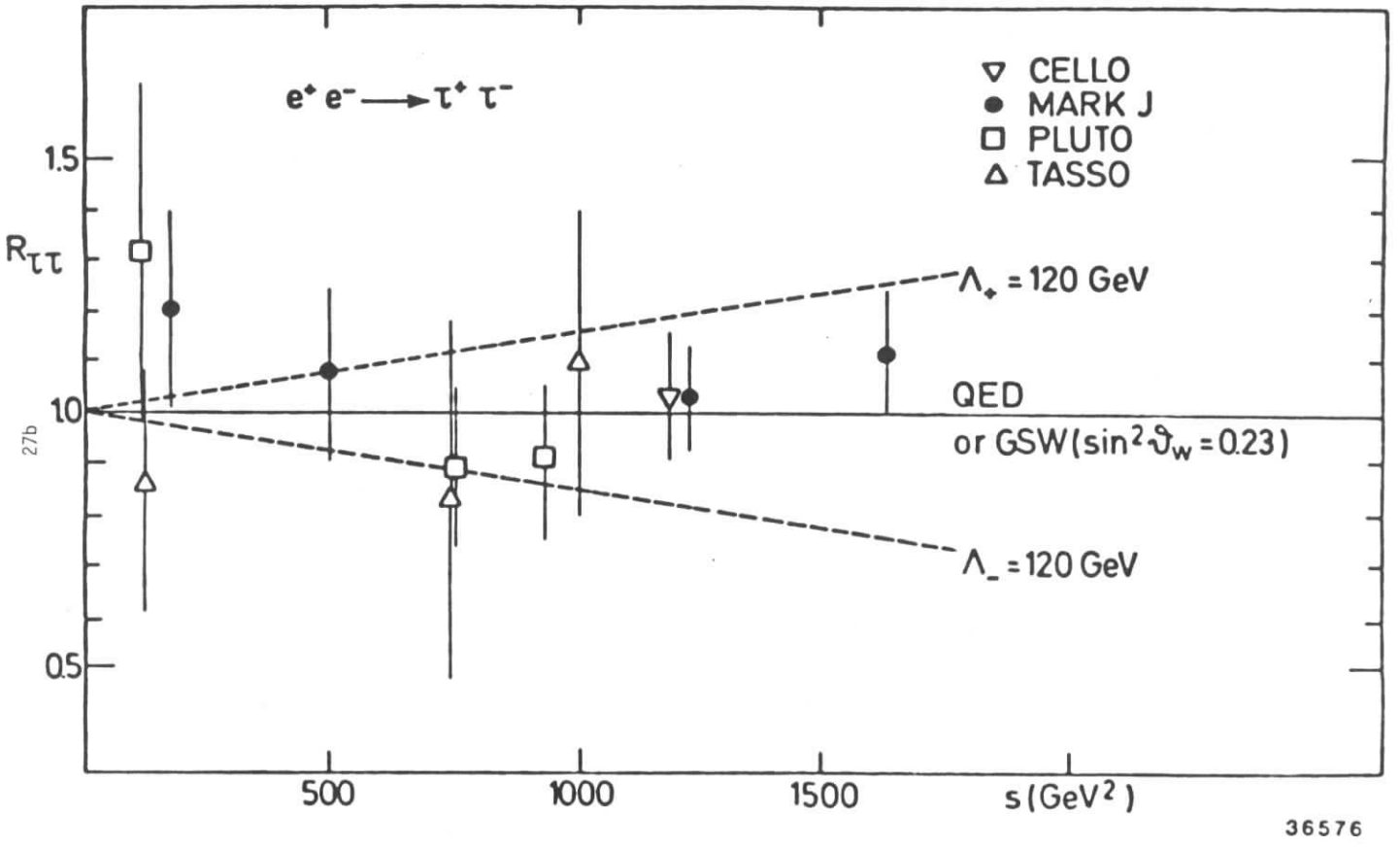

Fig. 12: Same as fig. 11 but $e^+e^- \rightarrow \tau^+\tau^-$

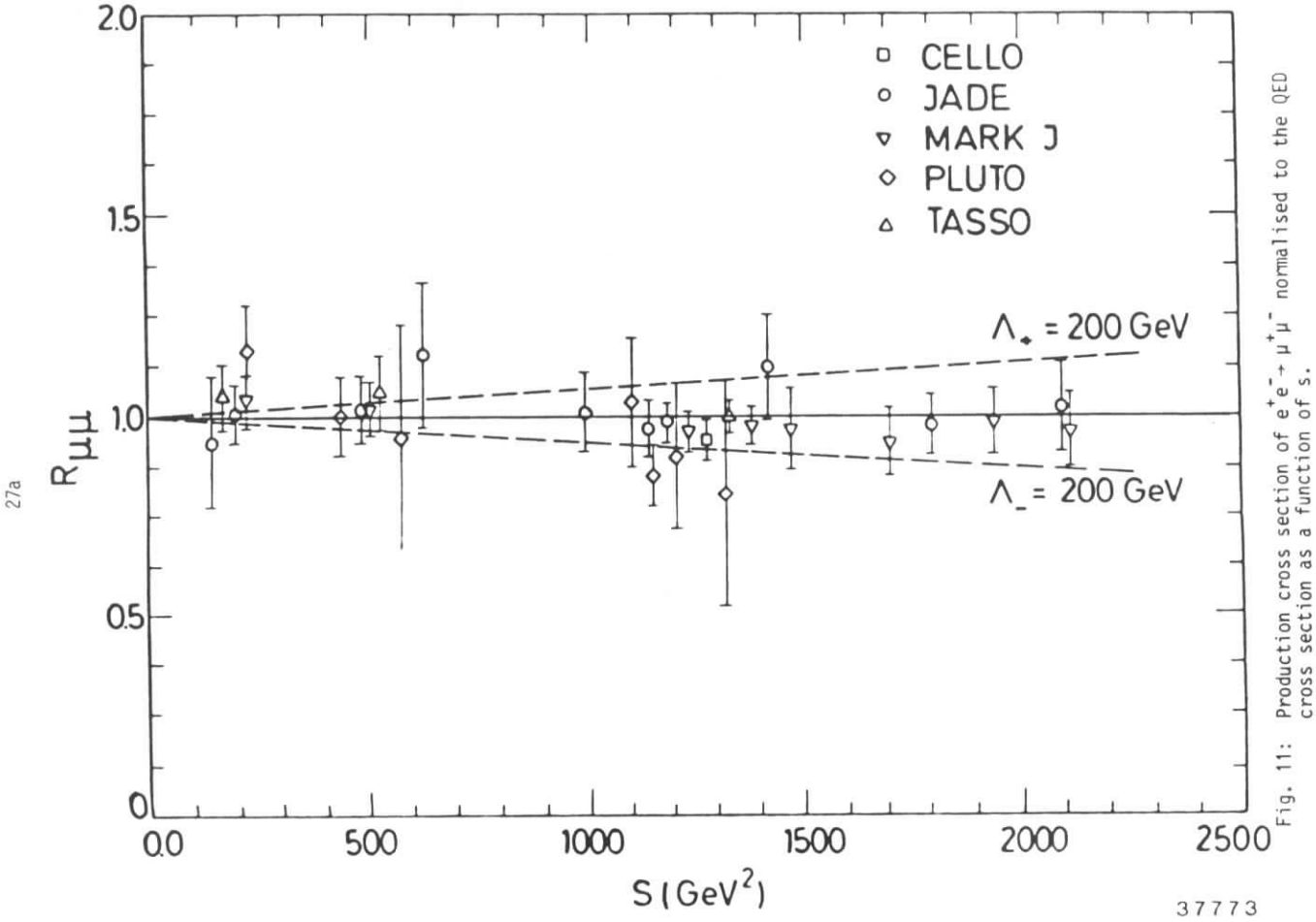

Fig. 11: Production cross section of $e^+e^- \rightarrow \mu^+\mu^-$ normalised to the QED cross section as a function of s.

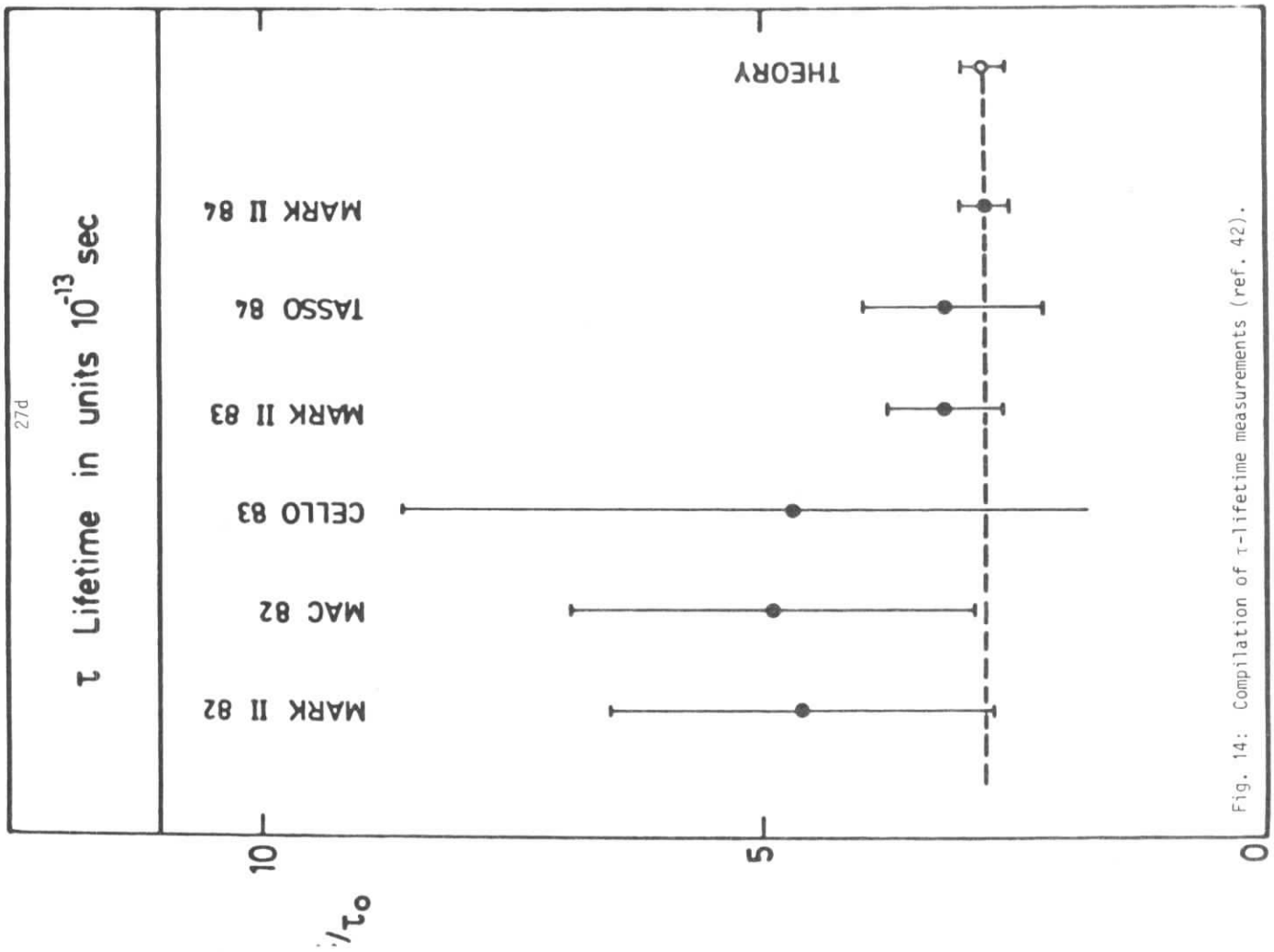

27d

Fig. 14: Compilation of τ-lifetime measurements (ref. 42).

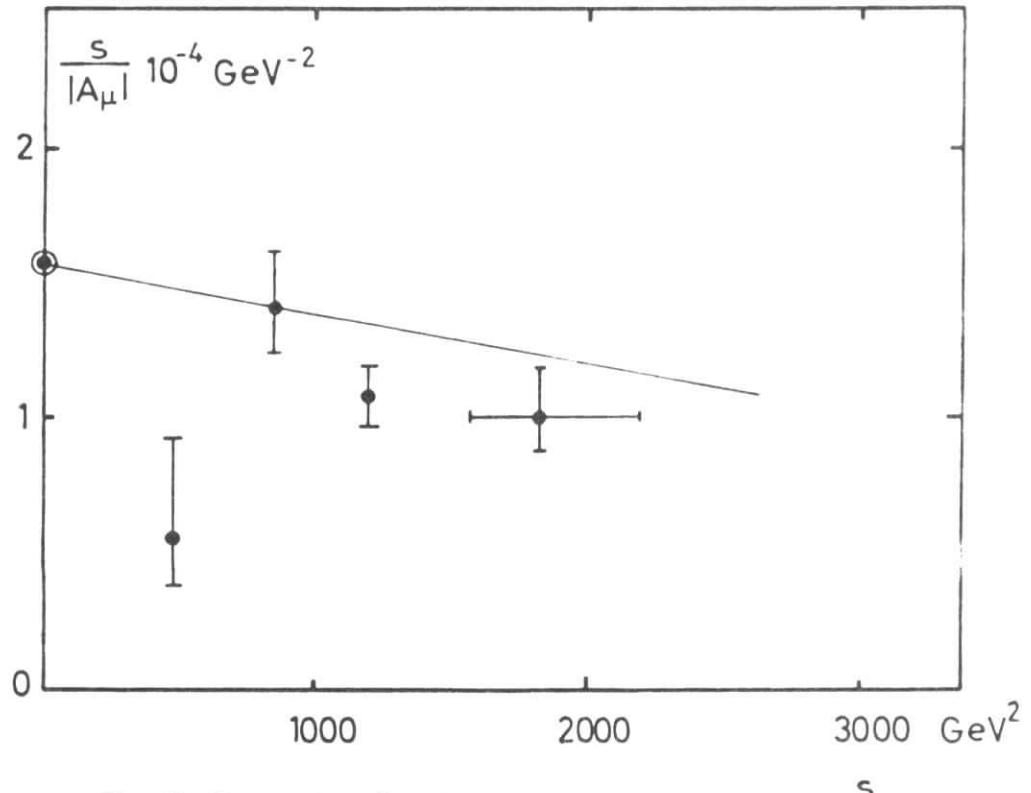

27c

Fig. 13: Z-propagator effect in the energy dependence of the angular asymmetry in $e^+e^- \to \mu^+\mu^-$. The fixpoint at $s = 0$ depends upon G/α. The line represents the prediction of the Standard Model for $m_Z = 93$ GeV as calculated from G, α and $\sin^2\theta = 0.217$.

conclude on a significant nontrivial s-dependence. However, the test can be sharpened by requiring a straight line through the fix point $\frac{2}{3}\mathcal{A}$ at $s = 0$ as given by the Standard Model. The line drawn in fig. 13 is the prediction of the Standard Model (m_Z = 93 GeV). The agreement with the data is fair. The highest energy point includes new data[36]:
$A_\mu = -(17.6 \pm 2.5)\%$ at average $\sqrt{s}$ = 42.5 GeV (expected: -14.7%).

MUON DECAY

The study of the decay $\mu^+ \to \bar{\nu}_\mu e^+ \nu_e$ or $\mu^- \to \nu_\mu e^- \bar{\nu}_e$ had an essential impact on the development of weak interaction physics. Although q^2 in this process is very small, high precision measurements provide valuable information. Four results will be quoted:

a) The MICHEL parameter ρ_M:

$$\frac{\rho_M^{meas}}{\rho_M^{V-A}} = 1.0024 \pm 0.0035$$

b) The lifetime of the μ^+ [37] : $\tau_\mu = (2.19695 \pm 0.00005)10^{-6}$ sec

with $\frac{1}{\tau_\mu} = \frac{G^2 m_\mu^5}{192\pi^3}\left(1 - 8\frac{m_e^2}{m_\mu^2}\right)\left(1 + 0.6\frac{m_\mu^2}{m_W^2} - \frac{\alpha}{2\pi}\left(\pi^2 - \frac{25}{4}\right)\right)$

follows $G = 1.166365\ (\pm 16)10^{-5}$ GeV^2 which is the most precise measurement of the FERMI coupling constant.

c) Search for the right handed currents in polarized μ^+-decay: by looking at the electron energy spectrum near the end point the assumption of a righthanded W is only consistent with the data if its mass exceeds 380 GeV[38].

d) New upper limit $\Gamma(\mu^+ \to e^+e^+e^-)/\Gamma(\mu^+ \to e^+\nu_e\bar{\nu}_\mu) < 1.6 \cdot 10^{-10}$ (90% CL)[39]

INVERSE MUON DECAY

The process $\nu_\mu e^- \to \mu^- \nu_e$ is induced by a lefthander and contains more information than the μ-decay (with its two neutrinos in the final state). This reaction was only some years ago observed, since a threshold at E_ν = 11 GeV is involved. The results from GARGAMELLE (1979) and CHARM (1980) give[40]

$$\frac{\sigma(\nu_\mu e \to \mu\nu_e)}{\sigma_{V-A}} = 0.98 \pm 0.18$$

THE TAU LEPTON

The heavy lepton $\tau^{\pm}$ [41] was the first member of the third generation, discovered 1975. It is produced in $e^+e^- \to \tau^+\tau^-$ for $\sqrt{s} > 2m_\tau$. All observations confirm that the τ behaves like a sequential lepton. Up till now the inverse process: $\nu_\tau N \to \tau^- + x$ has not yet been observed. Fig. 14 summarizes measurements of the τ-lifetime[42]. It agrees within 10% with the expected V-A prediction assuming μ-τ universality. Another check is provided by comparing the purely leptonic decays:

$$\frac{\tau \to \nu_\tau + \mu\,\bar{\nu}_\mu}{\tau \to \nu_\tau + e\,\bar{\nu}_e} = 0.97 \pm 0.08$$

where the standard model predicts 0.973.
As already mentioned above the weak neutral current (ττ) is tested by measuring the angular asymmetry of $e^+e^- \to \tau^+\tau^-$: g_A^τ agrees within 15% with the theoretical expectation (cf. table 6).

HIGHER ORDER QED-PROCESSES

The next figures shall demonstrate that even at $\sqrt{s}$ up to 40 GeV QED works very well. The processes considered are[43]:

$e^+e^- \to \gamma\gamma\gamma$ (fig. 15)
$e^+e^- \to e^+e^-\gamma$ (fig. 16)
$e^+e^- \to e^+e^-\mu^+\mu^-$ (fig. 17)

SEARCH FOR NEW HEAVY LEPTONS

Interactions of e^+e^- are ideal to look for new heavy leptons. The charged member of a forth sequential lepton doublet $\binom{\nu}{L}$ would be produced like

$$e^+e^- \to L^+L^- \qquad \sqrt{s} > 2m_L > 2m_\tau$$

with a cross section

$$\frac{1}{\sigma_\mu^{QED}} \frac{d\sigma}{d\cos\theta} = \frac{3}{8}\beta\,(1 + \cos^2\theta + (1-\beta^2)\sin^2\theta)$$

where β describes the threshold behaviour.
The signature of such events is characterized by missing momentum and non-collinear, non-coplanar topologies as a consequence of

$$L \to \nu_\tau + \text{anything} \to \begin{cases} \nu_\tau + \ell\bar{\nu}_e \\ \nu_\tau + q\bar{q}'\text{-jets} \end{cases}$$

The experiments at PETRA and PEP exclude such sequential charged leptons up to 21 GeV[44] (fig. 19).
Another type of heavy leptons has been searched for[45]:

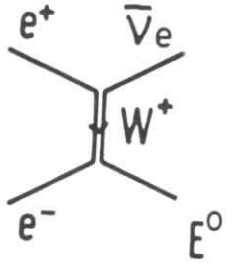

$e^+e^- \to \bar{\nu}_e E^0$

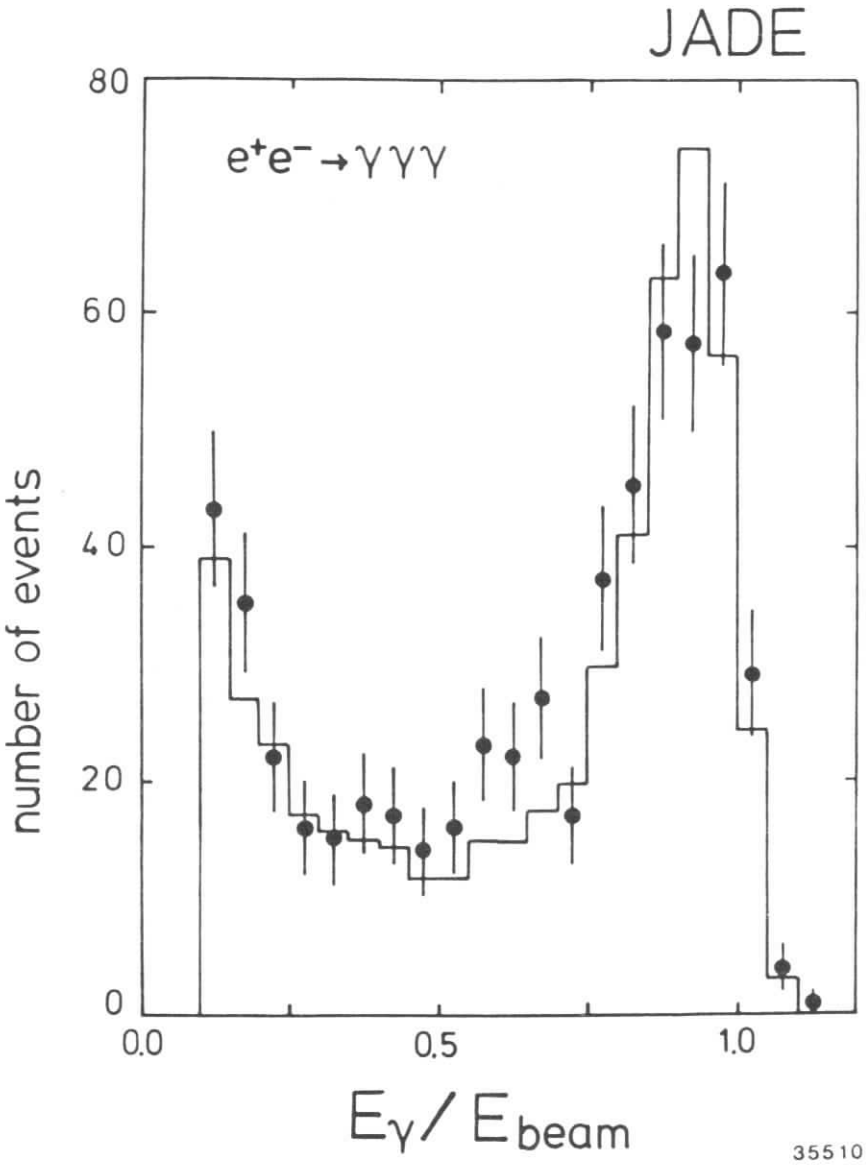

Fig. 15: Photon energy spectrum of $e^+e^- \to \gamma\gamma\gamma$ and comparison with QED.

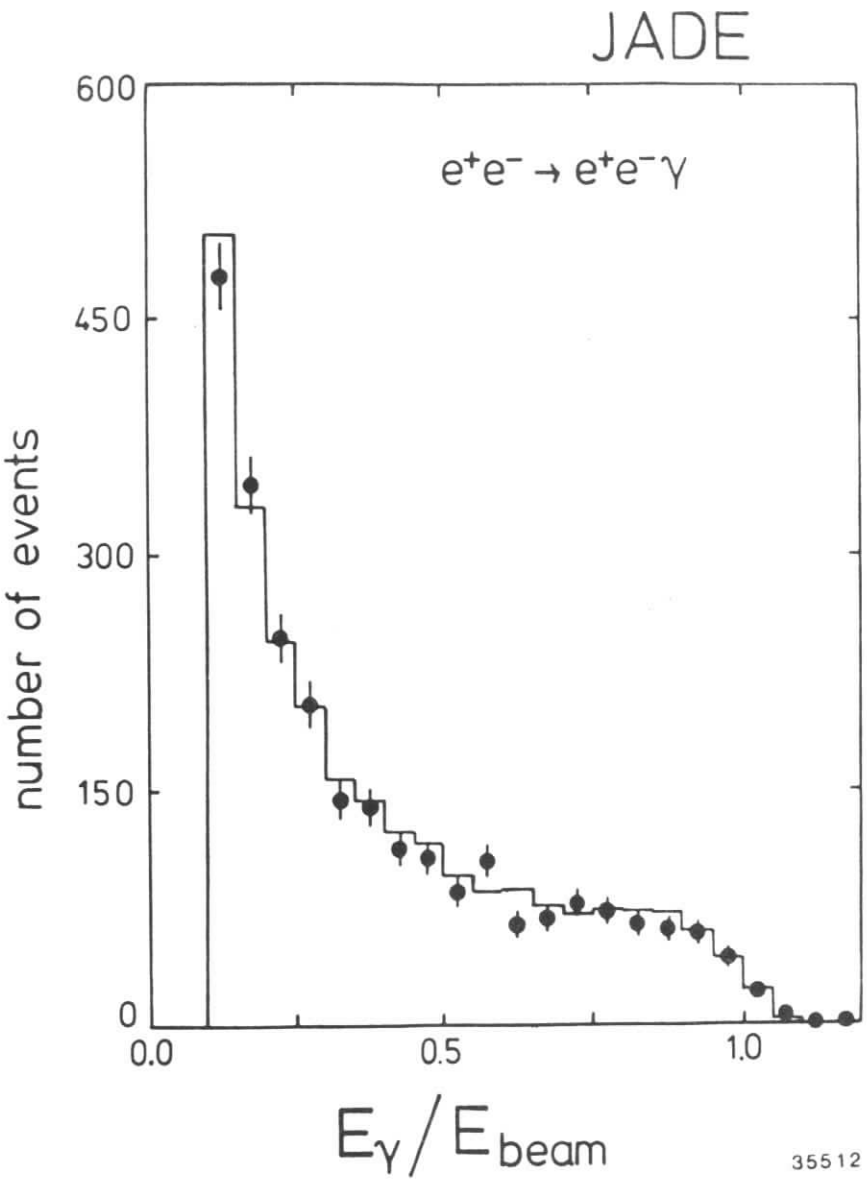

Fig. 16: Photon energy spectrum of $e^+e^- \to e^+e^-\gamma$ and comparison with QED.

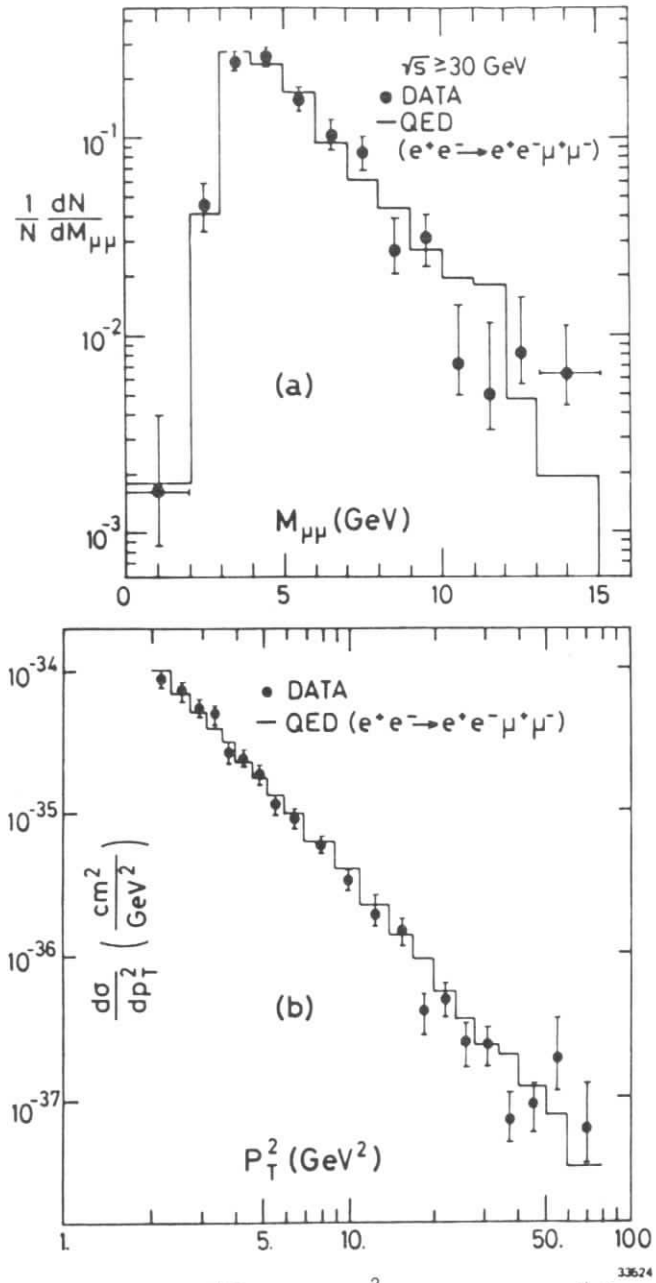

Fig. 17: Invariant $\mu^+\mu^-$ mass and P_T^2 distribution of $e^+e^- \to e^+e^-\mu^+\mu^-$ and comparison with QED.

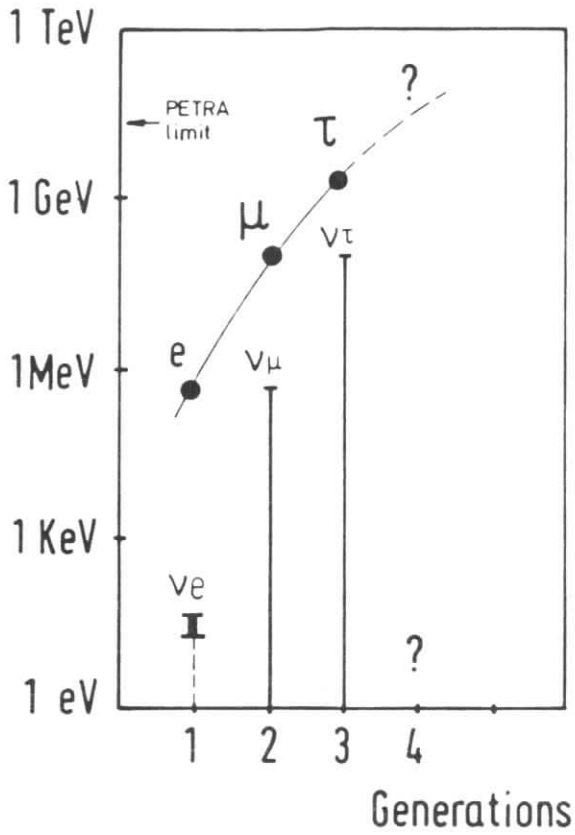

Fig. 18: Lepton masses vs generation number.

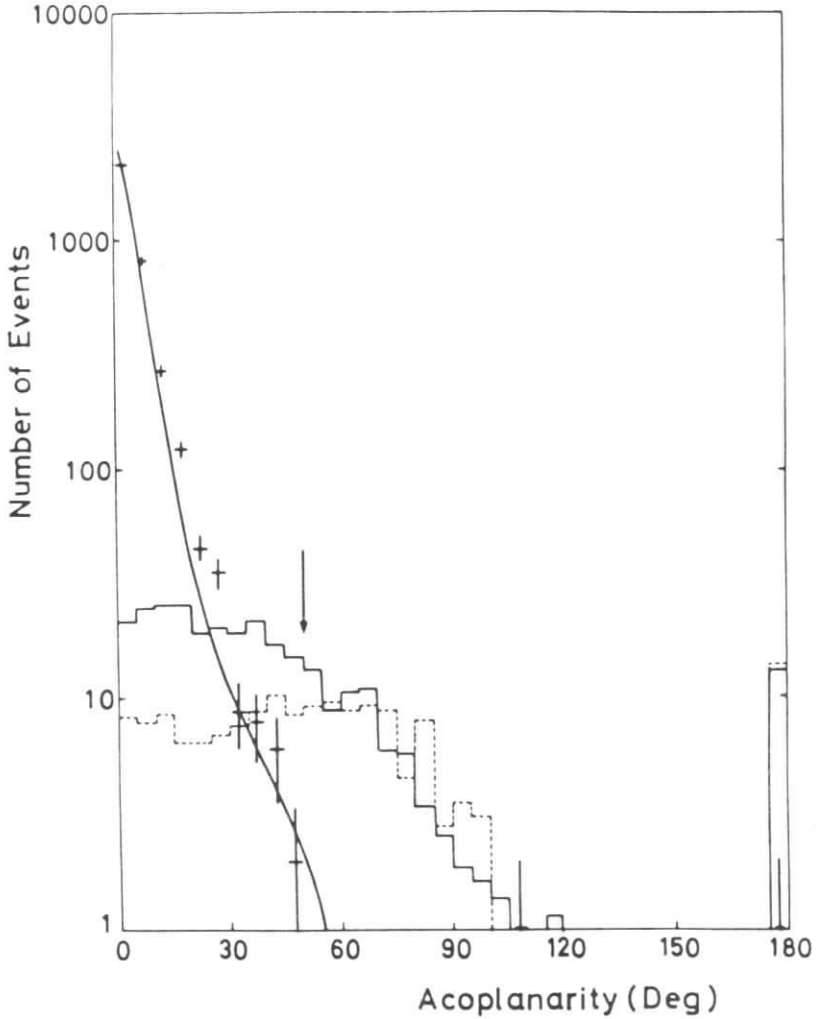

Fig. 19: The acoplanarity distribution of the data (crosses) compared with expectation from multihadron events (solid line). The two histograms refer to simulated $L^{\pm}$ events (solid) and E^{0} (dotted).

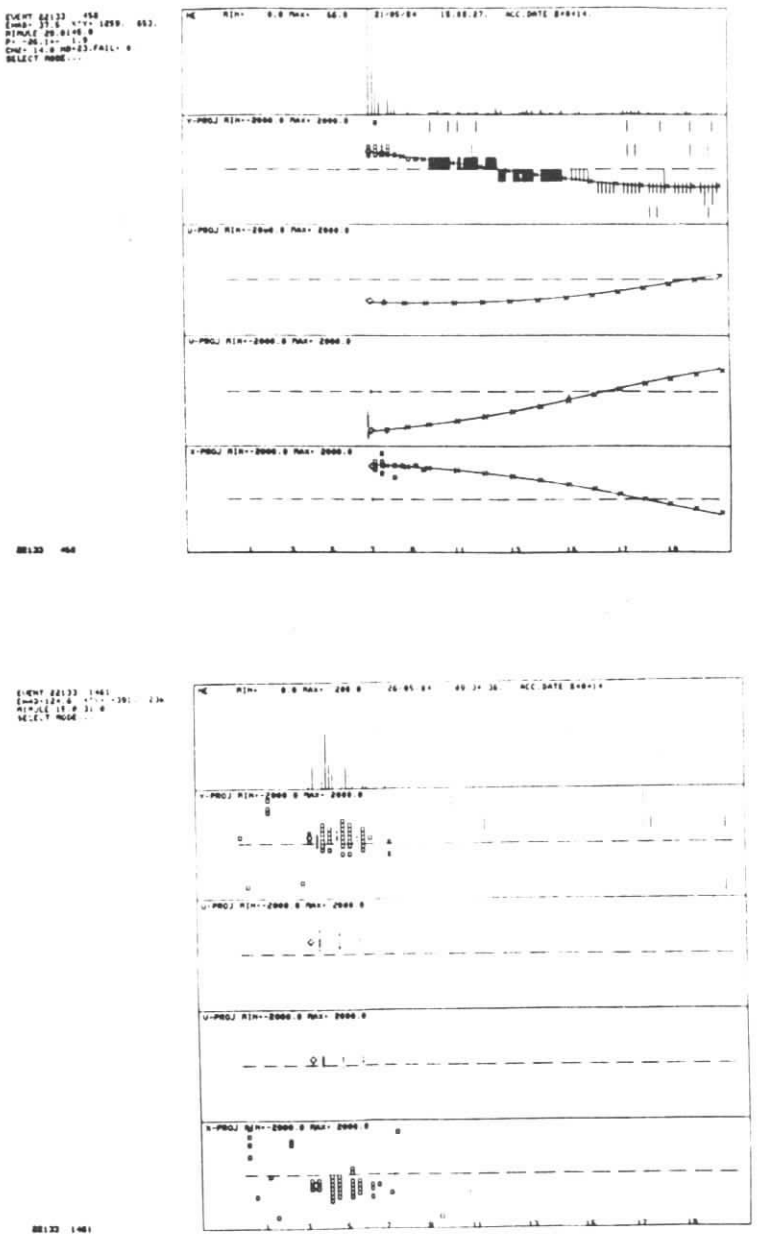

Fig. 20: Neutrino interactions seen in the CDHS apparatus[46].
a) Charged current event (CC), b) neutral current event (NC).

If produced, its decay is assumed to proceed according to

$$E^0 \rightarrow \begin{cases} e^- + u\bar{d} \text{ or } s\bar{c} \\ e^- + \bar{\ell}\, \nu_e \end{cases}$$

again with characteristic topologies depending upon the mass assumed for the E^0. From the absense of such event topologies a lower limit, $m_E > 22.5$ GeV with 95% confidence level, can be deduced.

Lecture 3 : SEMILEPTONIC NEUTRAL CURRENT INTERACTIONS

1. Introduction
2. The $Zq\bar{q}$ couplings
3. Electroweak results from e^+e^--experiments
4. Weak effects in charged lepton-nucleon scattering
5. Parity violation in Caesium
6. Conclusions on $Zq\bar{q}$

1. INTRODUCTION

The lepton vertices are well understood. This means, that the gauge bosons (γ, $W^\pm$, Z) can be used as probes for the electroweak and the strong properties of quarks. Typical experiments to investigate these two aspects are:

neutrino-nucleon scattering	($\nu N \to \nu$ or μ + anything)
charged lepton-nucleon scattering	($\ell^\pm N \to \ell^\pm$ + anything)
e^+e^- - annihilation into hadrons	($e^+e^- \to$ hadrons)

These deep inelastic scattering experiments revealed the weak neutral current structure of light quarks, to some extent also for heavy quarks, and the structure of nucleons appearing as if made of quasi free pointlike constituents. The color is a distinguishing property of quarks and causes a deep difference between quarks and leptons: leptons exist as free particles, whereas quarks, when leaving the interaction region, develop strong forces with the consequence of getting confined. Since the gauge bosons $W^\pm$, Z, γ couple only to the electroweak properties of the quarks, they are ideal tools to study the color aspects of quarks under well defined conditions. The results from deep inelastic scattering experiments are important input for the interpretation of hadron-nucleon experiments, including the recent $S\bar{p}pS$ collider experiments.

2. THE $Zq\bar{q}$ COUPLINGS

When the weak neutral currents were discovered 1973, it was immediately clear that a new chapter in physics was opened and that an extensive research program would start. Early contributions came from various neutrino experiments:

GARGAMELLE bubble chamber at CERN-PS
AACHEN-PADOVA setup at CERN-PS
HPWF calorimeter } at FNAL
CITF calorimeter }
12' ANL bubble chamber
7' BNL bubble chamber
15' FNAL bubble chamber

1975 an experiment at SLAC with polarized electrons scattering off deuterons reported the observation of a parity violating asymmetry, interpreted as a (γ, Z^0)-interference effect, and leading to a 10% measurement of $\sin^2\theta$ in agreement with neutrino data.

1977 the first neutrino experiments were carried out using the CERN-SPS thus reaching neutrino energies up to 200 GeV. Compared to the CITF- and HPWF-apparatus running already since a few years in this energy regime the new CDHS calorimeter at CERN was a second generation apparatus (fig. 20). The big european bubble chamber BEBC, of similar size as the 15' bubble chamber, started - upstream in the same neutrino beam as CDHS - its 8 years lasting research program. Soon after, the fine grain marble calorimeter of the CHARM collaboration joined the other two. GARGAMELLE ran for a short while at the SPS before it broke down. At Serpuchov two experiments were operating: the bubble chamber CKAT and a counter apparatus. Dedicated experiments were performed on ν, $\bar{\nu}p$ at BNL and ν, $\bar{\nu}e$ scattering at CERN and BNL. At FNAL the new calorimeter of the CCFRR collaboration came into operation. The big bubble chambers got upgraded with an external muon identifier (EMI), which ensured an efficient distriction of charged current from neutral current induced events (fig. 21).
With the advent of the high energy e^+e^- colliders PETRA and PEP electro-weak effects got accessible in a new energy regime. The latest achievement was the observation of weak phenomena at the $S\bar{p}pS$ collider, culminating 1983 in the discovery of the weak gauge bosons.

All data available up to 1979 have been analysed by KIM et al.[48].
Three of their results are quoted here:

a) Use all neutrino data: 4 parameters are fitted

$u_L = 0.340 \pm 0.033$ $\quad \alpha = 0.589 \pm 0.067$

$d_L = -0.424 \pm 0.026$ $\quad \beta = 0.937 \pm 0.062$

$u_R = -0.179 \pm 0.019$ $\quad \gamma = -0.272 \pm 0.081$

$d_R = -0.017 \pm 0.058$ $\quad \delta = 0.101 \pm 0.093$

$\sqrt{u_L^2 + d_L^2} = 0.544 \pm 0.007$

$\sqrt{u_R^2 + d_R^2} = 0.180 \pm 0.015$

fit quality: χ^2/d.o.f. = 13.5/24

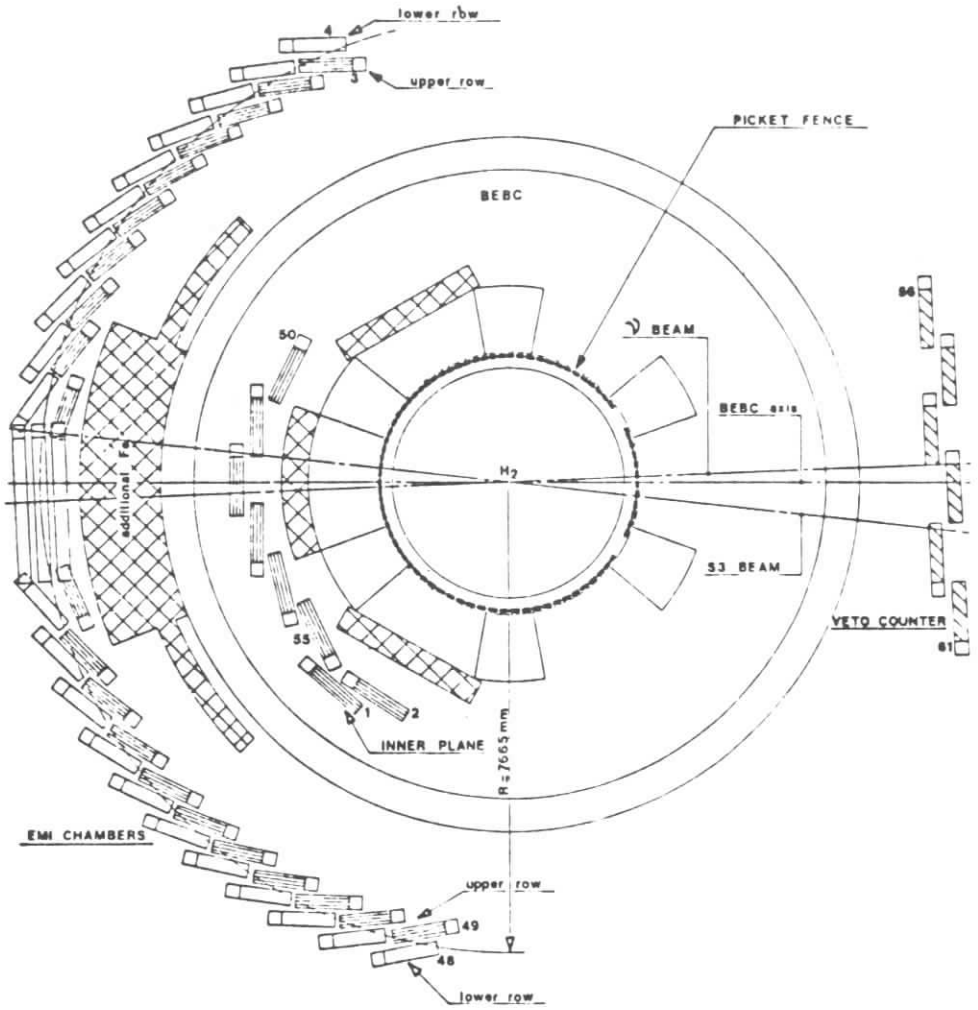

Fig. 21: Top view of the bubble chamber BEBC in its hybridized version with veto plane, picket fence and 2-plane muon identifier. The neutrino beam enters from right[47].

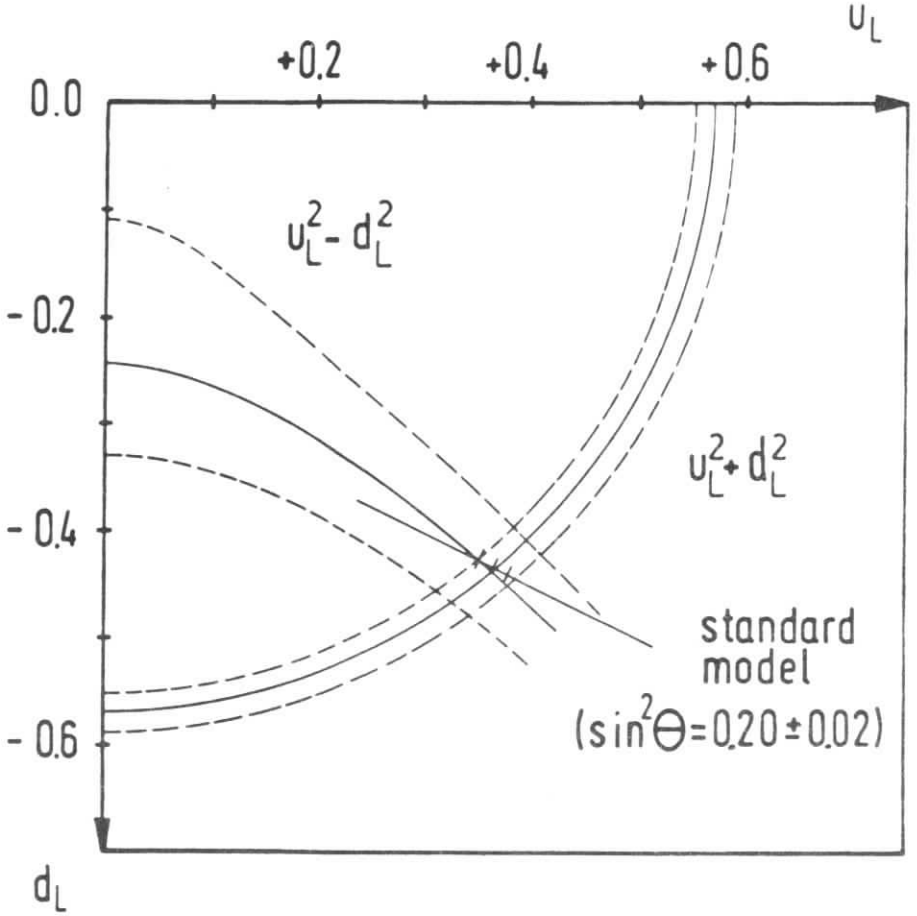

Fig. 22: Constraints of the BEBC ν, $\bar{\nu}$ D_2 measurements on the lefthanded couplings and comparison with Standard Model.

b) Use all data: 2 parameters are fitted

$$\sin^2\theta = 0.234 \pm 0.013 \qquad \rho = 1.002 \pm 0.015$$

c) Use all data: 1 parameter is fitted

$$\sin^2\theta = 0.233 \pm 0.009 \qquad \chi^2/\text{d.o.f.} = 33.1/45$$

It was an important achievement that already after 5 years of research, mainly in neutrino-nucleon scattering, the host of models describing weak neutral currents basically reduced to what is called today the Standard Model. The chiral couplings of the light quarks u and d could be uniquely determined from the data. In the Standard Model these 4 couplings are expressed in terms of only one parameter, namely $\sin^2\theta$, and precisely this fact is borne out by the data, although still with sizeable uncertainty in the righthanded sector (d_R). The measurements of $u_R^2 + d_R^2$ gave a value significantly different from 0 and demonstrated that the weak neutral gauge bosons couple also to righthanded quarks.

An unsatisfactory feature in the determination of the chiral couplings consisted in the fact that many experimental results with rather different systematic errors got combined. Furthermore, the interpretation of inclusive pion production data required a distinction of pions associated to current fragments from pions associated to target fragments which is not trivial at low energies. Also the single pion data, for example $\nu n \rightarrow \nu n\pi^0$ or $\nu p \rightarrow \nu n\pi^+$, can only be interpreted within models describing weak isobar production[49]. In a recent bubble chamber experiment in BEBC[50] the double rôle of deuterium, being an isoscalar target and providing quasi-free proton and neutron targets, was successfully used to get a simultaneous measurement of 4 neutral to charged current ratios (cuts: $E_H > 5$ GeV, $P_T^H > 1.5$ GeV/c):

$$R_{\nu p} = \frac{\sigma(\nu p \rightarrow \nu x)}{\sigma(\nu p \rightarrow \mu^- x)} = 0.49 \pm 0.05$$

$$R_{\nu n} = \frac{\sigma(\nu n \rightarrow \nu x)}{\sigma(\nu n \rightarrow \mu^- x)} = 0.25 \pm 0.02$$

$$R_{\bar{\nu}p} = \frac{\sigma(\bar{\nu}p \to \nu x)}{\sigma(\bar{\nu}p \to \mu^+ x)} = 0.26 \pm 0.04$$

$$R_{\bar{\nu}n} = \frac{\sigma(\bar{\nu}n \to \nu x)}{\sigma(\bar{\nu}n \to \mu^+ x)} = 0.57 \pm 0.09 \quad \text{(first measurement)}$$

Each ratio involves a different combination of the 4 chiral couplings squared. In valence quark approximation the first 2 ratios would be:

$$R_{\nu p} = (2u_L^2 + d_L^2) + \frac{1}{3}(2u_R^2 + d_R^2)$$

$$R_{\nu n} = (u_L^2 + 2d_L^2) + \frac{1}{3}(u_R^2 + 2d_R^2)$$

It was thus possible to obtain from the 4 ratios all 4 chiral couplings:

$$u_L^2 = 0.133 \pm 0.026 \pm 0.015$$

$$d_L^2 = 0.192 \pm 0.026 \pm 0.015$$

$$u_R^2 = 0.020 \pm 0.019 \pm 0.004$$

$$d_R^2 = 0.002 \pm 0.019 \pm 0.004$$

If only $\sin^2\theta$ is fitted to the data a 10% measurement results:

$$\sin^2\theta = 0.20 \pm 0.02.$$

The prediction of the Standard Model is illustrated in fig. 22 for the lefthanded sector. A significant test of the righthanded sector is limited by the precision in the $\bar{\nu}$-data.
Recent ν and $\bar{\nu}$ experiments using isoscalar targets have provided accurate measurements of

$$R_\nu = \frac{\sigma(\nu N \to \nu x)}{\sigma(\nu N \to \mu^- x)} = (u_L^2 + d_L^2) + \frac{1}{3}(u_R^2 + d_R^2)$$

$$R_{\bar{\nu}} = \frac{\sigma(\bar{\nu}N \to \bar{\nu}x)}{\sigma(\bar{\nu}N \to \mu^+ x)} = (u_L^2 + d_L^2) + 3(u_R^2 + d_R^2)$$

The actual evaluation of these ratios is quite complicated by the nucleon structure. For instance, the contributions of charged and neutral current interactions with sea quarks have to be evaluated; then, in the case of flavor changing transitions quark masses and the KOBAYASHI-MASKAWA matrix elements have to be taken into account. Finally, quarks are not really free. This illustrates, that although a ratio is measured its interpretation in terms of $u_L^2 + d_L^2$, $u_R^2 + d_R^2$ or in terms of ρ and $\sin^2\theta$ will necessarily be affected by small systematic uncertainties. The present status is shown in fig. 23[51] and fig. 24[52]. It is interesting to note that the ρ-parameter is measured with an accuracy of $\pm$ 0.02 and agrees with 1, as ecpected if the HIGGS representation is a doublet (assumed in the Standard Model). There are now three determinations of $\sin^2\theta$ which have each an accuracy comparable to the previous average of all experiments in KIM et al. (1981). It is appropriate to apply 1-loop corrections to R_ν and $R_{\bar{\nu}}$ to obtain the renormalized value of $\sin^2\theta$. The uncorrected value is then lowered by typically 5%[53]. All recent data on isoscalar, when combined, give[54]

$$\sin^2\theta^{corr} = 0.223 \pm 0.007.$$

Not all data are published yet.
A careful study of the systematic limitation in determining $\sin^2\theta$ from $R_\nu = \frac{\sigma(\nu N \to \nu N)}{\sigma(\nu N \to \mu^- N)}$ has been carried out in the context of the SPS fixed target workshop 1981 [11] and is believed to be $\Delta\sin^2\theta < 0.005$. The ratio $R_{\bar{\nu}}$ is not suited, since for values of $\sin^2\theta \approx 0.22$ $\Delta R_{\bar{\nu}} \approx 0$ $\Delta\sin^2\theta$. Both the CHARM and the CDHS collaborations have investigated the possibility to decrease the experimental uncertainties to match the above limit and came to an affirmative conclusion[55,56]. The importance to really reach the accuracy in $\sin^2\theta$ of 0.005 has already been discussed in the second lecture.

Once accurate measurements of the squares of the weak neutral current couplings (for the light flavors) exist, the sign ambiguities can be removed even with experiments of minor precision. For instance, the observation (fig. 25) of a prominent Δ^+ (1236) resonance in $\nu p \to \nu p\pi^0$ in the GARGAMELLE propane experiments allows to conclude:

$$u_L d_L = \frac{1}{16}(-(\alpha+\beta)^2 + (\gamma+\delta)^2) < 0$$

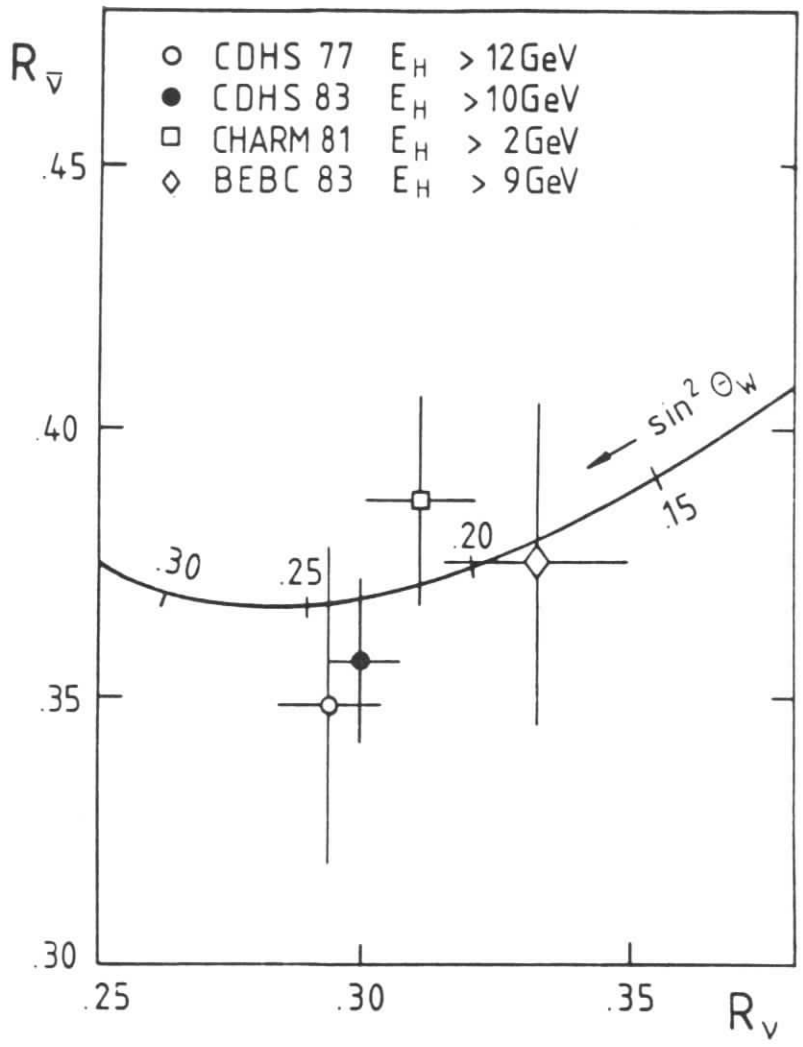

Fig. 23: Comparison of R_ν and $R_{\bar{\nu}}$ with the prediction of the Standard Model. The CDHS data in this plot are preliminary[51]. In the meantime the final numbers are available[54] ($R_{\bar{\nu}}$ increased from 0.357 ± 0.015 to 0.363 ± 0.015).

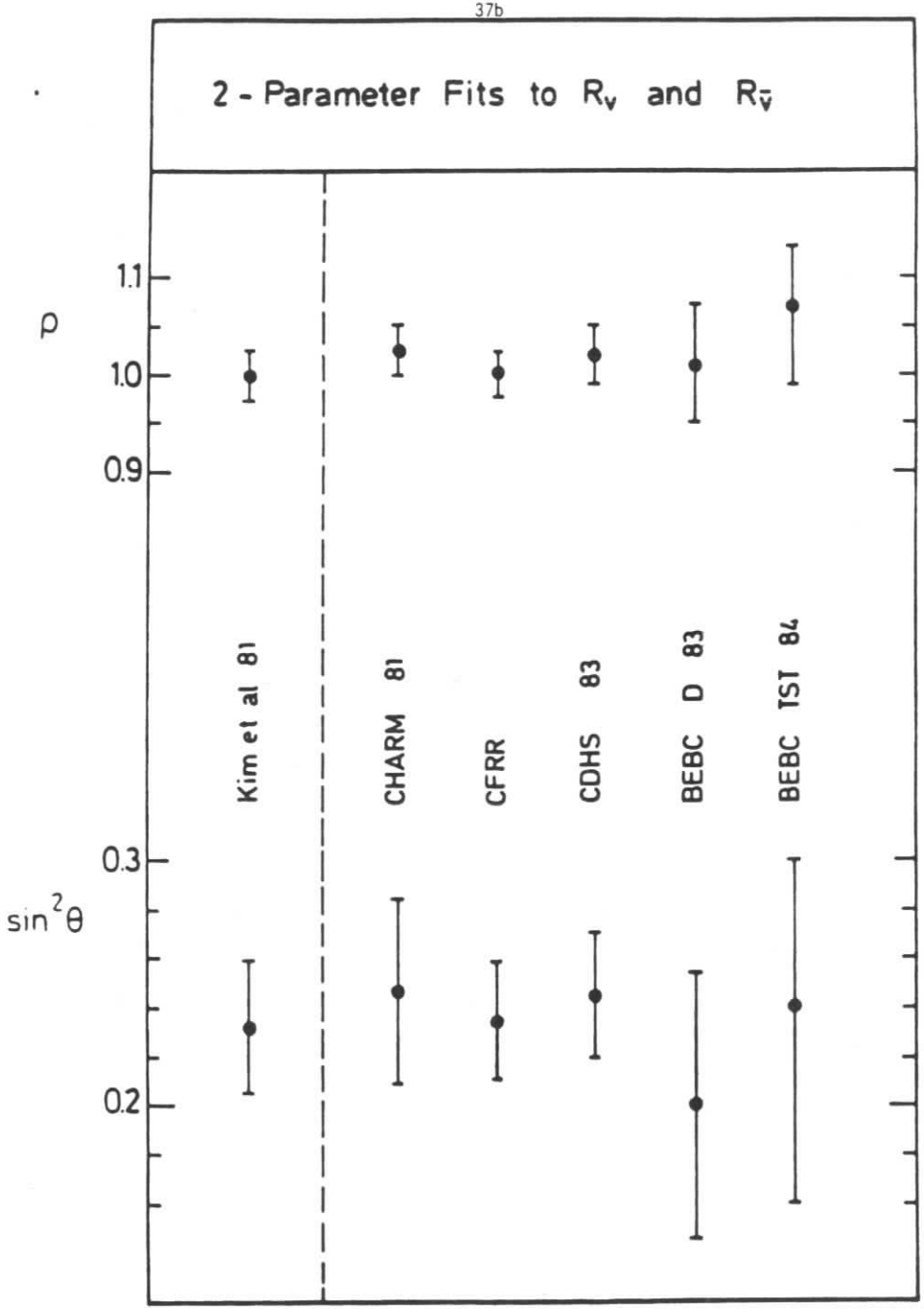

Fig. 24: Comparison of simultaneous ρ and $\sin^2\theta$ fits from recent experiments. The final point, indicated KIM et al.[48], is the combined fit of all data up to 1979.

Fig. 25: Observation of the Δ^0 (1236) resonance induced by weak neutral currents (ref. 57). For comparison the exclusive $p\pi^0$ state in charged current events.

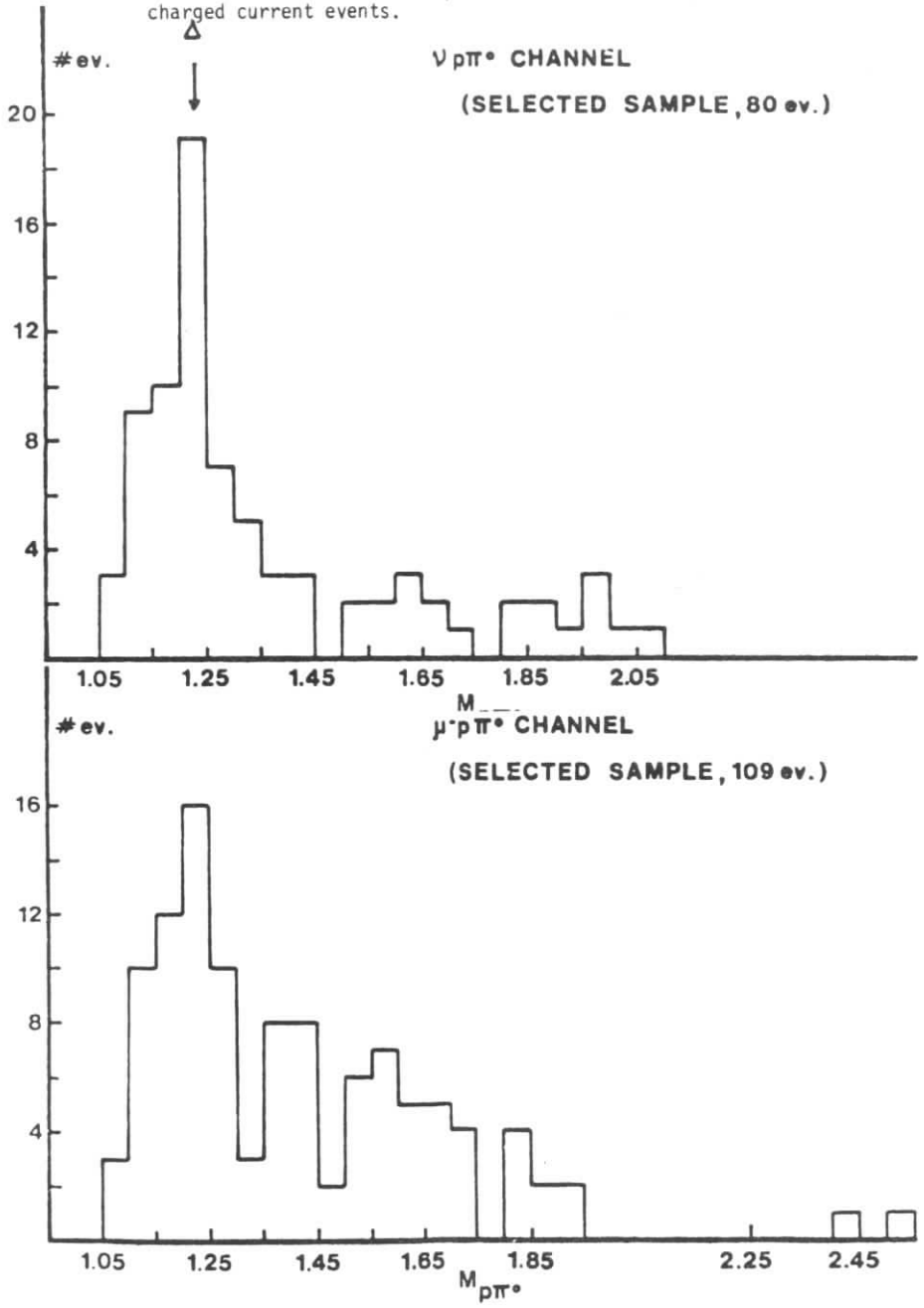

since the isovector term dominates the isoscalar term. The other ambibuity is solved by a form factor analysis of the elastic scattering experiments $\nu p \to \nu p$ and $\bar{\nu} p \to \bar{\nu} p$[58] yielding $u_L u_R < 0$.
The recent observation of coherent π^0 production in neutrino nucleus scattering provides a direct test of the axial vector coupling[59]

$$|\beta| = 0.93 \pm 0.12$$

where 1 is predicted by the Standard Model.

3. ELECTROWEAK RESULTS FROM e^+e^- EXPERIMENTS

The processes to be considered here are $e^+e^- \to$ hadrons. The final state is dominated by a forward and a backward jet at PETRA and PEP energies. These jets are induced by u, d, s, c, b - quarks (resp. antiquarks) in the relative proportion 4 : 1 : 1 : 4 : 1. The interference between the electromagnetic (γ) and the weak (Z^0) amplitude leads to observable effects in the hadron production rate and the quark angular asymmetries.
The first quantity is defined

$$R = \frac{\sum_q \sigma(e^+e^- \to q\bar{q})}{\sigma(e^+e^- \to \mu^+\mu^-)^{QED}}$$

$$= 3 \sum_q \{Q_q^2 - 2Q_q \chi v_e v_q + 0(\chi^2)\} (1 + \delta_{QCD})$$

with χ, defined in lecture 2, of order 10% at PETRA/PEP energies. The electroweak contribution is proportional to

$$v_e(\tfrac{4}{3} v_u - v_d)$$

and therefore small, since $v_e \approx 0$ for $\sin^2\theta = 0.22$. The factorized form of the weak couplings reflects the assumption of just one massive neutral gauge boson. Results are given in table 7 and fig. 26.

Table 7 $\sin^2\theta$ from data on $e^+e^- \to$ hadrons (ref. 60)

EXPT	$\sin^2\theta$
JADE	0.23 ± 0.05
MARK J	$0.28 \,^{+\,0.08}_{-\,0.05}$
TASSO	$0.30 \,^{+\,0.23}_{-\,0.07}$

The other quantity, the angular asymmetry, measures at these energies only the product $a_e a_q$, provided the quark flavor q can be isolated:

$$A_q = -\,7.5\% \left(\frac{\sqrt{s}}{35\ \text{GeV}}\right)^2 \frac{g_A^e g_A^q}{Q_q}$$

Note that the fractional quark charge enhances the asymmetry. Two methods have been applied to isolate $e^+e^- \to c\bar{c}$ and $e^+e^- \to b\bar{b}$:

i) reconstruction of D^0 and $D^{*\pm}$ (fig. 40, 28)
ii) use of semileptonic c- and b-decays (fig. 40, 28)

Results from PETRA at $\sqrt{s}$ = 34.5 GeV from JADE, MARK J, TASSO and from PEP at $\sqrt{s}$ = 29 GeV from HRS, MARK II, MAC are summarized[61] in table ($g_A^e = -1$ is assumed):

MACHINE	g_A^c	g_A^b
PETRA	1.22 ± 0.40	-1.00 ± 0.30
PEP	2.40 ± 1.70	-1.10 ± 0.50

The axial couplings agree in magnitude and sign with the prediction of the standard model. The study of e^+e^--interactions gives access to the weak couplings of c and b quarks which are members of the 2nd and 3rd fermion generation.

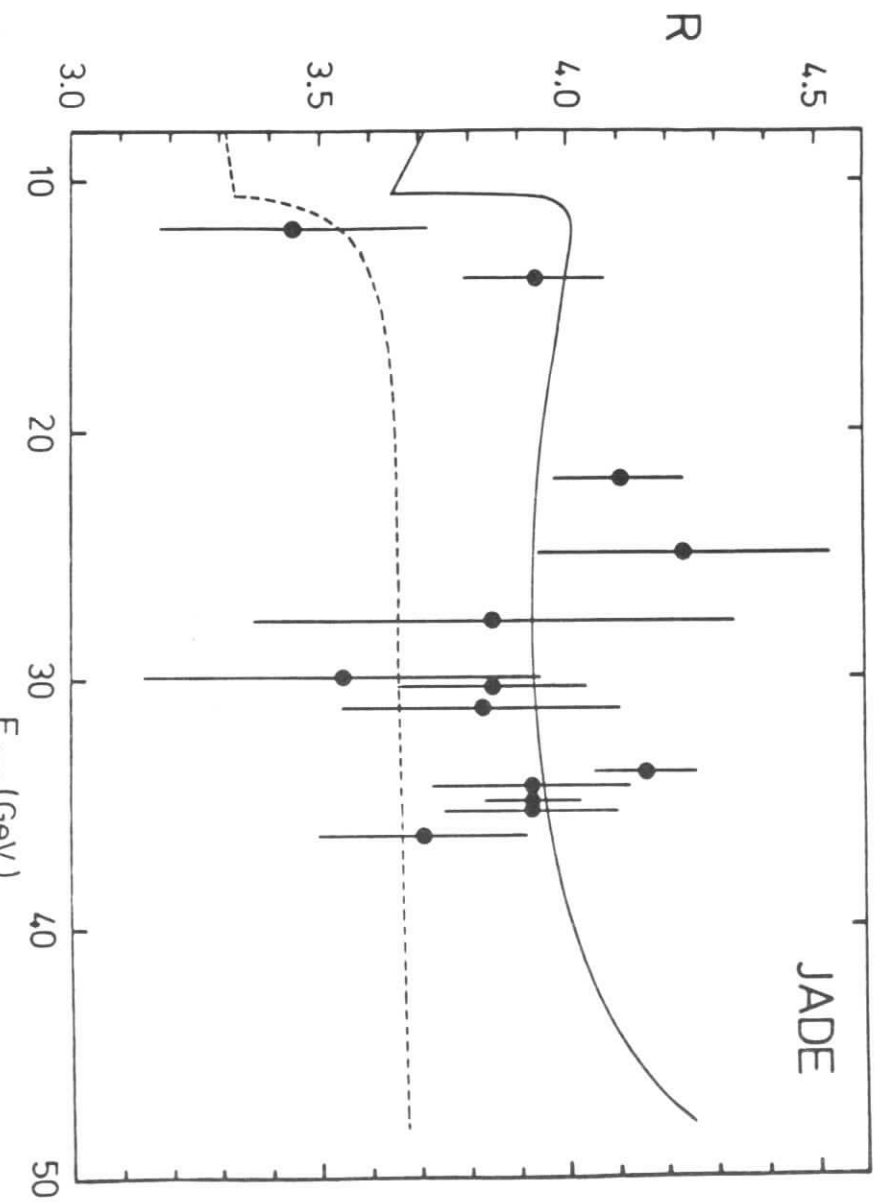

Fig. 26: The ratio R compared to predictions of Standard Model with $\sin^2\theta = 0.23$ and $\sin^2\theta = 0.20$. The dotted curve is the expectation of the naive quark-parton model.

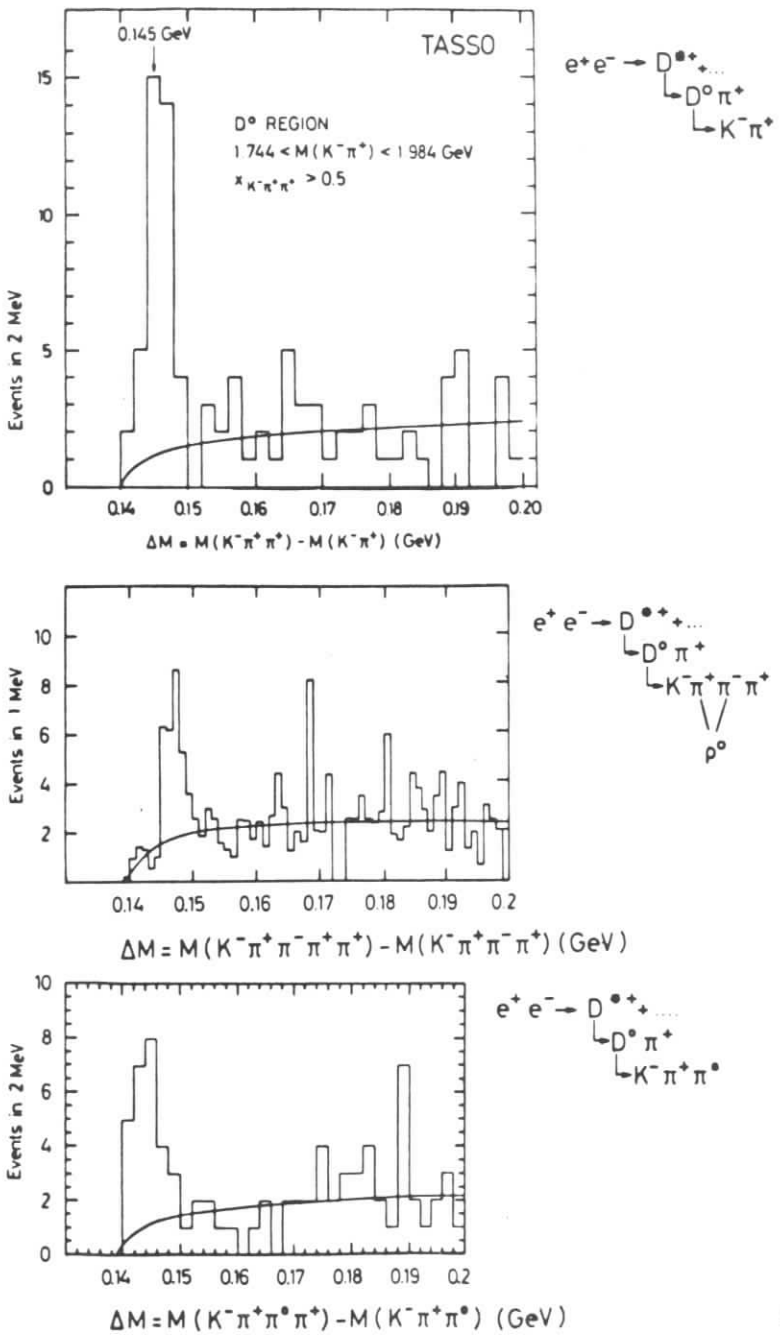

Fig. 27

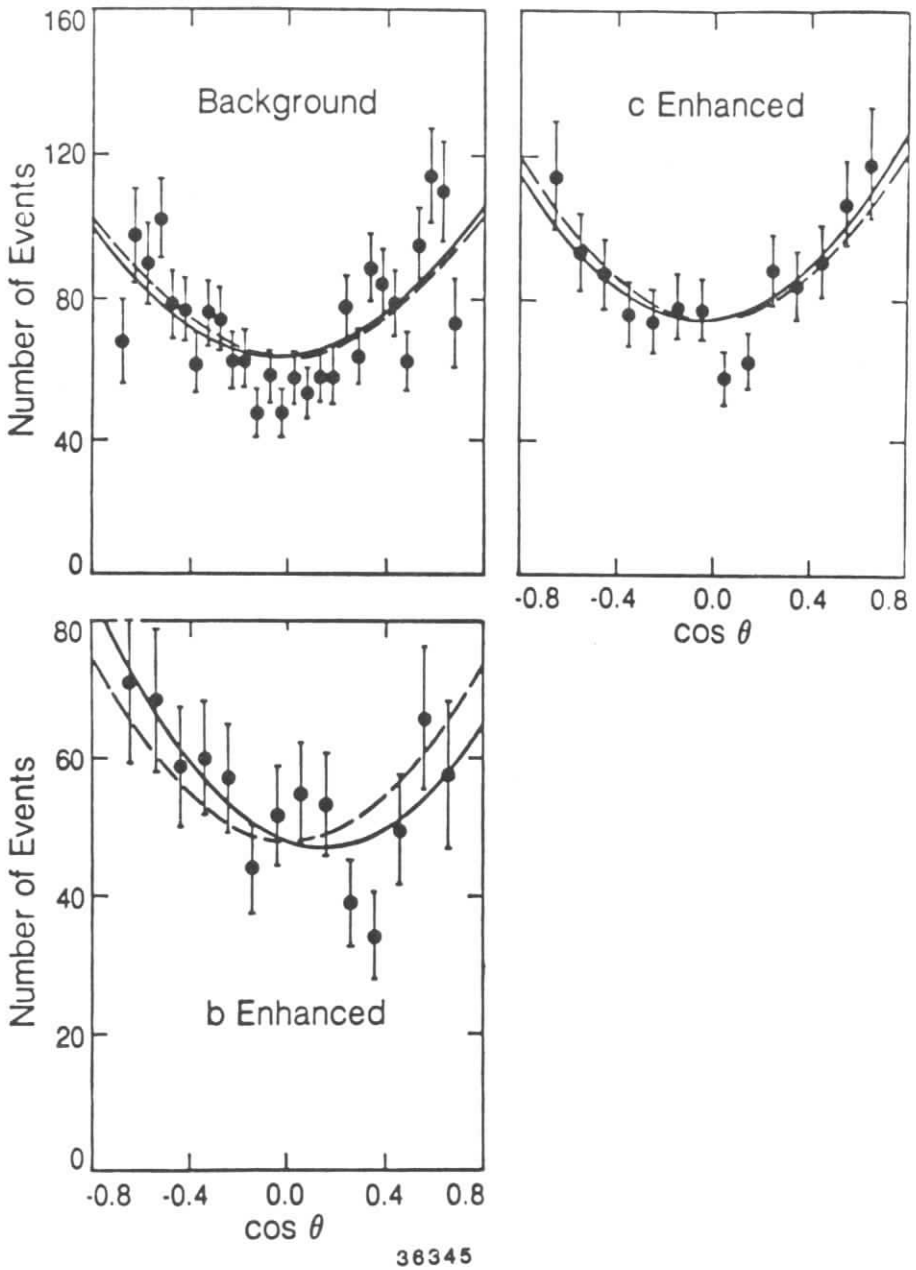

Fig. 28: Asymmetries in c- and b-enriched samples from various e^+e^- - experiments (ref. 61).

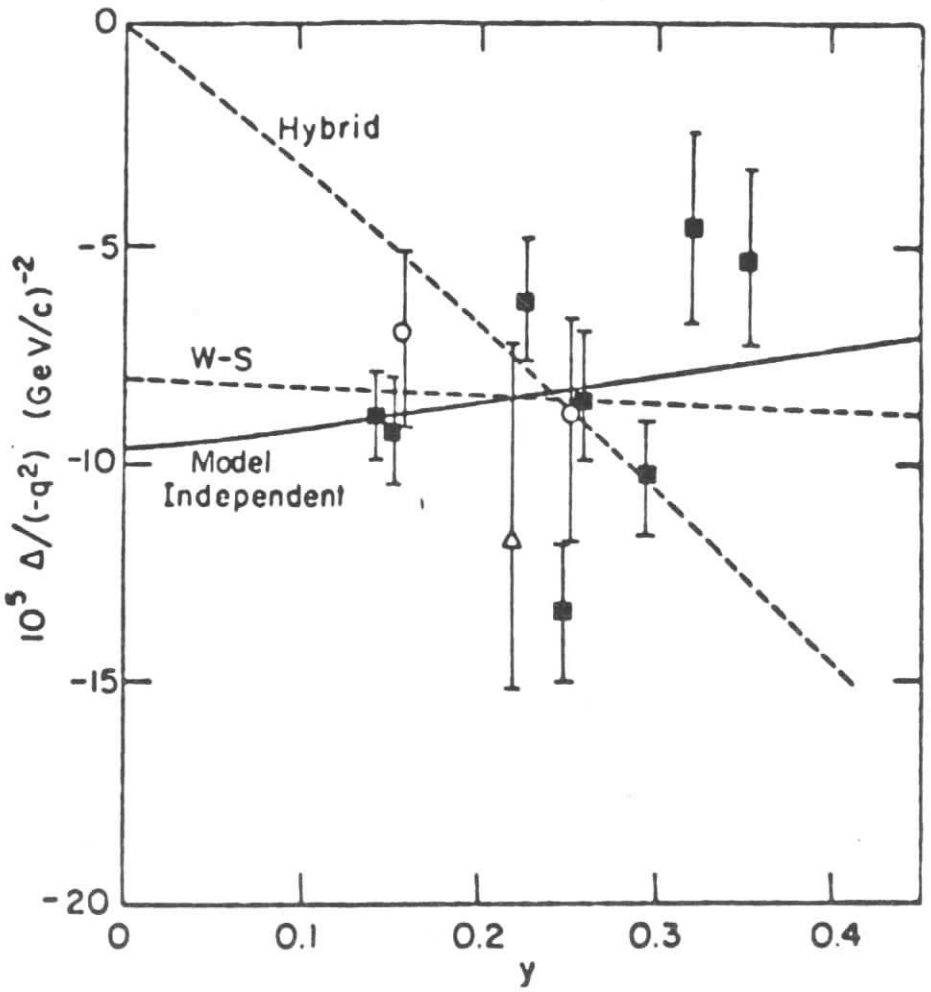

Fig. 29: Asymmetry vs y compared to the Standard Model and a hybrid model, where the righthanded electron is assumed to be a member of a weak doublet.

4. WEAK EFFECTS IN CHARGED LEPTON-NUCLEON SCATTERING

There are results from two experiments on electroweak asymmetries involving the product of charged lepton coupling and quark coupling. The effect is of the order

$$\frac{G}{e^2}\,Q^2 \approx 10^{-4}\,\frac{Q^2}{GeV^2}$$

and requires a good control of systematic errors.

a) The SLAC experiment[62]: polarized $e^- + D \to e^- +$ anything.
A fairly detailed description of this classic experiment is given in the 1981 CERN summer school lectures[4b]. The quantity measured is the parity violating asymmetry

$$A = \frac{d\sigma(e_R)-d\sigma(e_L)}{d\sigma(e_R)+d\sigma(e_L)} = \frac{G\rho Q^2}{\sqrt{2}\,e^2}\,\frac{18}{5}\left\{a_1 + a_2 f(y)\,\frac{q(x)-\bar{q}(x)}{q(x)+\bar{q}(x)}\right\}$$

≈ 1 for $x > 0.2$

$$\frac{A}{Q^2} = -(0.57 \pm 0.27)\,10^{-4}\ GeV^{-2}$$

$$a_1 = 0.30 \pm 0.08 = \frac{2}{3}\,a_e\,(2v_u - v_d) = -\frac{1}{2}\left(1 - \frac{20}{9}\sin^2\theta\right)$$

$$a_2 = 0.15 \pm 0.25 = \frac{2}{3}\,v_e\,(2a_u - a_d) = -\frac{1}{2}\left(1 - 4\sin^2\theta\right)$$

Results from 2 parameter fit: $\rho = 1.74 \pm 0.36$ $\sin^2\theta = 0.25\ ^{+0.03}_{-0.10}$
and from 1 parameter fit ($\rho \equiv 1$): $\sin^2\theta = 0.224 \pm 0.020$.
The y-dependence (cf. fig. 29) is incompatible with the assumption, that the righthanded electron is a member of a weak doublet. This experiment with its precise determination of $\sin^2\theta$ supported strongly the Standard Model. At that time there was no other individual experiment with such a precision.

b) The NA4 Experiment[63]: $\mu^{\pm}$ C $\rightarrow \mu^{\pm}$ + anything.

The naturally polarized μ beam from the CERN-SPS is scattered off carbon. The asymmetry

$$B = \frac{d\sigma(\mu_R^+) - d\sigma(\mu_L^-)}{d\sigma(\mu_R^+) + d\sigma(\mu_L^-)} = -\frac{G\rho Q^2}{\sqrt{2}e^2}\ \frac{18}{5}\ f(y)\ \frac{q(x) - \bar{q}(x)}{q(x) + \bar{q}(x)}\ (b_1|\lambda| + b_2)$$

is measured using data at 200 GeV and 120 GeV. The μ-helicity is denoted by λ. The measurement of B leads to

$$b_1|\lambda| + b_2 = \frac{2}{3}(v_\mu|\lambda| - a_\mu)\ (2a_u - a_d) = 0.45 \pm 0.11\ ^{+0.05}_{-0.07}$$

and from this $\sin^2\theta = 0.23 \pm 0.07 \pm 0.04$. Assuming $\sin^2\theta = 0.23$ the weak isospin of the righthanded muon comes out to be $I_3^R(\mu) = 0.00 \pm 0.06 \pm 0.04$ in agreement with the standard assignment of righthanded muons in SU(2)-singlets.

If $2a_u - a_d = \frac{3}{2}$ is assumed, then one gets

$v_e = 0.15 \pm 0.25$ from the SLAC-MIT experiment

$v_\mu = -0.06 \pm 0.14$ from the NA4 experiment

This can be compared with the combined results from ν_μe-experiments giving $v_e = 0.002 \pm 0.058$ (cf. lecture 2).

5. PARITY VIOLATION IN CAESIUM

Significant parity violating effects have been observed in bismuth, lead, thallium and caesium[64]. The recently published results of the experiment of M.A. BOUCHIAT et al.[65] will be mentioned in this section. A circularly polarized laser beam (direction $\vec{k}$) is used to excite the Cs 6S F = 3 state to 7S F = 4 in a constant STARK field with $\vec{E}$ perpendicular to $\vec{k}$. The effective dipole operator is given by

$$\vec{d} = -\alpha\vec{E} - i\beta\vec{\sigma}\times\vec{E} + M_1\vec{\sigma}\times\vec{k} - i\ \mathrm{Im}\ E_1\ \vec{\sigma}$$

where the first 2 terms are STARK induced, the third term is due to the magnetic dipole and the last term is the weak neutral current induced electric dipole. One looks for an interference between the E_1 and β-term. Two measurements were carried out:

$$\mathrm{Im}E_1/\beta = -(1.78 \pm 0.26 \pm 0.12)\ \mathrm{mV/cm} \qquad \Delta F = 1$$
$$-(1.34 \pm 0.22 \pm 0.11)\ \mathrm{mV/cm} \qquad \Delta F = 0$$

It follows:

$$Q_W^{exp} = -66.5 \pm 7.2 \pm 5.1 = -0.574\ (N - (1-4\sin^2\theta)Z)$$

thus $\sin^2\theta^{corr} = 0.205 \pm 0.034 \pm 0.024$ in good agreement with other measurements (cf. fig. 30).

CONCLUSIONS

1. In the first decade after the discovery of weak neutral currents the electro-weak parameter $\sin^2\theta$ has been measured over a big range of space- and timelike-momentum transfers squared. This is illustrated in fig. 30. All determinations are compatible with each other. The data from the neutrino-quark sector are the most precise measurements.

2. On the basis of α, G, $\sin^2\theta^{\nu q}$ the masses of the weak gauge bosons can be predicted within the Standard Model:

$$m_W = \frac{37.2810 \pm 0.0003}{\sqrt{1-0.0696 \pm 0.002}\ \sin\theta}\ \mathrm{GeV} \quad \text{and} \quad m_Z = \frac{m_W}{\cos\theta}$$

Using the corrected value from KIM et al (1981) the masses can be calculated (including 1-loop corrections):

$$m_W = 83.0\ ^{+2.9}_{-2.7}\ \mathrm{GeV}$$

$$m_Z = 93.8\ ^{+2.4}_{-2.2}\ \mathrm{GeV}$$

These values anticipated on the basis of the Standard Model have been measured 1983 by the UA-experiments at the CERN $\bar{S}pS$ collider and are

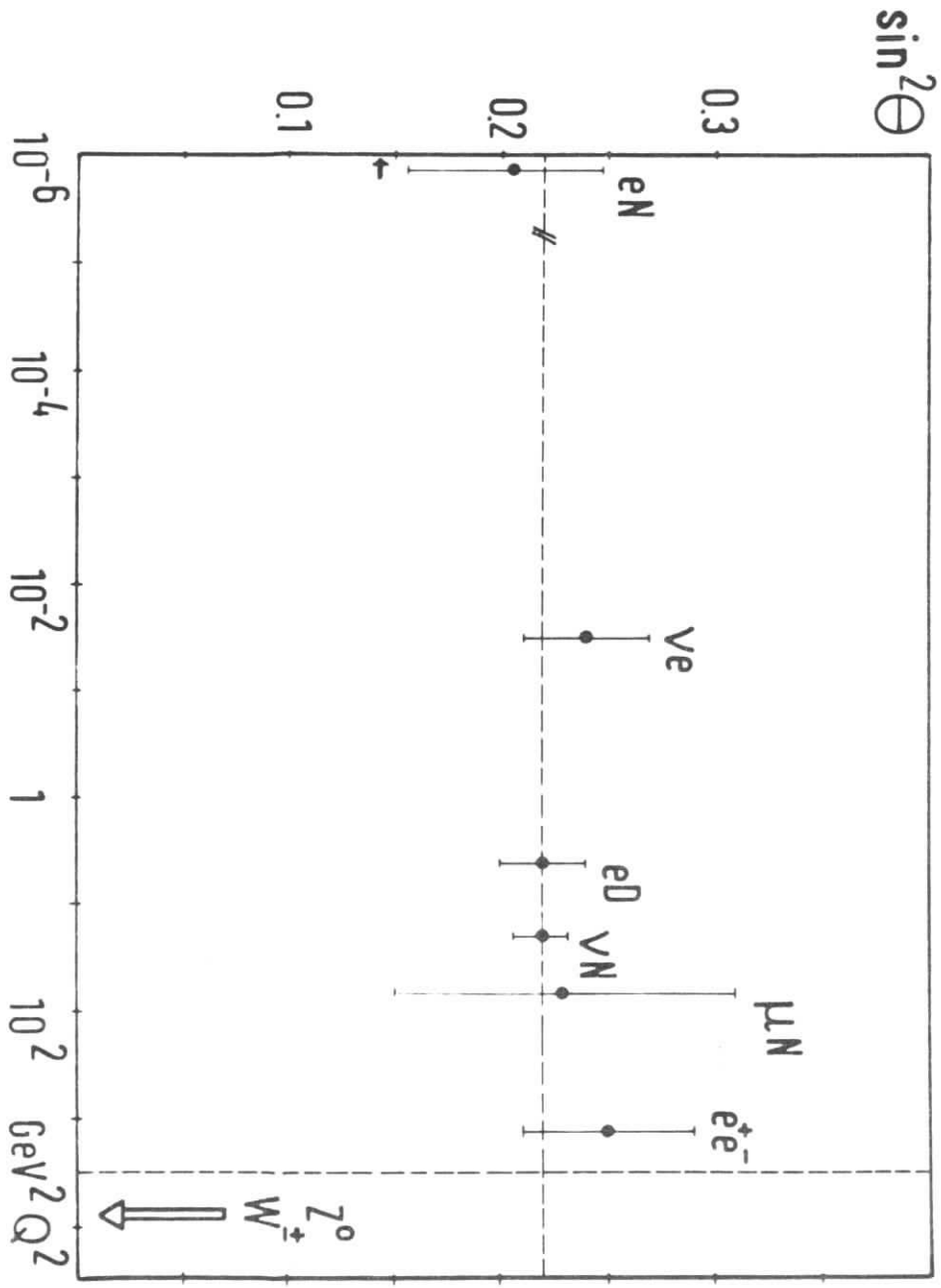

Fig. 30: Comparison of measurements of $\sin^2\theta$ in various types of low energy experiments.

(average over values from UA1 and UA2):

$$m_W = 82.2 \pm 1.8 \text{ GeV}$$

$$m_Z = 93.2 \pm 1.5 \text{ GeV}$$

in good agreement with the predicted masses within the Standard Model.
This is a great success.
Sofar, all tests described refer to leading order only. The next step will be tests sensitive to 1-loop corrections which are in progress.

Lecture 4: SEMILEPTONIC CHARGED CURRENT INTERACTIONS
(Selected Topics)

1. The naive quark-parton model
2. The strange sea in the nucleon
3. Limits on right-handed currents
4. ν_e-interactions
5. The KOBAYASHI-MASKAWA matrix
6. Determination of the B-lifetime
7. Search for top quarks
8. B-decays

1. THE NAIVE QUARK-PARTON MODEL

The deep inelastic scattering experiments $eN \to e$ + anything at SLAC and later on $\nu N \to \mu^-$ + anything, $\bar{\nu}N \to \mu^+$ + anything, $\mu N \to \mu$ + anything have led to a simple picture of the nucleon. At sufficiently high $Q^2 = -q^2$ (the 4-momentum transfer squared) the intermediate vector bosons interact incoherently with quasifree, pointlike partons identified with quarks and antiquarks. Since the scattering process is purely spacelike a frame can be found in which the gauge boson carries only 3-momentum, i.e. no energy. This particularly simple frame is called the BREIT frame:

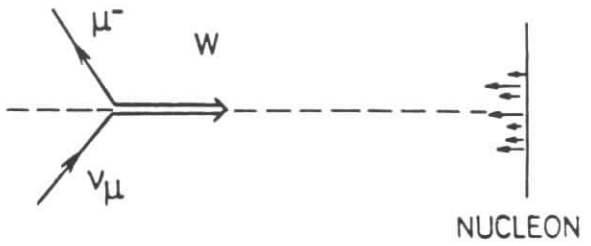

The W interacts either with a lefthanded quark-parton or a righthanded antiquark-parton according to the V-A structure of charged weak currents. Angular momentum conservation implies a helicity -1 W to couple to a quark and a helicity +1 W to an antiquark. This determines the angular distribution: an isotropic contribution (from W^+q)

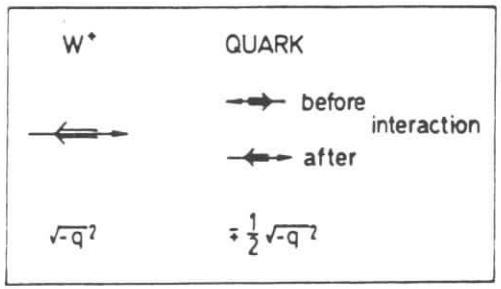

and a contribution $\sim(1-\cos\theta^*)=(1-y)^2$ from $W^+\bar{q}$, where 1-y is the muon energy in units of the energy of the incoming neutrino. In the approximation of

spin 1/2 quark-partons with zero intrinsic transverse momentum a helicity 0 W has nothing to couple to, therefore the angular distribution has no term $(1-y)^1$. It is now trivial to write down the differential cross section of deep inelastic νp-scattering:

$$d^2\sigma(\nu p) = \sum_f P_f(x)dx \cdot d\sigma(\nu f)$$

$$= \frac{G^2}{\pi} 2ME_\nu \left[x\, P_d(x)\, 1 + x\, P_{\bar{u}}(x)\, (1-y)^2 \right] dxdy$$

where $x = \frac{1}{2} \frac{\sqrt{-q^2}}{p}$ is the fractional momentum of the parton in the proton, $P_f(x)$ is the probability density to find a quark-parton with flavor f in the proton and $d\sigma(\nu f)$ the elastic cross section of the subprocess. In the above formula only the flavors of the first generation are taken into account. The νp cross section depends only on the scaling variables x and y. This is called BJORKEN scaling. Precise measurements have shown that scaling is not strictly fulfilled (see lecture 5), but for many applications a quite good approximation.
Due to the V-A structure neutrino and antineutrino experiments have the unique feature of differentiating between quarks and antiquarks in the nucleon and thus between valence and sea quarks. For instance, a proton is composed of $(uud)^{valence}$ and $(u\bar{u} + d\bar{d} + s\bar{s} + \ldots)^{sea}$. This implies sumrules for the quark-parton densities $P_f(x)$:

$$\int_0^1 dx\, (P_u(x) - P_{\bar{u}}(x)) = 2$$

$$\int_0^1 dx\, (P_d(x) - P_{\bar{d}}(x)) = 1$$

$$\int_0^1 dx\, (P_f(x) - P_{\bar{f}}(x)) = 0 \qquad \text{for } f = s, c, b, t$$

In fig. 31 recent measurements of the fractional momentum distributions by the CDHS group[66] are shown. Note the substantial rise of the strange sea. There is no direct evidence of the charmed sea yet.
The comparison of charged lepton nucleon (coupling Q_f^2) with neutrino - nucleon scattering (V-A coupling) shows that quarks are fractionally charged (fig. 35).

2. THE STRANGE SEA IN THE NUCLEON

Forgetting about the quarks in the third generation there are 4 charm changing charged current interactions:

$$\nu d \to \mu^- c \qquad \text{rate} \sim |U_{cd}|^2$$

$$\nu s \to \mu^- c \qquad \sim |U_{cs}|^2$$

$$\bar{\nu} \bar{s} \to \mu^+ \bar{c} \qquad \sim |U_{cs}|^2$$

$$\bar{\nu} \bar{d} \to \mu^+ \bar{c} \qquad \sim |U_{cd}|^2$$

Only the first reaction takes place on a valence quark, but is suppressed by the mixing matrix element squared: $|U_{cd}|^2 \approx \sin^2\theta_c$ (θ_c = CABIBBO angle) ≈ 0.05. Reaction 4 is negligible compared to reaction 3. Reactions 1, 2, 3 are of similar strength. All subprocesses are flat in y and are sizeable, where the quark momentum distributions (xd(x), xs(x), $x\bar{s}(x)$) are sizeable, i.e. for small values of x. In a recent analysis the CDHS group[67a] has detected the final state charmed quark by its semileptonic decay:

$$c \to \mu^+ \nu_\mu + \text{anything}$$

$$\bar{c} \to \mu^- \bar{\nu}_\mu + \text{anything}$$

Therefore, the opposite sign dimuon events in the $\bar{\nu}$ - run allow to extract the strange sea ($x\bar{s}(x)$). The result is shown in fig. 32 and compared to the shape of the distribution $x\bar{u}(x) + \bar{x}\bar{d}(x) + 2x\bar{s}(x)$ as measured directly in normal $\bar{\nu}$ interactions. There is a slight dependence on how the charm threshold is treated. The strange sea and the nonstrange sea have the same form. The neutrino dimuon data get two contributions, one from the valence

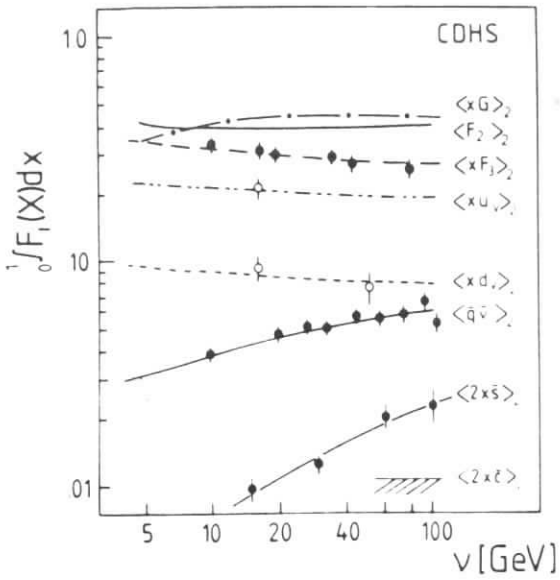

Fig. 31:
Flavor composition
of the nucleon

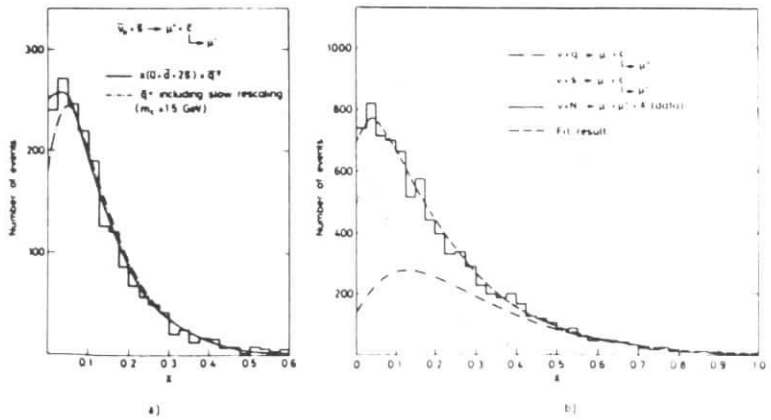

Fig. 32: The strange sea in the nucleon (ref. 67a)

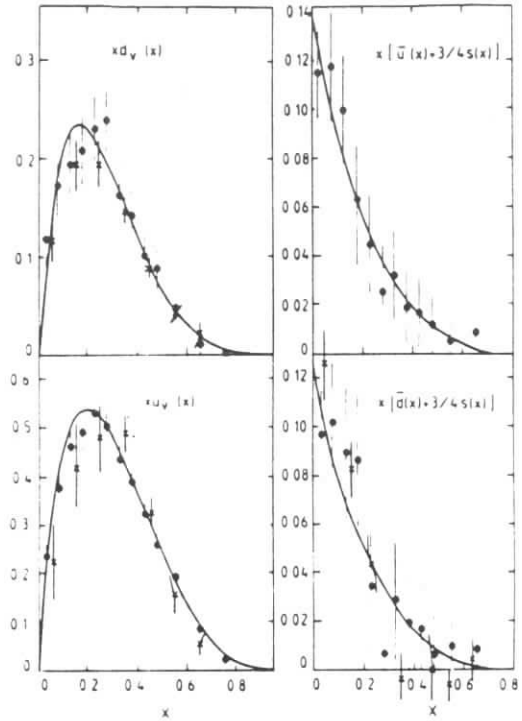

Fig. 33: The nonstrange quark distributions (ref. 67b)

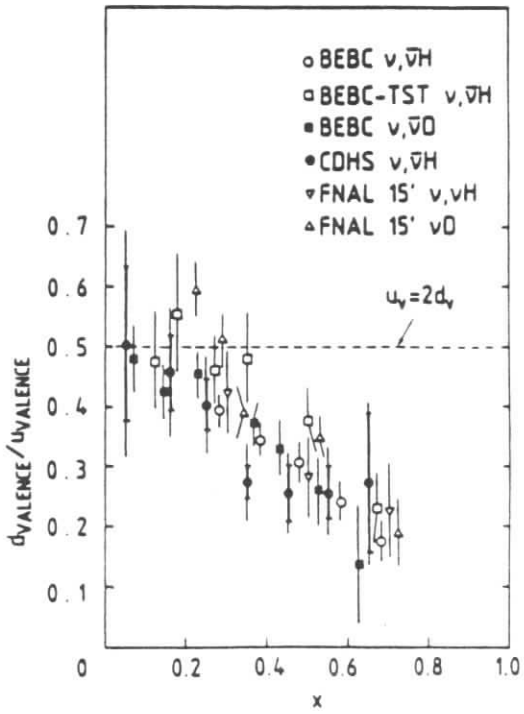

Fig. 34: The d/u ratio (ref. 68)

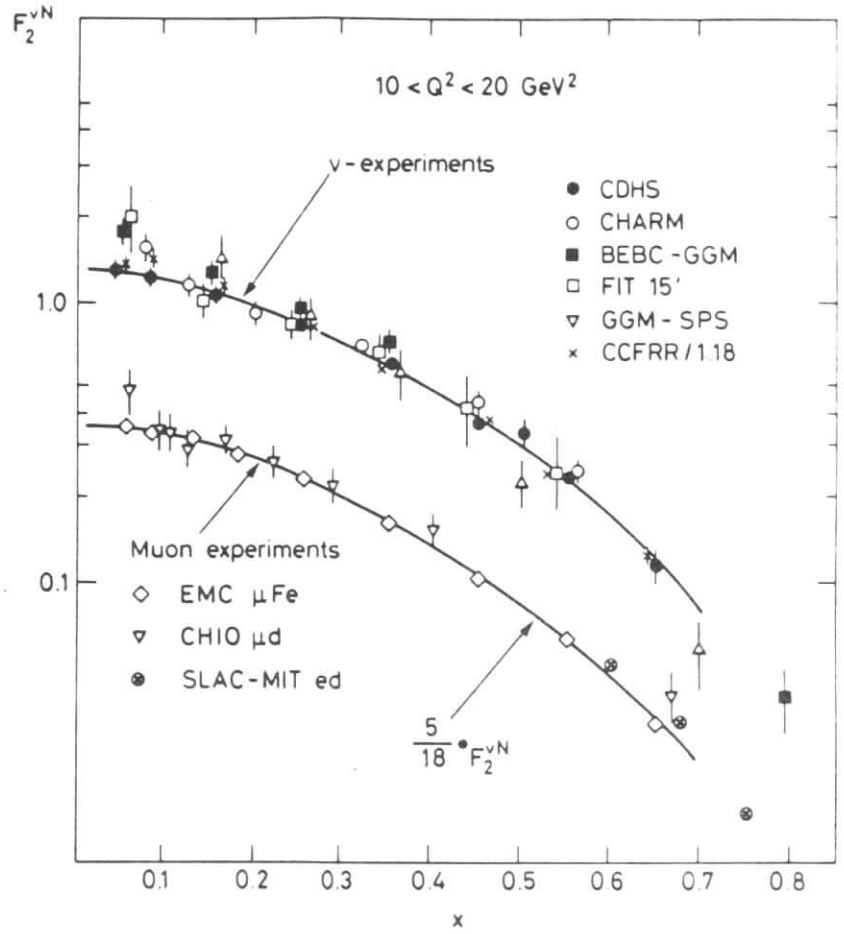

Fig. 35: Comparison of ν and μ deep inelastic experiments (ref. 66)

quarks and one from the strange sea. A good fit is obtained (fig. 32). The dimuon data confirm the GIM construction[17], which is a special case of the KOBAYASHI-MASKAWA scheme. The matrix elements $|U_{cd}| = 0.24 \pm 0.03$ and $|U_{cs}| > 0.59$ (90% CL) have been derived from the dimuon data.
Early neutrino experiments[69] have given already indirect evidence of semileptonic charm decay in correlation with strange particle production. In the bubble chamber BEBC filled with hydrogen, i.e. free protons, some rare cases of fully reconstructable charmed particle decays did occur. Fig. 36 shows a famous event[70]. The 3 C-fit resulted in a very accurate mass measurement of D^0 and D^{*+}. It should be mentioned that there are ν, ν induced dimuon events where the two muons have the same charge. No satisfactory explanation of their anomalous rate has sofar been proposed[71].

3. LIMITS ON RIGHT-HANDED CURRENTS

The effective Lagrangian for the semileptonic charged current process $\nu_\mu d \to \mu^- u$ is

$$L_{eff}^{cc} = \frac{G}{\sqrt{2}} (\bar{\psi}_u \gamma_\lambda (1 + \gamma_5)\psi_d) (\bar{\psi}_\mu \gamma^\lambda (1+\gamma_5)\psi_{\nu_\mu})$$

and excludes by construction righthanded weak current. It is convenient to generalize this Lagrangian in the following way:

$$L_{eff}^{cc} = \frac{G}{\sqrt{2}} (\bar{\psi}_\mu \gamma_\lambda (1+\gamma_5)\psi_\nu) \left[\bar{\psi}_u \gamma_\lambda (C_L(1+\gamma_5) + C_R(1-\gamma_5))\psi_d\right]$$

and to test on $C_R \neq 0$ by comparison with the measured y-distributions at large x. The differential cross section is now modified:

$$\frac{1}{\sigma^o} \frac{d^2\sigma(\nu N)}{dxdy} = \left[q(x) + \left(\frac{C_R}{C_L}\right)^2 \bar{q}(x)\right] + (1-y)^2 \left[\bar{q}(x) + \left(\frac{C_R}{C_L}\right)^2 q(x)\right]$$

$$\equiv q_L(x) + (1-y)^2 q_R(x)$$

$$\frac{1}{\sigma^o} \frac{d^2\sigma(\bar{\nu}N)}{dxdy} = q_R(x) + (1-y)^2 q_L(x)$$

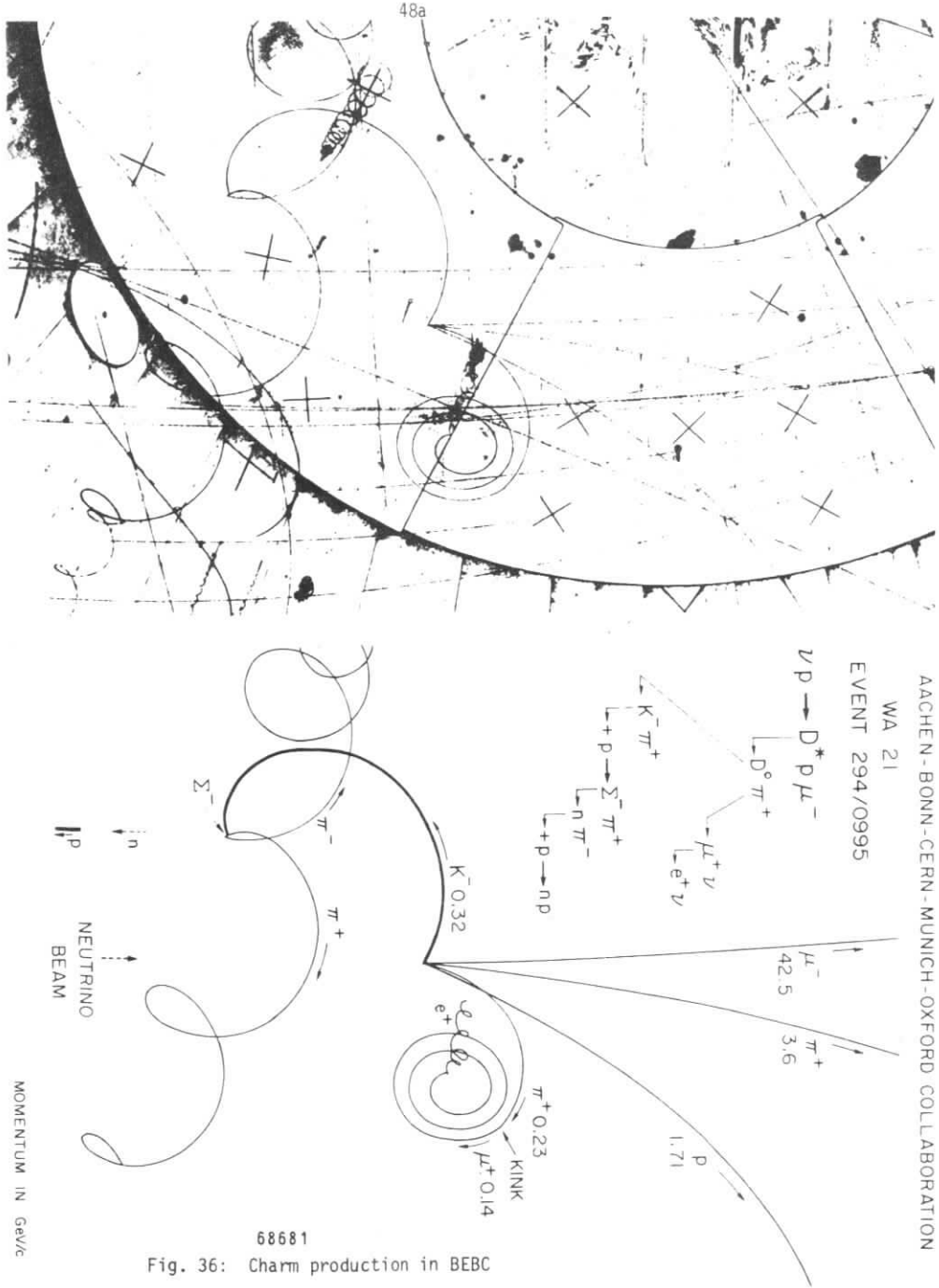

Fig. 36: Charm production in BEBC

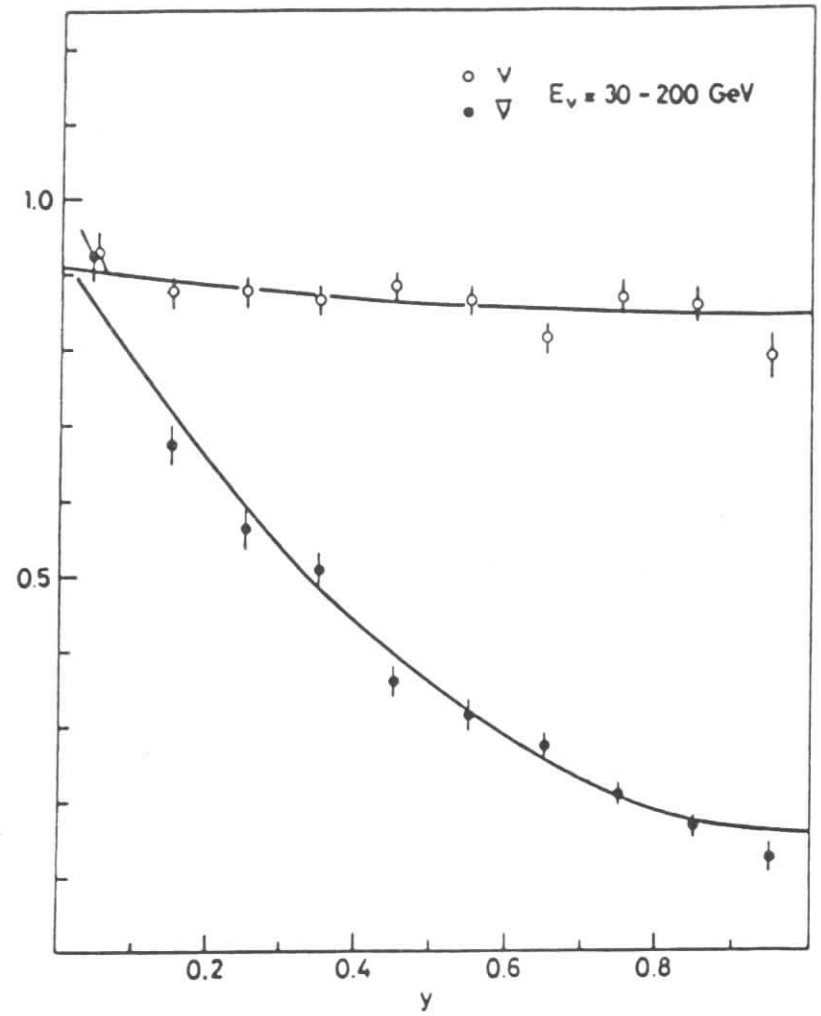

Fig. 37: y-distributions in ν- and $\bar{\nu}$-Fe charged current interactions (ref. 72)

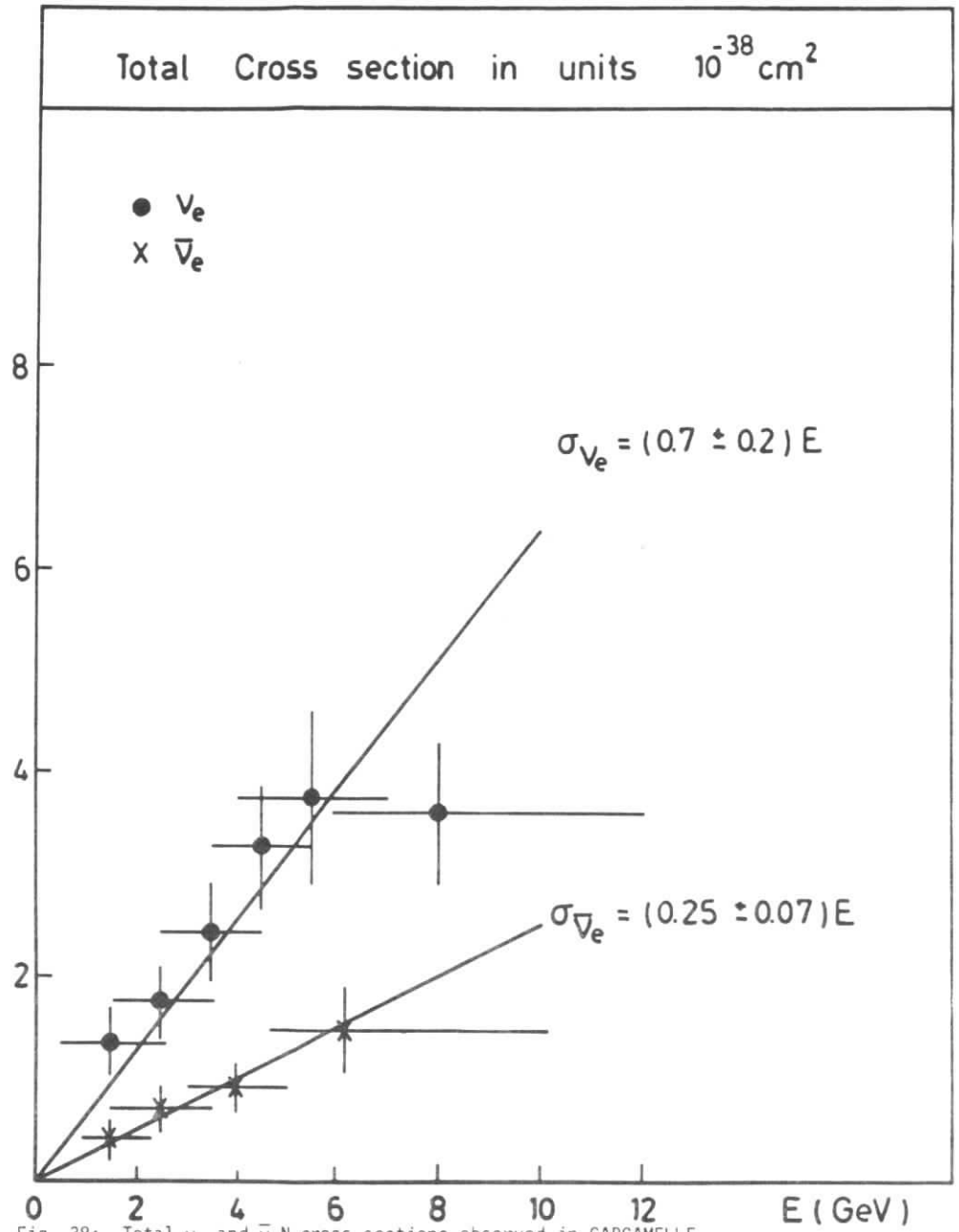

Fig. 38: Total ν_e and $\bar{\nu}_e$N cross sections observed in GARGAMELLE

where $q(x)$ and $\bar{q}(x)$ are the relevant quark and antiquark distributions. The ν and $\bar{\nu}$ induced differential cross sections are accurately measured (fig. 37), thus the CDHS Collaboration[72] could conclude

$$(\frac{C_R}{C_L})^2 < 0.005 \text{ at } 50\% \text{ CL.}$$

4. ν_e - INTERACTIONS

Neutrino beams at accelerators are derived from π- and K-decays and are therefore predominantly ν_μ or $\bar{\nu}_\mu$ beams depending on the selected parent charge. Nevertheless, these beams contain a contamination of ν_e and $\bar{\nu}_e$ at the 1% level and the GARGAMELLE experiments at the PS did collect quite a few ν_e, $\bar{\nu}_e$N interactions. Fig. 38 shows the total cross sections vs the neutrino energy[73]. The linear rise, characteristic for low energy experiments, manifests scaling behaviour. The slopes agree well with the ones measured in ν_μ, $\bar{\nu}_\mu$ experiments and constitute a check of e - μ universality at the level of 30%.

The very first antineutrino induced interaction was observed in a reactor which produces an $\bar{\nu}_e$-beam[74].

Physics in a ν_e-beam derived via the cascade $\pi^+ \to \mu^+ \nu_\mu$ and $\mu^+ \to \bar{\nu}_\mu e^+ \nu_e$ is considered at Los Alamos[75].

5. THE KOBAYASHI-MASKAWA MATRIX

The KM-matrix[76] is the extension of the GIM matrix from 2 to 3 quark generations. Instead of

$$\begin{pmatrix} d \\ s \end{pmatrix}^{GIM} = \begin{pmatrix} \cos\theta & \sin\theta \\ -\sin\theta & \cos\theta \end{pmatrix} \begin{pmatrix} d \\ s \end{pmatrix}$$

with 1 angle, the CABIBBO angle, there is now

$$\begin{pmatrix} d \\ s \\ b \end{pmatrix}^{KM} = \begin{pmatrix} c_\beta c_\theta & c_\beta s_\theta & s_\beta \\ -c_\gamma s_\theta - s_\gamma s_\beta c_\theta e^{i\delta} & c_\gamma c_\theta - s_\gamma s_\beta s_\theta e^{i\delta} & s_\gamma c_\beta e^{i\delta} \\ -c_\gamma s_\beta c_\theta + s_\gamma s_\theta e^{-i\delta} & -c_\gamma s_\beta s_\theta - s_\gamma c_\theta e^{-i\delta} & c_\gamma c_\beta \end{pmatrix} \begin{pmatrix} d \\ s \\ b \end{pmatrix}$$

with 3 angles θ, β, γ, 1 phase δ and c, s standing for cos, sin.
For example:

$$J_\lambda^{ud'} = \bar{\psi}_u \gamma_\lambda (1-\gamma_5)\,(c_\beta c_\theta \psi_d + c_\beta s_\theta \psi_s + s_\beta \psi_b).$$

Instead of the above notation due to MAIANI[77] an alternative notation has recently been proposed by WOLFENSTEIN[78] who expands the unitary, nearly unit KM matrix in terms of a small parameter.
There are detailed analyses of experiments relevant for the determination of the KM matrix elements[79]. Here, only a few ingredients will be mentioned:

Nuclear β-decay	$U_{ud} = 0.9735 \pm 0.0015$
K_{e3}-decays Y-decays (WA2) }	$U_{us} = 0.221 \pm 0.002$
$\nu, \bar{\nu}N \to \mu\bar{\mu}x$ (CDHS)	$U_{cd} = 0.23 \pm 0.03$ $\lvert U_{cs}\rvert > 0.59$ (90% CL)
CLEO, CUSB $\frac{b\to u}{b\to c}$	$\left\lvert\frac{U_{ub}}{U_{cb}}\right\rvert < 0.15$ (90% CL)
b-lifetime $0.5 < \tau_b < 1.4$ psec	$\frac{\sin^2\beta}{a_\beta^2} + \frac{\sin^2\gamma}{a_\gamma^2} = 1$ $a_\beta = 0.598\, a_\gamma$; $a_\gamma = \frac{0.058}{\sqrt{\tau_b/\text{psec}}}$

The constraints are shown in fig. 39. Only a small region remains.
The B-lifetime measurements determine essentially $|\sin\gamma|$. The statistical and systematic uncertainties in measuring the B-lifetime are for the time being quite large. Therefore, the upper limit of the JADE result[80] and the lower limits of the MARK II[81] and MAC[82] results are used.

6. DETERMINATION OF B-LIFETIME

In e^+e^- interaction at PETRA and PEP energies the quark-antiquark jets occur b-flavored at a rate 1 : 11. The natural mixture can be made b-rich or c-rich applying certain selection criteria. First of all a fast muon is requested in a multihadron event. The second criterion uses the fact that B-hadrons are heavy and fast objects, giving rise to high transverse momentum particles and a characteristic event shape. For instance fig. 40 shows the composition of the transverse momentum distribution of prompt muons, i.e. those coming from b- and c-decays. It is obvious that a cut in $P_T(\mu)$ around 1 GeV/c generates a b-rich ($P_T > 1$ GeV/c) and a b-poor sample ($P_T < 1$ GeV/c). The background due to hadrons misidentified as muons or $K_{\mu 2}$, $\pi_{\mu 2}$ decays in flight, which is of the order 20 - 30%, has been subtracted.
A schematic $b\bar{b}$ event with $b \to \mu + c$ is displayed in fig. 41. The muon track originating from the B-vertex is extrapolated from the inner detector to the interaction region. The measured distance δ of closest approach to the e^+e^--interaction point (fig. 41) is related to the lifetime of B-hadrons[80]:

$$\delta = \ell \sin\alpha = \frac{\ell}{L} c\tau \quad f(\alpha^*)$$

where ℓ is the actual decay length, $L = \beta\gamma c\tau$ the average decay length of the B with velocity β and lifetime τ, α^* the decay angle of the μ in the B rest frame. It is assumed that the B flight direction is well approximated by the reconstructed event axis. Assuming $\tau = 1$ psec the typical average δ is around 150 μm (depending on P_T-criterion). This is to be compared with the track uncertainty σ after extrapolation, which is 450 μm for JADE, 250 μm for MARK II, 800 μm for MAC. The statistical precision

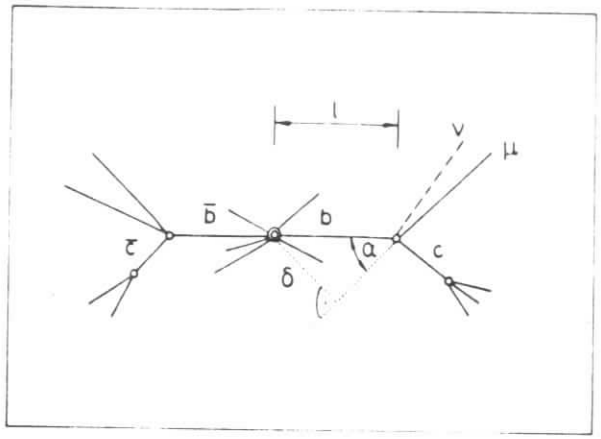

Fig. 41a:

Sketch of an event $e^+e^- \to b\bar{b}$ and semileptonic b-decay. The extrapolated μ-track fails the e^+e^- interaction point. This point is either determined from the event itself or assumed a priori using external information.

using n B-events is $\sigma/\sqrt{n}$. With the help of an extensive Monte Carlo simulation the observed δ-distribution is expressed in terms of $b \to \mu$, $c \to \mu$, and hadrons $\to \mu$. The published results are

Expt.	#b (estimated)	lifetime
JADE	12	< 1.4 psec
MARK II	67	$1.20^{+0.45}_{-0.36} \pm 0.3$ ps
MAC	112	$1.8 \pm 0.6 \pm 0.6$ ps

If the lifetime is indeed high, say 1.5 psec, it should be possible to measure the B-decay vertex distribution. In this case the average length is

$$\bar{L} = \overline{\beta\gamma}\, c\tau \approx 3 \times 0.45 \text{ mm} \approx 1.4 \text{ mm},$$

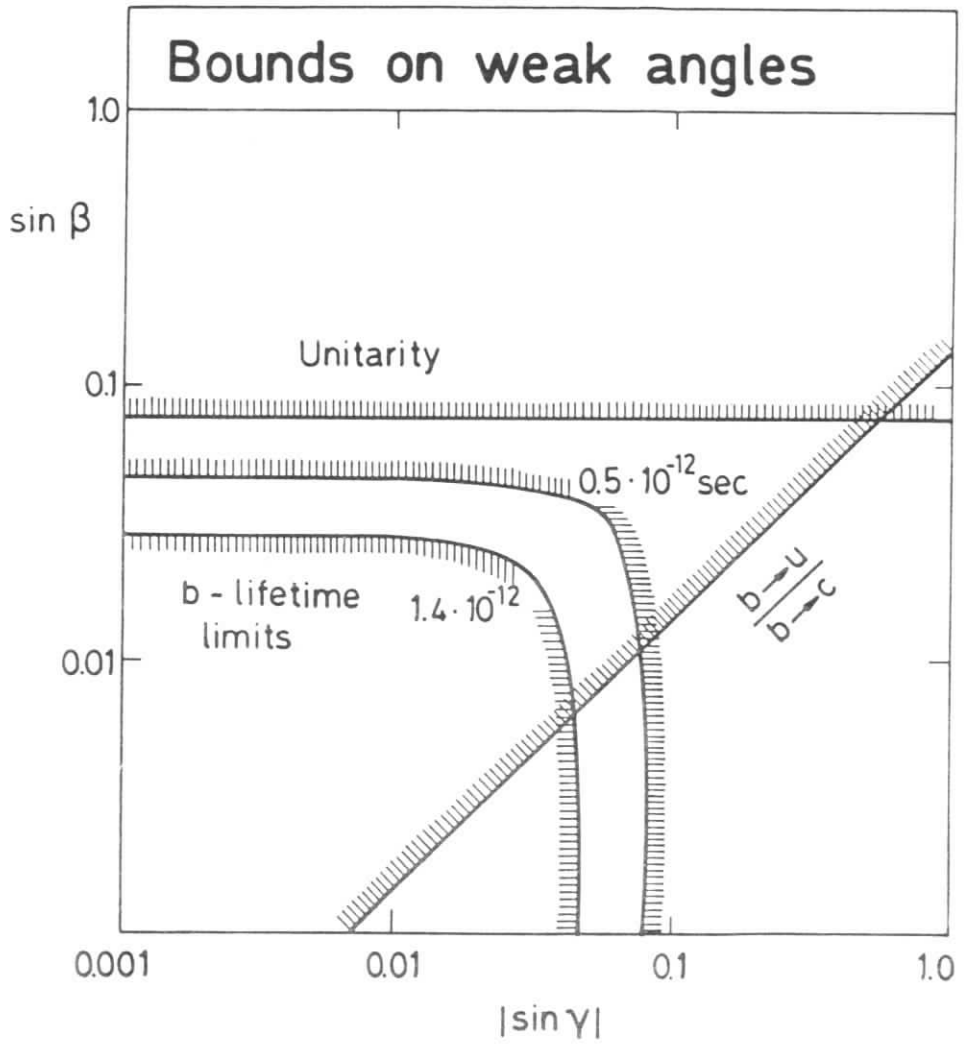

Fig. 39: Bounds on weak angles

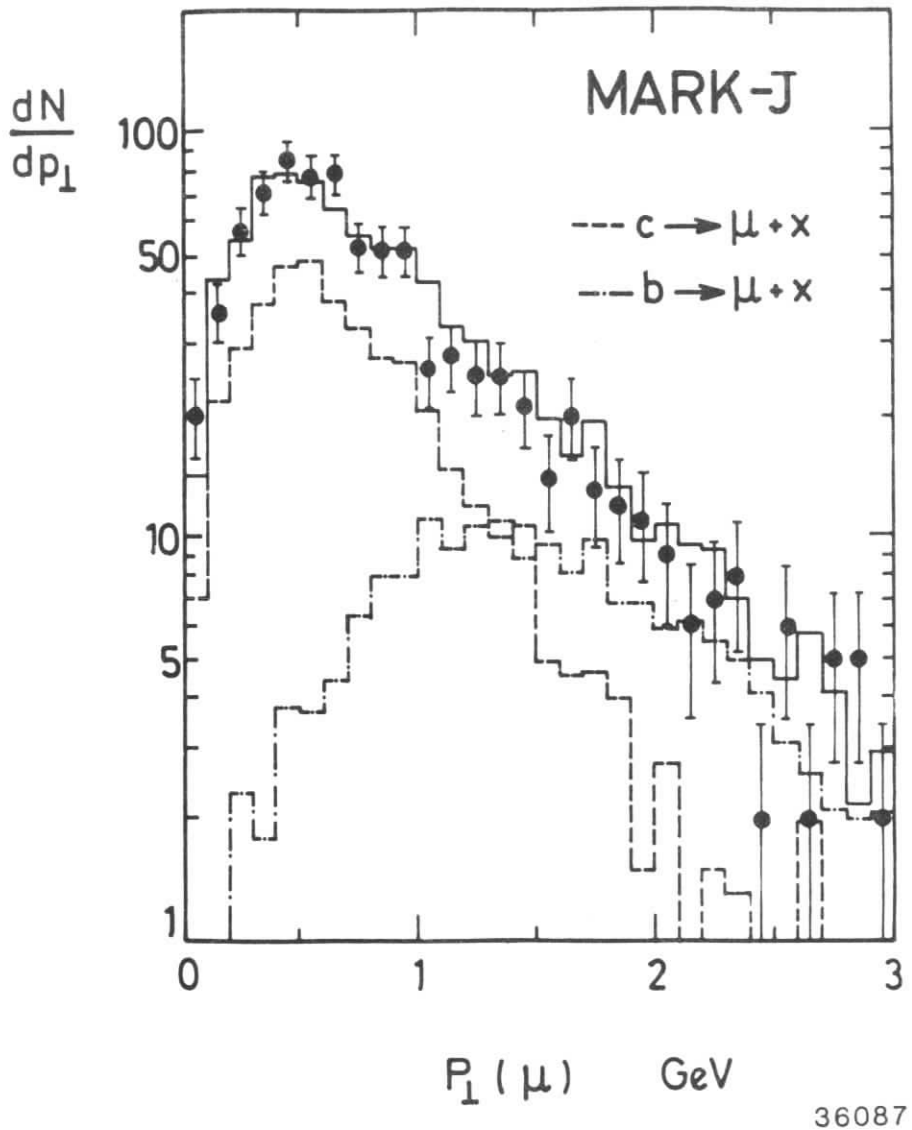

Fig. 40: Transverse momentum distribution of prompt muons in multihadron events. The dotted histograms are Monte Carlo predictions of the contributions from semi-leptonic c- and b-quark decays. The nonprompt background is subtracted.

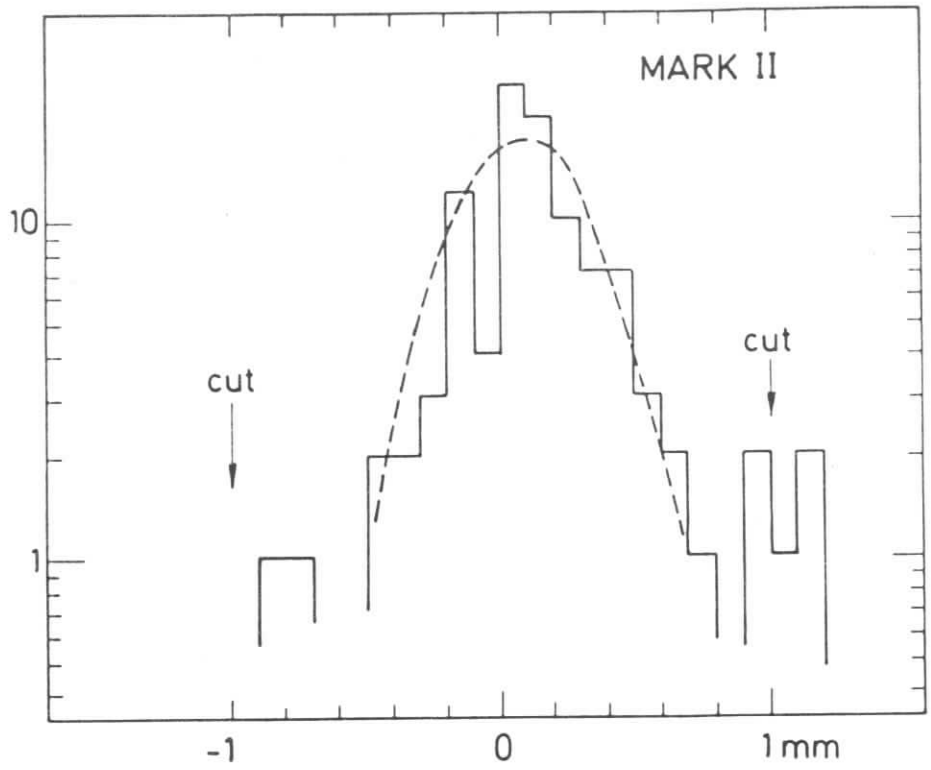

Fig. 41b: The observed impact parameter distribution of 104 muons in the b-enriched event sample of MARK II (ref. 81). The average is (106 ± 29) μm. The dotted curve is a GAUSSian distribution with width 250 μm.

this means effectively about 1 mm in the plane perpendicular to the beam. In an apparatus with a vertex detector a fair fraction of the B-decay vertices will be detectable and open new perspectives for B-physics.

7. SEARCH FOR TOP-QUARKS

A substantial amount of time at PETRA was devoted to search for t quarks (fig. 42). The machine was operated in a scanning mode. The step size of ΔE = 30 MeV corresponds to the machine energy resolution. For each point each of the 4 running experiments collected 60 nb^{-1}. This gives just enough multihadron events to detect a resonance in

$R = \frac{\sigma(e\bar{e} \to q\bar{q})}{\sigma_0(e\bar{e} \to \mu\bar{\mu})}$. Assuming a BREIT-WIGNER resonance shape one obtains

$$\int \sigma(E)dE = \frac{6\pi^2}{M^2} \Gamma_e \frac{\Gamma_h}{\Gamma}$$

with M = mass of $t\bar{t}$ and Γ_e resp. Γ_h being the leptonic resp. hadronic widths. Fitting a GAUSS curve width ΔE and varying position along the energy axis ($\sqrt{s}$) on top of the constant continuum due to u, d, s, c, b events the limit $\Gamma_e \frac{\Gamma_h}{\Gamma}$ < 1 keV (50% CL) is obtained to be compared with $\Gamma_e(t\bar{t}) \approx 5$ KeV as extrapolated from $\phi(s\bar{s})$, $J/\psi(c\bar{c})$, $\Upsilon(b\bar{b})$. In conclusion, there is no indication of a resonance due to $t\bar{t}$ with Q_t = 2/3 and its mass must exceed 22.6 GeV.
At the time of these lectures the UA1-group[8] claimed the observation of a few events containing the flavor top so long searched for. No precise mass was quoted, but is well above the PETRA limit.

8. B-DECAYS

Hadrons containing b-quarks are abundantly produced at e^+e^- machines (CESR, DORIS, PETRA, PEP). The CLEO group[84] at CORNELL succeeded in reconstructing B-mesons starting from a sample of identified D^0, $D^{*\pm}$ and adding 1 or 2 charged pions. They obtained for the masses:

$m(B^-) = (5270.8 \pm 2.3 \pm 2.0)$ MeV

$m(B^0) = (5274.2 \pm 1.9 \pm 2.0)$ MeV.

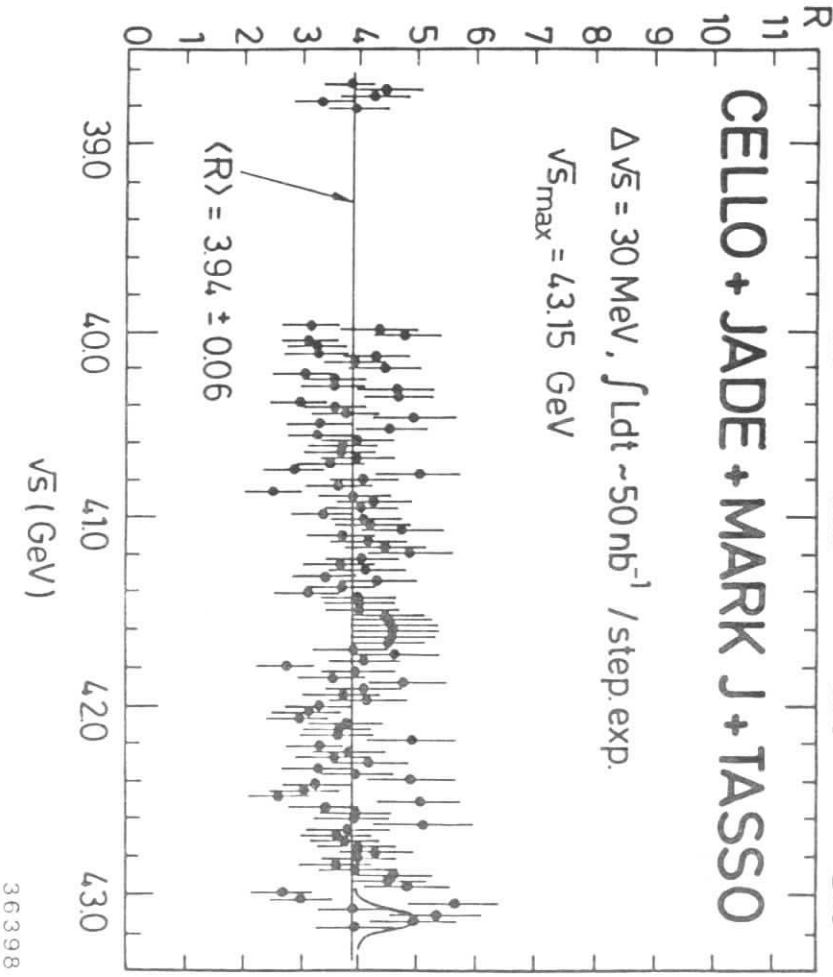

Fig. 42: Search for top in the highest PETRA energy range

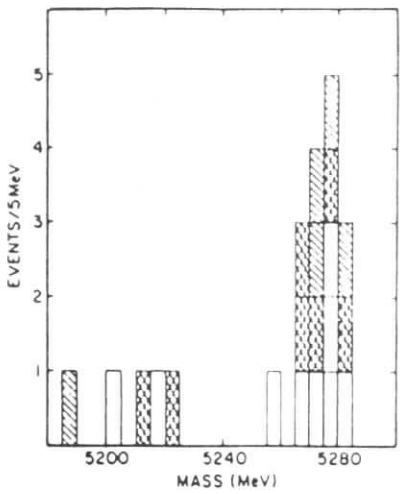

Fig. 43: The mass spectrum for B meson candidates with restrictive cuts on the D mass.

There are many investigations using continuum events, of which 1 : 11 contain B-hadrons.

a) Semileptonic B-decay: In the free quark model this decay proceeds like

$$b \to (c,u) + \begin{cases} \ell\bar{\nu}_\ell & \ell = e, \mu, \tau \\ q\bar{q}' & q = d, s \end{cases}$$

Thus, the branching ratio into $\mu\bar{\nu}_\mu$ is expected to be

$$BR_\mu = \frac{1}{(1+1+0.3) + 3(1+0.3)} = 16\%$$

The two terms in the denominator count the lepton and quark flavors. Heavy flavors are suppressed (phasespace). The average over all PETRA/PEP measurements[85] is (11.8 ± 0.6)%, which indicates that the use of the free quark model is too naive and hadronic corrections must be taken into account.

b) The electron spectrum in b-decays near the kinematic endpoint is sensitive to the mass of the accompanying flavor. Measurements of CUSB and CLEO[86] show that $b \to u + e\bar{\nu}_e$ is suppressed against $b \to c + e\bar{\nu}_e$ (fig. 44):

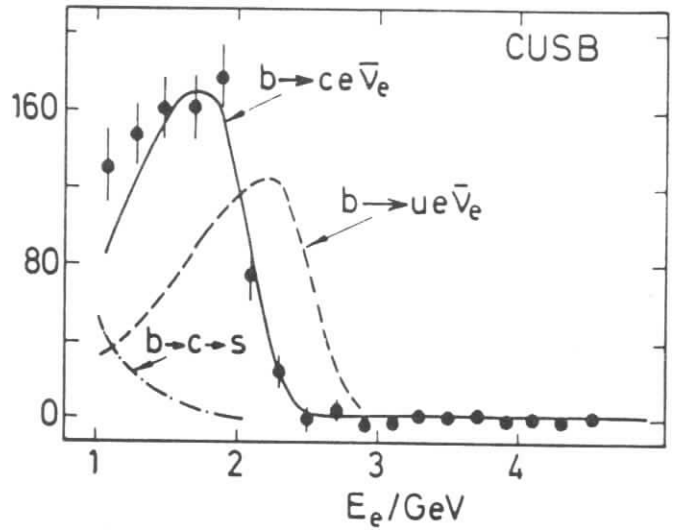

Fig. 44: Electron momentum spectrum and comparison with theory (Altarelli et al.)

for founding the KOBAYASHI-MASKAWA matrix elements U_{cb} and U_{ub} (see sect. 5).

c) The standard model forbids at tree level flavor changing neutral weak currents. Searches have been made for $b \to (s, d) + \ell\bar{\ell}$. 4 experiments reported[85]

$$\frac{\#\ B \to \ell\bar{\ell} + X}{\#\ B \to \text{all}} < 0.7\% \text{ at } 50\% \text{ CL.}$$

d) The CLEO group compared $B \to D^0 + X$ with $b \to c + \ell\bar{\nu}_\ell$ and got good agreement. This is support for the V - A structure and dominance of the spectator model.

Lecture 5: STRONG INTERACTIONS

1. The claims of QCD
2. Asymptotic freedom (qualitative)
3. The basic problem
4. Gluons
5. Scaling violation in deep inelastic scattering (DIS)
6. The structure function $xF_3(x, Q^2)$
7. Analysis of F_2 and π^{ν}
8. α_s from e^+e^--interactions

1. THE CLAIMS OF QCD

Quantum chromodynamics, together with the existence of flavored quarks, describes the structure of all hadrons. Hadrons are composites of quarks. The force between quarks is derived from the local SU(3) gauge group. The analog rôle of electric charge and photon in QED is played by color and gluon in QCD. There is a crucial difference: the color gauge group is nonabelian. Gluons, unlike photons, will interact with themselves. At decreasing distance the force gets smaller and smaller. This is called asymptotic freedom and allows for a perturbative treatment. On the contrary, at increasing distance the force gets stronger and stronger, hindering quarks to leave the interaction region as free particles. This aspect is called confinement and is an unsolved problem. An account of the development of QCD can be found in ref. 88.

2. ASYMPTOTIC FREEDOM (QUALITATIVE)

a) Deep inelastic scattering: The SLAC-MIT experiment 1967 has initiated an important research line. At high Q^2 it turned out that the nucleon structure function $F_2(x, Q^2)$ is essentially independent of Q^2. This phenomenon was called scaling or BJORKEN-scaling. A simple interpretation due to FEYNMAN is to think of the nucleon as being made of quasi-free partons later on identified with quarks. The eN experiments were paralleled by the neutrino experiments in GARGAMELLE. The comparison of eN and νN experiments (cf fig. 35) confirmed the assignment of fractional charges to quarks. Furthermore, it turned out that quarks and antiquarks carry only about 50% of the nucleon momentum. This was taken as evidence for the existence of another type of partons in the nucleon which are not "seen" in reactions induced by γ or $W^{\pm}$, Z. These inert partons were called gluons. More detailed experimental investigations, again at SLAC, have shown 1974 that scaling did not hold exactly. The small scaling violation attracted a strong theoretical interest and was the beginning of a big experimental effort both in ℓN and ν, $\bar{\nu}$N experiments extending Q^2 up to 200 GeV^2.

b) $e^+e^- \to q\bar{q}$: One of the most fundamental observable is the total hadronic cross section normalized to the QED $\mu^+\mu^-$ production cross section:

$$R = \frac{\Sigma\sigma(e^+e^- \to q\bar{q})}{\sigma(e^+e^- \to \mu^+\mu^-)^{QED}} = 3\left[(\tfrac{2}{3})^2 + (\tfrac{1}{3})^2 + (\tfrac{1}{3})^2 + (\tfrac{2}{3})^2 + (\tfrac{1}{3})^2\right] = \frac{11}{3} = 3.67$$

The factor 3 takes the three color degrees of freedom of quarks into account. The five terms represent the electric quark charges squared for the flavors u, d, s, c, b assuming $\sqrt{s}$ to be above the threshold for $b\bar{b}$ and below the threshold for $t\bar{t}$ production. A glance at fig. 45 shows that this simple theoretical calculation is a quite good approximation provided the resonance regions are avoided. This means that away from thresholds strong interactions between quarks are small. Theoretically expected deviations due to γ, Z^0 interference have been considered in lecture 3, deviations due to strong interactions will be discussed below.

3. THE BASIC PROBLEM

As mentioned above quarks are quasifree pointlike particles only at small distance scale. In this regime the force due to strong interactions is weak and perturbation calculations can be performed. However, observations are made at large distance scale. The transition from quarks and gluons to the observed hadrons should in principle be described by nonperturbative QCD, however sofar without success. For this reason more or less sophisticated models for the hadronisation process have been invented and investigated. They contain free parameters which are fixed by fitting the model predictions to experimental data. Various models give a reasonably good phenomenological description of all experimentally investigated distributions.

The hadronic final states in e^+e^--interactions, for instance, are interpreted with the help of such models to deduce the properties of perturbative QCD, in particular the strong coupling constant $\alpha_s(Q^2)$. At the present time the extraction of the running coupling constant $\alpha_s(Q^2)$ is model dependent. A better understanding of the hadronisation process must be attained.

4. GLUONS

More than 10 years ago the determination of $\int_0^1 F_2(x)dx \approx 0.5 \neq 1$ in lepton nucleon deep inelastic scattering experiments led to the conclusion that there

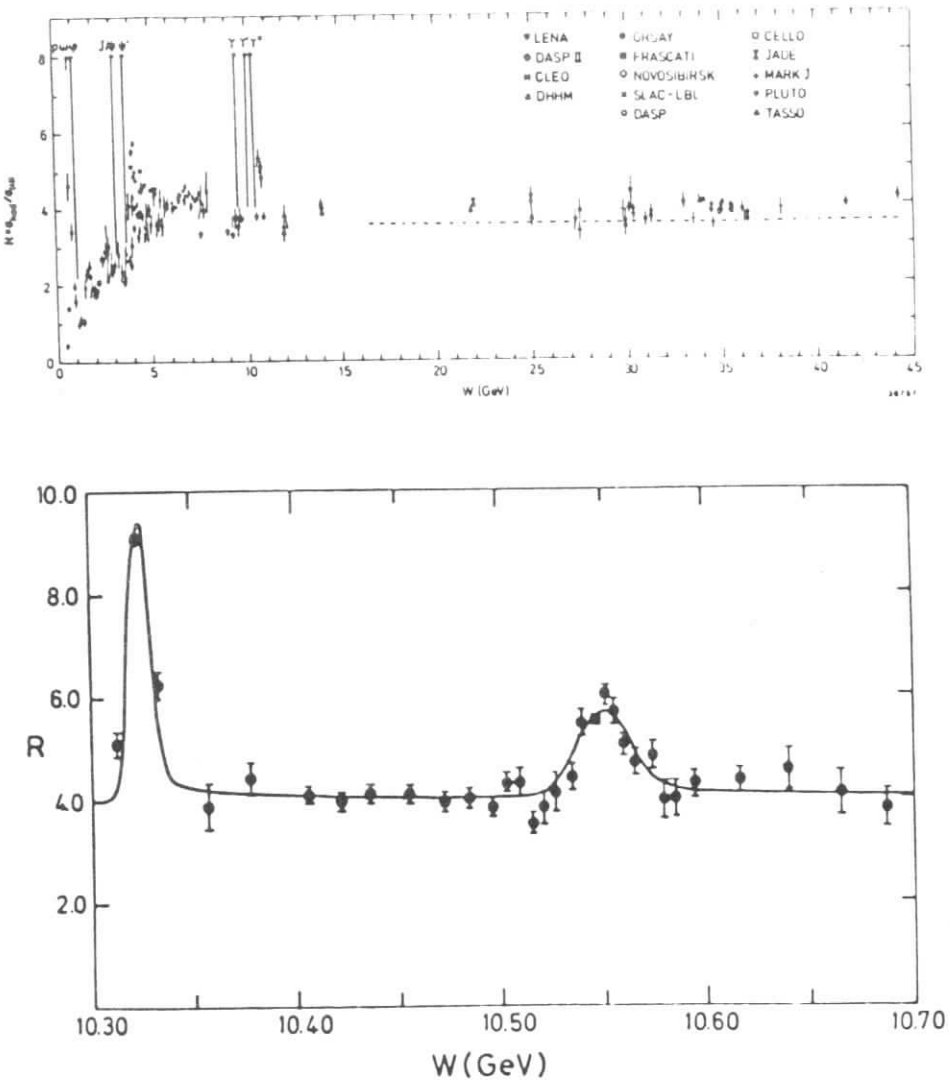

Fig. 45: The total hadron cross section in units of the QED-cross section $\sigma(e^+e^- \to \mu^+\mu^-)$. The dotted line in the upper figure is the prediction of the naive quark parton model. The figure below shows two resonances in the Y-region (CLEO 1981).

must be partons in the nucleon which do not couple to γ and $W^{\pm}$. The carriers of the missing momentum were named gluons or more vaguely glue. A few months after the start up of PETRA clear 2-jet and, at about 10 times lower rate, 3-jet events have been observed. At these high energies the process $e^+e^- \to q\bar{q}$ with the subsequent hadronisation of the q and $\bar{q}$ running off in opposite directions appears as two jets. The 3-jet events (fig. 46, 47) were then interpreted as $e^+e^- \to q\bar{q}g$ with a hard gluon giving rise to the third jet. The gluon bremsstrahlung spectrum disfavors hard gluons. Therefore, in most of the hadron events jets will only be broadened. The same kind of broadening is also observed in the forward jet in lepton nucleon scattering. The observed p_T behaviour in νN and μN experiments agree well (fig. 48)[89].

Structure function analyses favor the spin 1 assignment to gluons. In events $e^+e^- \to$ 3-jets the angular distribution contains information about the gluon spin and agrees with the assumption of vector gluons (fig. 46). ISR data (fig. 49) and $S\bar{p}pS$ data[3] support this.

A crucial feature of QCD is the selfinteraction of gluons giving rise to processes like $g \to g + g$ (triple gluon vertex). In reactions induced by γ and Z, W the triple gluon vertex occurs in second or higher order in α_s. In 3-jet events, as observed in e^+e^--interactions, the gluon-jet should be different than the quark- or antiquark-jet. The JADE collaboration at PETRA has investigated this question for some time and indeed noticed differences[91]. The most direct way of looking for gluon selfinteraction is in hard scattering processes in pp (ISR) or $p\bar{p}$ (CERN collider) collisions. In understanding the behaviour of the ratio K^-/π^- as opposed to K^+/π^+ for various energies as a function of $x_T = 2p_T/\sqrt{s}$ (fig. 49) the ABCDHW collaboration[90] at the ISR is led to the conclusion that the hard scattering process $qg \to qg$, which includes also the triple gluon vertex, contributes significantly. The qualitative argument is this: K^- being composed of $\bar{u}s$ cannot be formed in first generation by a knocked out valence quark (u,d) of the colliding protons. Most likely is the assumption that a hard gluon splits into $s\bar{s}$ with the $\bar{s}$ picking up a u quark from the vacuum to from a K^-.

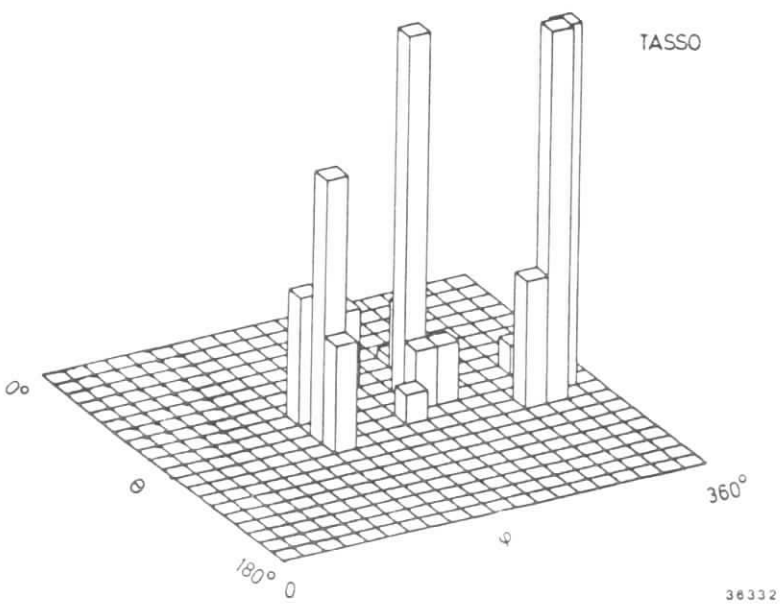

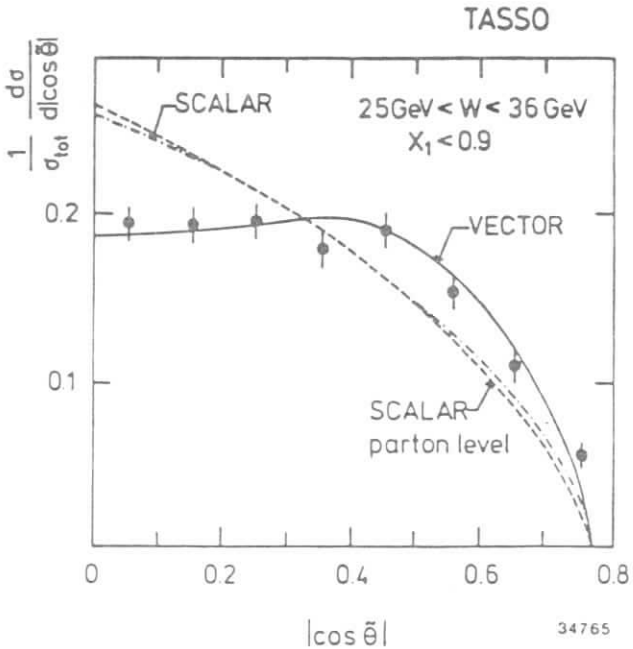

Fig. 46: TASSO 3-jet event and ELLIS-KARLINER analysis (ref. 89).

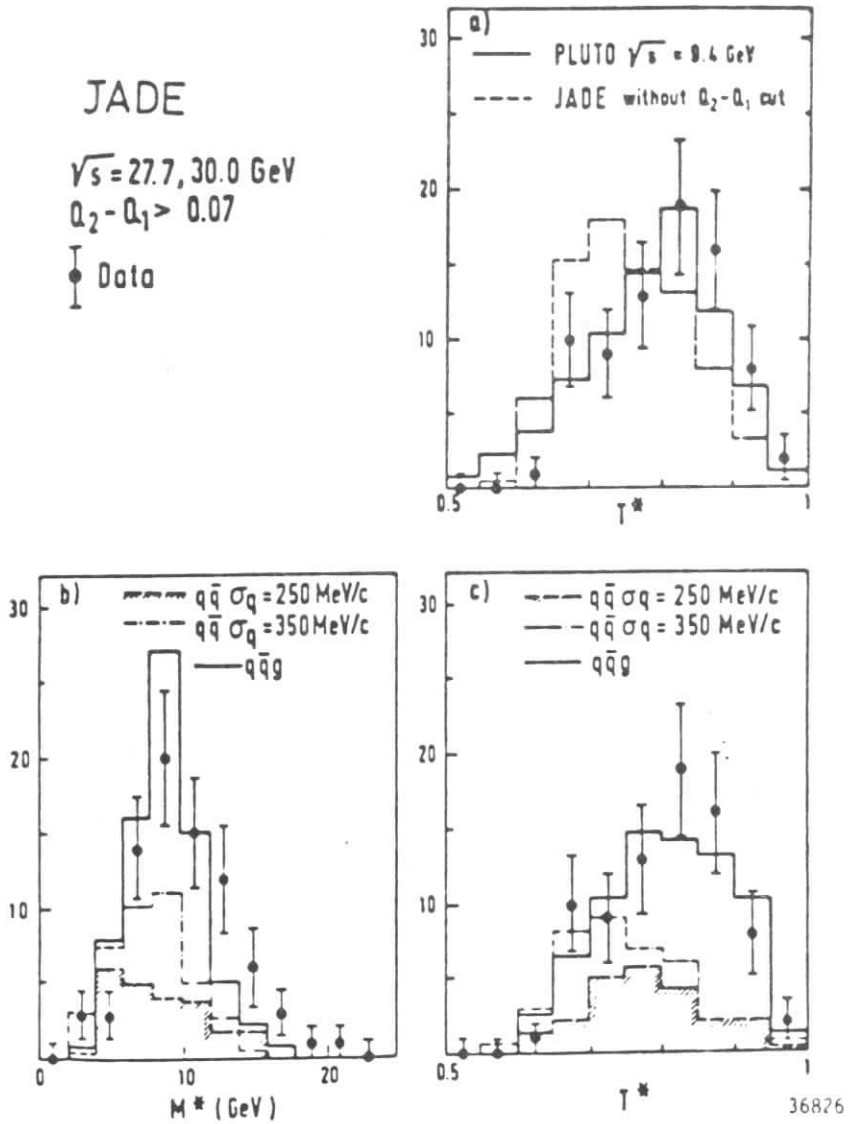

Fig. 47: The JADE analysis of planar events. The 3-jet character is recognized by investigating the "fat" jet in its own rest frame (ref. 89).

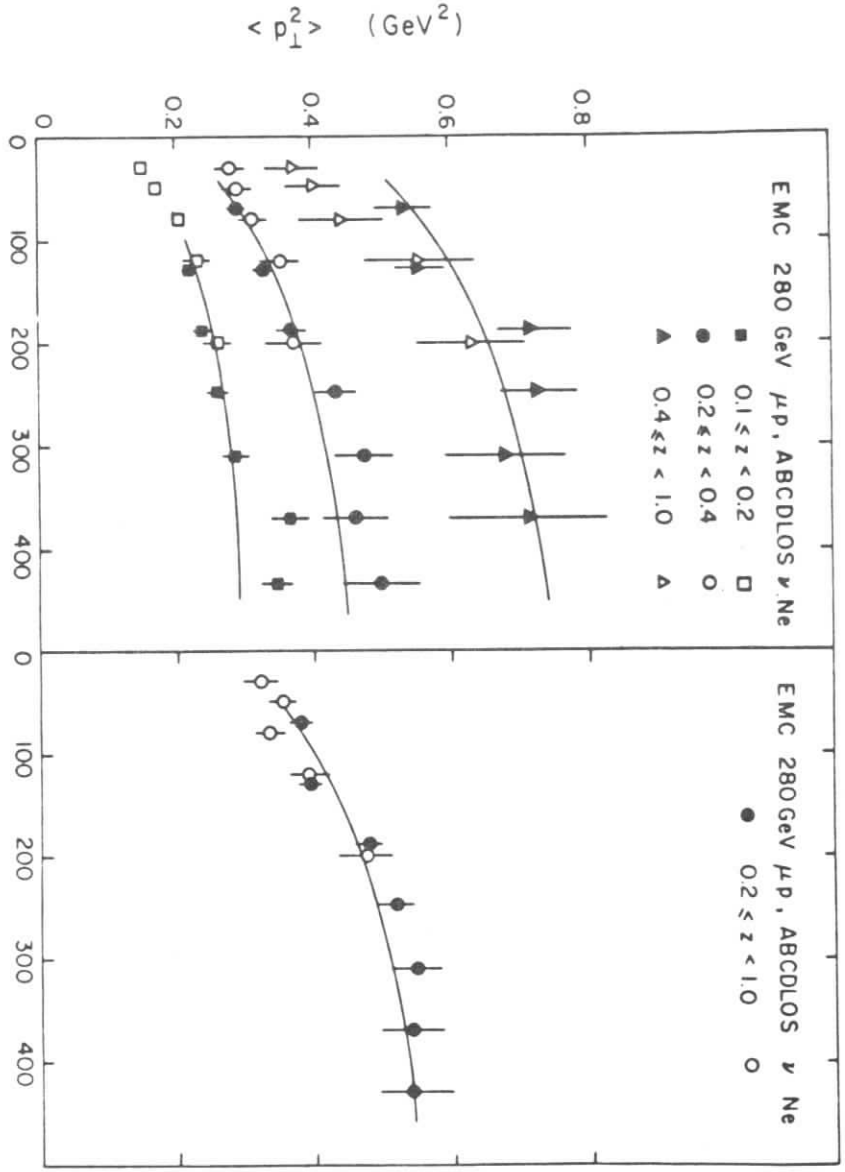

Fig. 48: Transverse jet broadening in νN_e (BEBC) and μp (EMC).

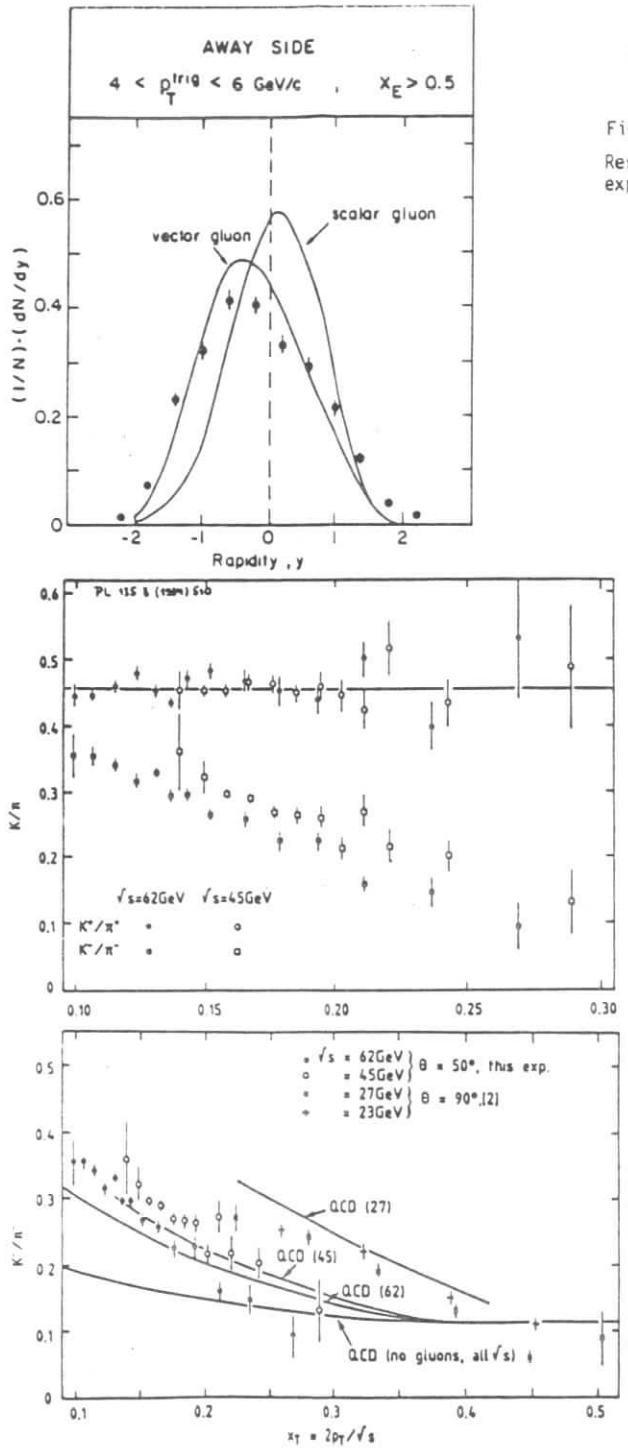

Fig. 49:

Results from an ISR experiment.

5. SCALING VIOLATION IN DI-SCATTERING

The inclusive processes

$$\nu_\mu N \to \mu^- + \text{anything}$$
$$\bar{\nu}_\mu N \to \mu^+ + \text{anything}$$
$$\ell N \to \ell + \text{anything} \quad (\ell = e, \mu)$$

can be written in terms of 3 resp. 2 structure functions:

$$d^2\sigma(\nu N) = \sigma_0^\nu dxdy \left[\left(1-\frac{y}{2}\right)^2 2xF_1^\nu(x,Q^2) + (1-y)F_2^\nu(x,Q^2) + y\left(1-\frac{y}{2}\right)xF_3^\nu(x,Q^2)\right]$$

$$d^2\sigma(\bar{\nu}N) = \sigma_0^\nu dxdy \left[\left(1-\frac{y}{2}\right)^2 2xF_1^\nu(x,Q^2) + (1-y)F_2^\nu(x,Q^2) - y\left(1-\frac{y}{2}\right)xF_3^\nu(x,Q^2)\right]$$

$$d^2\sigma(\ell N) = \sigma_0^\ell dxdy \left[\left(1-\frac{y}{2}\right)^2 2xF_1^\ell(x,Q^2) + (1-y)F_2^\ell(x,Q^2)\right]$$

N is assumed to be an isoscalar target. The heavy target calorimeters are nearly isoscalar. From the measured outgoing charged lepton and the hadronic energy ν the three variables

$$x = \frac{Q^2}{2M\nu} \qquad y = \frac{\nu}{E} \qquad Q^2 = 2EE'(1-\cos\vartheta)$$

can be computed. E is the energy of the incoming lepton. In neutrino experiments this quantity must be obtained from the final state. In narrow band beams there is however a correlation between the radial position of a ν event and its energy.

The aim of the experiments is to extract from the data

$$xF_3(x,Q^2)$$
$$F_2(x,Q^2)$$
$$R \equiv \frac{F_2(x,Q^2)\left(1+\frac{Q^2}{\nu^2}\right) - 2xF_1(x,Q^2)}{2xF_1(x,Q^2)} \equiv \frac{F_L(x,Q^2)}{2xF_1(x,Q^2)}$$

The ν and $\bar{\nu}$ experiments are unique in getting access to the structure function xF_3.

In the quark-parton model the structure functions have a simple interpretation:

$$xF_3(x) = x(q(x)-\bar{q}(x))$$
$$F_2(x) = x(q(x)+\bar{q}(x))$$
$$R(x) = 0$$

with the abreviation $q(x) \equiv u(x)+d(x)+s(x)+c(x)$. $R = 0$ is called the CALLAN-GROSS relation and reflects the fact that quarks have spin 1/2. It is interesting to note that xF_3 depends only on the valence quarks in the nucleon, since due to the difference $q(x)-\bar{q}(x)$ the sea contribution drops out. Not so for F_2, which has both a valence and a sea contribution.

6. THE STRUCTURE FUNCTION $xF_3(x,Q^2)$

From the difference of the differential cross sections of νN and $\bar{\nu}N$ data the structure functions xF_3 is obtained as follows:

$$xF_3(x,Q^2) = \frac{\pi}{G^2M^2E} \frac{d^2\sigma(\nu N)-d^2\sigma(\bar{\nu}N)}{(1-(1-y)^2dxdy} = xq(x,Q^2) - x\bar{q}(x,Q^2)$$

High statistics is needed since the difference of the cross sections is involved. The valence distributions are measured up to $x \approx 0.65$. The QCD-interpretation of xF_3 is given in terms of the ALTARELLI-PARISI equation[92]:

$$\frac{\partial}{\partial \ell n Q^2} xF_3(x,Q^2) = \frac{\alpha_s(Q^2)}{2\pi} \int_0^1 P_{qq}\left(\frac{x}{z}\right) zF_3(z,Q^2) \frac{xdz}{z^2}$$

The left hand side is directly measured (the slopes in fig. 50). The integral on the right hand side is a convolution of xF_3, which is measured up to 0.65, with a theoretically known function P_{qq}. Thus, the running coupling constant can be deduced.
In practice, a parametrisation (cf. fig. 51)

$$xF_3(x,Q_o^2) = a_3(1+b_2x)(1-x)^{c_3} \qquad \text{for } Q_o^2 = 4.5\ \text{GeV}^2$$

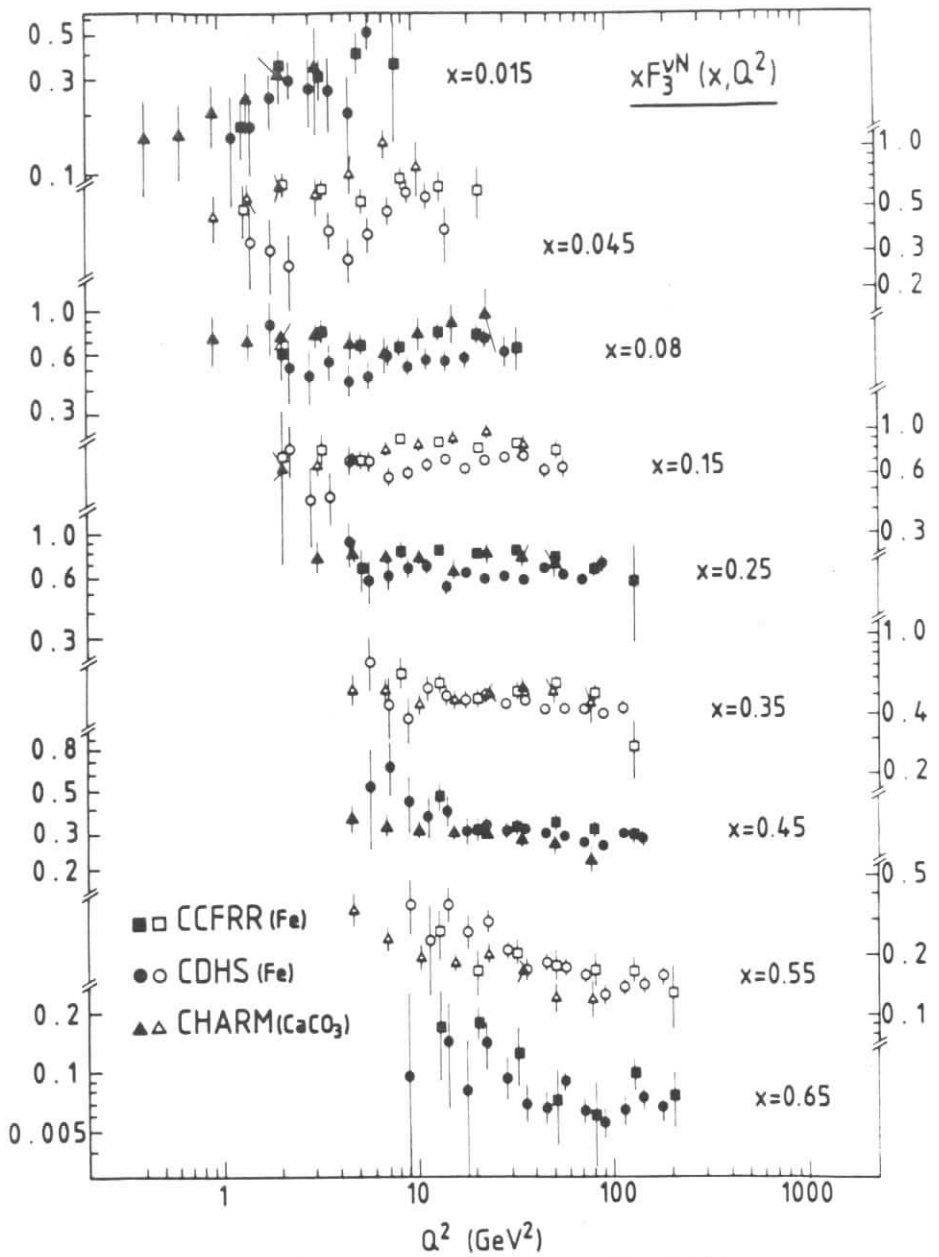

Fig. 50: The nucleon structure function xF_3 from 3 high statistics neutrino experiments (ref. 93).

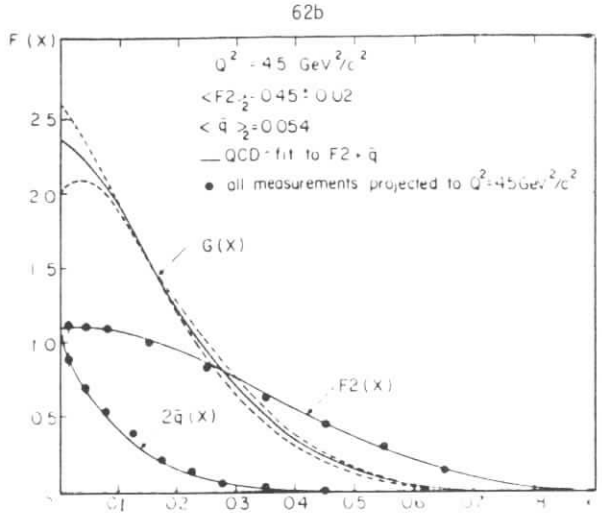

Fig. 51: The structure functions F_2, $\bar{q}^{\nu}$ and G(x) for fixed Q^2 obtained from a QCD fit to F_2 and $\bar{q}^{\nu}$ (ref. 95).

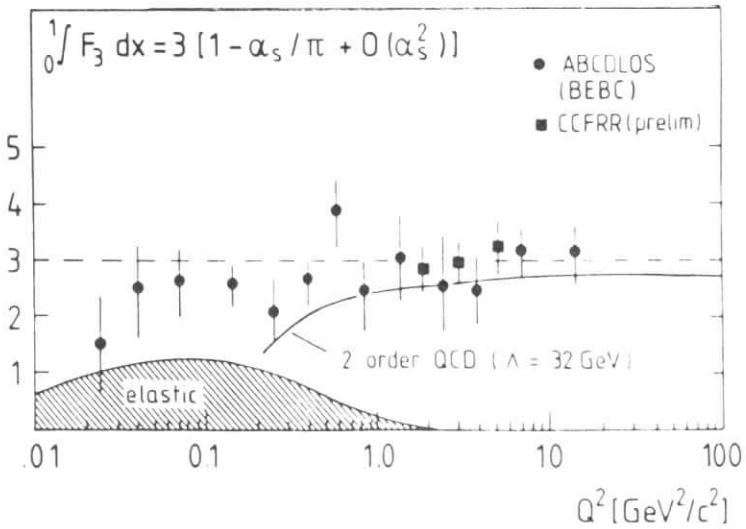

Fig. 52: The GROSS-LLEWELLYN-SMITH sumrule (ref. 96).

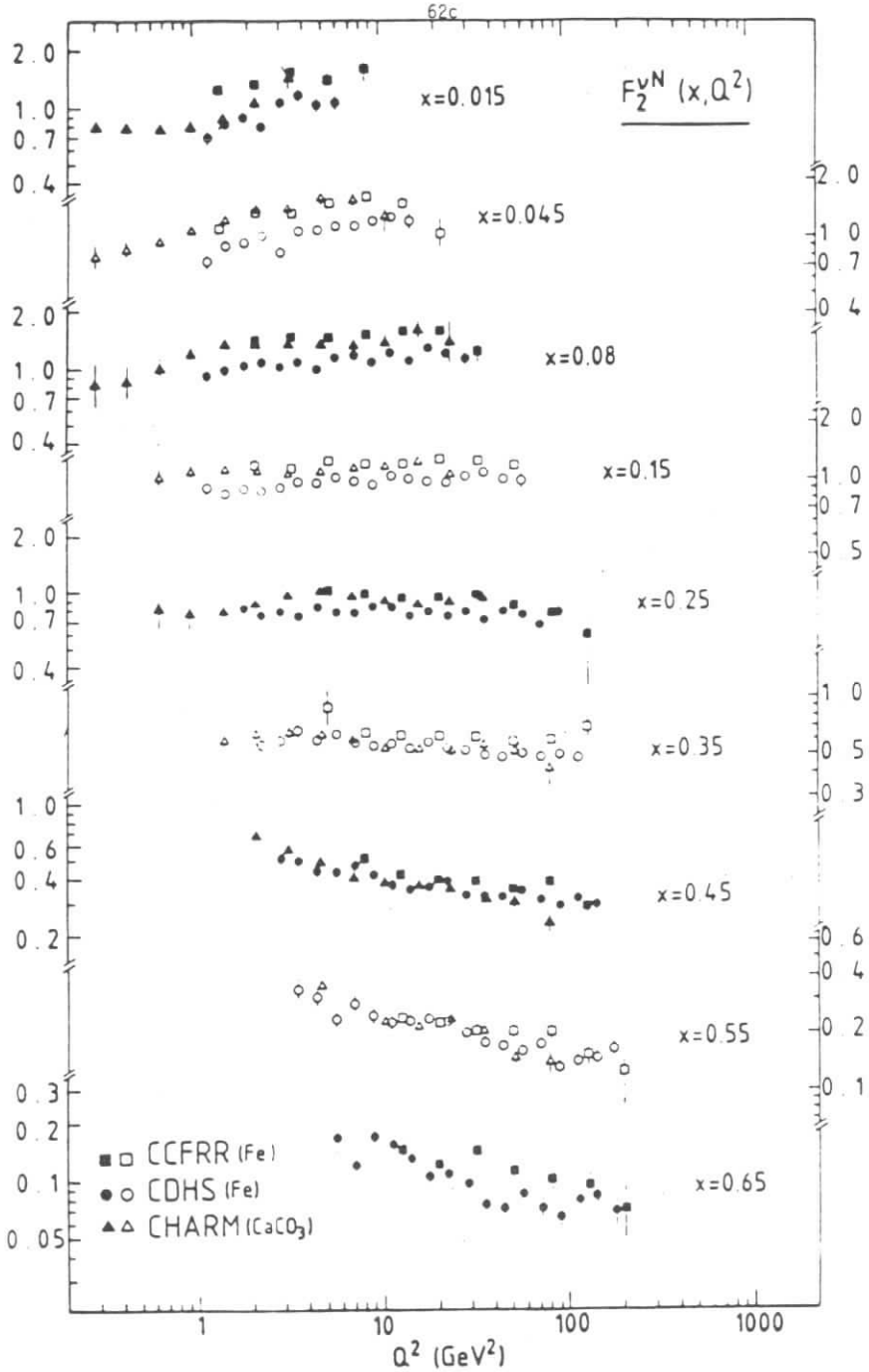

Fig. 53: The nucleon structure function F_2 from 3 high statistics neutrino experiments (ref. 93).

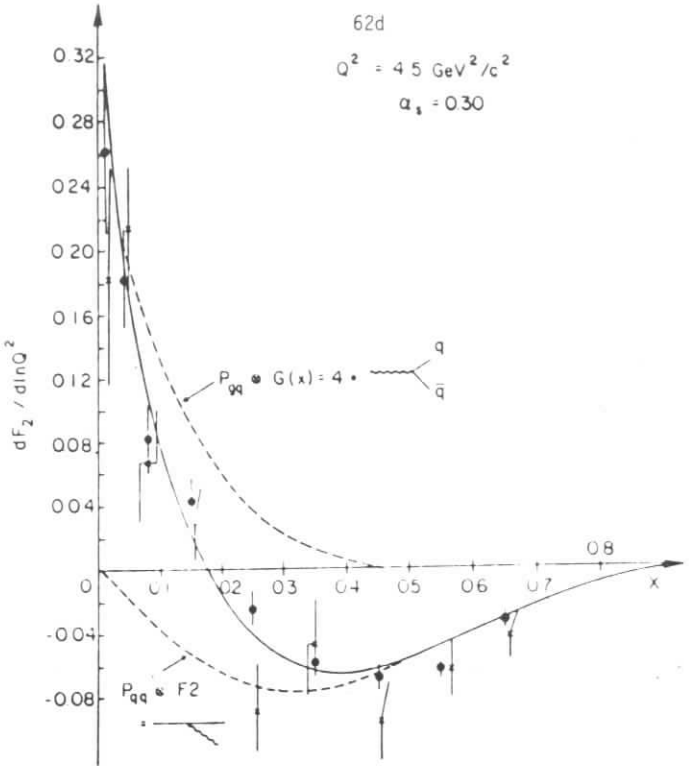

Fig. 54a: QCD interpretation of the slopes $dF_2/d\ln Q^2$ (ref. 95).

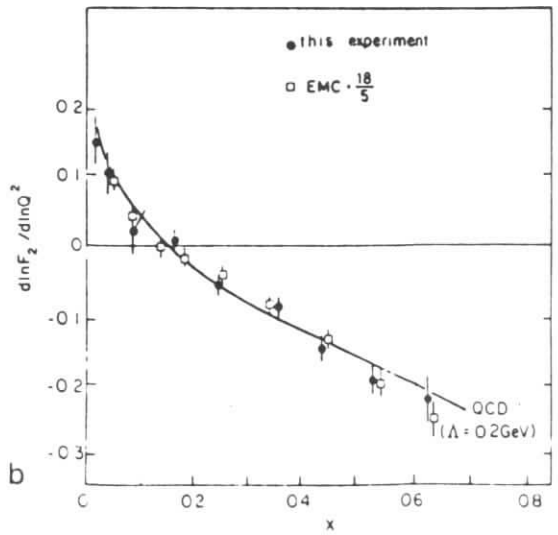

Fig. 54b:

Comparison between CDHS (νFe) and EMC (μFe) (ref. 95).

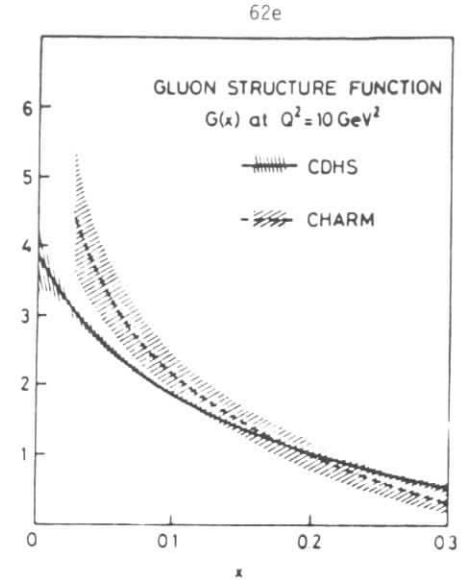

Fig. 55: The gluon distribution function

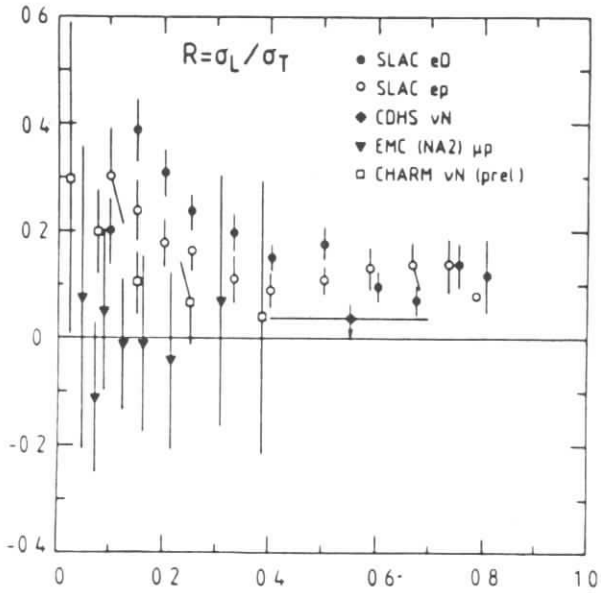

Fig. 56: Compilation of data on σ_L/σ_T (ref. 95).

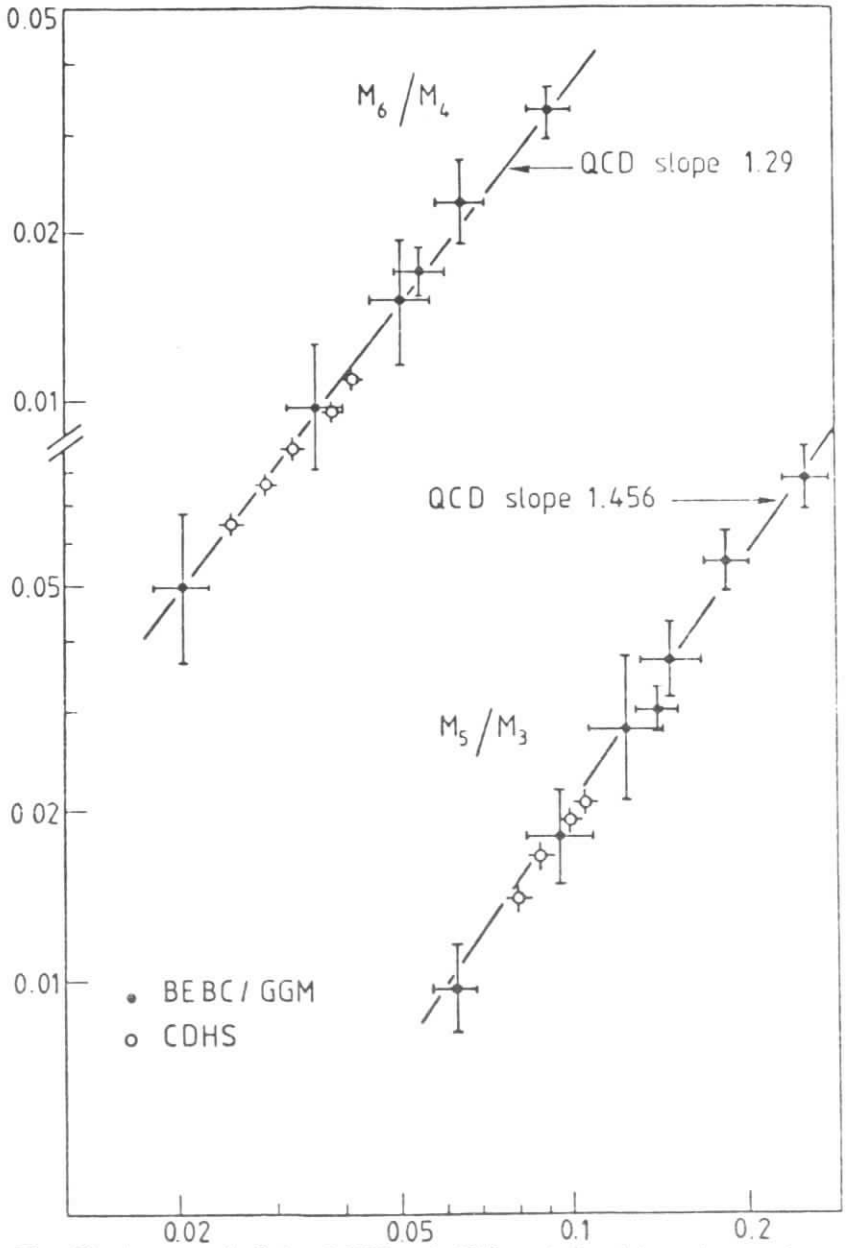

Fig. 57: Log moment plots of BEBC and CDHS neutrino data and comparison of slopes with QCD predictions (ref. 98).

is assumed, furthermore the GROSS-LLEWELLYN-SMITH sumrule (fig. 52)

$$\int_0^1 F_3 dx = 3(1 - \frac{\alpha_s}{\pi})$$

is used to constrain a_3. In order to avoid the high twist region cuts are applied: $Q^2 > 2$ GeV^2 and $W^2 > 11$ GeV^2. Under these conditions the CDHS collaboration[95] has obtained the result

$$\Lambda_{\overline{MS}} = 0.2^{+0.2}_{-0.1} \text{ GeV}$$

This result does not depend upon the gluon distribution function. It is per constructionem insensitive to the gluon selfcoupling. However, it is sensitive to the spin of the gluon and supports in fact its vector nature. The QCD mass scale parameter $\Lambda_{\overline{MS}}$ ($\overline{MS}$ = modified minimal subtraction) is related to $\alpha_s(\mu)$ through[94]

$$\Lambda^{(n)}_{\overline{MS}} = \mu \exp\left(\frac{1}{b_0\alpha_s(\mu)} - \frac{b_1}{b_0} \ln \frac{-2}{b_0\alpha_s(\mu)}\right) \text{ with}$$

$$b_0 = \frac{1}{2\pi}\left(11 - \frac{2}{3}n\right), \quad b_1 = -\frac{1}{4\pi^2}\left(51 - \frac{19}{3}n\right), \quad n = \#\text{ flavors with mass} < \mu.$$

7. ANALYSIS OF F_2 AND $\overline{q}^{\overline{\nu}}$

The structure function F_2 is extracted from the sum of the ν and $\bar{\nu}$ nucleon data:

$$\frac{1}{\sigma_0}\frac{d^2}{dxdy}(\sigma(\nu N) + \sigma(\bar{\nu}N)) = (1+(1-y)^2)\,F_2(x,Q^2) - \Delta F$$

with $\sigma_0 = \frac{G^2 ME}{\pi}$ and the term $\Delta F \equiv y^2 F_L - 2x(s-c)(1-(1-y)^2)$, which is small for $x > 0.3$. Nevertheless, the extraction of F_2 needs assumptions about $R = \frac{F_L}{2xF_1}$ and about the nonstrange sea. Results from 3 experiments are shown in fig. 53. The QCD interpretation of F_2 is more complicated then the one of xF_3. The change of F_2 w.r. to $\ln Q^2$ receives two contributions, one due to the process $q \to q + g$ and another due to $g \to q+\bar{q}$ (fig. 54). This means that the gluon distribution function is a necessary input. In order to get a handle on the shape of the gluon distribution function the CDHS collaboration[97] considered a suitably chosen combination of the differential

ν and $\bar{\nu}N$ cross section, namely

$$\overline{q}^{\bar{\nu}} \equiv x(\bar{u}+\bar{d}+2\bar{s}) = \frac{1}{1-(1-y)^4} \frac{1}{\sigma_o} \left| \frac{d^2}{dxdy} (\sigma(\bar{\nu}N)-(1-y)^2\sigma(\nu N)) + \delta \right|$$

where δ depends upon the strange and charmed sea $x(s-\bar{c})$ and the structure function F_L with the property that $\delta \to 0$ as $y \to 1$. The term $(1-y)^2\sigma(\nu N)$ subtracts the amount of scattering off quarks. At $y = 0.5$ this represents about 50%. Thus the specific sea quark combination $x(\bar{u}+\bar{d}+2\bar{s})$ is directly measurable. It has an important property: at large x, say $x > 0.4$, the sea $\overline{q}^{\bar{\nu}}$ is negligible over the measured Q^2-range. This implies a constraint on the shape of the gluon distribution function. Qualitatively speaking its shape cannot be too broad, otherwise the Q^2-evolution of $\overline{q}^{\bar{\nu}}$ would generate a nonnegligible contribution at large x due to $g \to q + \bar{q}$.
The simultaneous evaluation of F_2 and $\overline{q}^{\bar{\nu}}$ yields $\Lambda_{\overline{MS}}$ and the gluon distribution function G(x) (fig. 55). Also the CHARM collaboration has obtained G(x) from their data and has a new analysis in progress. The measured $\overline{q}^{\bar{\nu}}$ distribution can be used to obtain

$$F_2^{NS}(x,Q^2) \equiv F_2(x,Q^2) - 2(\overline{q}^{\bar{\nu}}(x,Q^2) - xs(x,Q^2)) \qquad x > 0.3$$

which is now independent of the sea like xF_3. Thus a nonsinglet analysis is possible and has been performed in both ν and μ experiments. Two results may be quoted:

$$\Lambda_{\overline{MS}} = 0.17^{+0.17}_{-0.11} \qquad \text{EMC} \quad \text{(ref. 99)}$$

$$0.30 \pm 0.15 \qquad \text{CDHS} \quad \text{(ref. 95)}$$

In conclusion, there is good agreement between the 5 highest statistics experiments, i.e. CDHS, CFFRR, CHARM, EMC, NA4. All agree in the observation of substantial scaling violation. If interpreted within QCD the strong interaction coupling constant is small in the Q^2-range from 5 till 100 GeV^2. However, the systematic uncertainties are for the time being too big to conclude about the running of $\alpha_s(Q^2)$.
There is a second type of QCD analyses based upon the moments of structure functions (fig. 57). A detailed account may be found in ref. 4b.

8. α_s FROM e^+e^- - INTERACTIONS

Over the past 5 years many QCD analyses have been performed by the experimental groups at PETRA and PEP. Early analyses were done in 1st order perturbation theory. When the 2nd order calculations became available more refined analyses were done. This section restricts to three groups of results.

a) R-measurements: The R-value

$$R \equiv \frac{\sigma(e^+e^- \to \text{hadrons})}{\sigma_\mu^{QED}} = R_o \{1 + \frac{\alpha_s}{\pi} (1 + c \frac{\alpha_s}{\pi}) + \dots\}$$

with R_o as calculated in the quark parton model including electroweak effects, $c = 0.08$ in the $\overline{MS}$ scheme (see lectures by R. Petronzio) is an inclusive quantity and is supposed to offer a clean way of measuring α_s. "Clean" refers to the believe that for $\sqrt{s} > 15$ GeV nonperturbative effects are negligible. Indeed, R at a given energy $\sqrt{s}$ could be used to define α_s.
Unfortunately, R-measurements are not easy. The average over 5 results obtained by JADE, MARK J, TASSO and MAC, MARK II[100] at $\langle s \rangle = 1170$ GeV^2

$$\langle \alpha_s \rangle = 0.190 \pm 0.015 \pm 0.047$$

The error is dominated by systematics.

b) R. FIELD[101] has compared 4 observables with calculations in 2nd order at the parton level. The argument is this:

$$\text{Obs (W)}^{exp} = \text{Obs (W)}^{parton} + \text{Had (W)}$$

the experimentally observed quantity is written as a sum of the calculated quantity at parton level plus the unknown nonperturbative contribution (Had). In 2nd order perturbation in terms of α_s:

$$\text{Obs (W)}^{parton} = c_o \alpha_s(W) (1 + c_1 \alpha_s(W) + \dots)$$

with theoretically known c_o and c_1. It follows in 1st approximation:

$$\alpha_s^{(1)}(W) = \frac{\text{Obs(W)}^{exp} - \text{Had(W)}}{c_o}$$

2nd approximation: $\alpha_s^{(2)}(W) = \dfrac{\alpha_s^{(1)}}{1 + c_1\alpha_s^{(1)}}$

$\alpha_s^{(1)}$ can only be obtained provided the term Had(W) is known. This is, of course, not the case. Nevertheless, the sign of Had(W) decides on whether $\alpha_s^{(2)}(W)$ is a lower (Had(W) > 0) or an upper bound (Had(W) < 0) of the true value.

R. FIELD remarked that for the quantities 1-T (T = thrust of an event $e^+e^- \to$ hadrons) and M_h^2/s (in each multihadron event the so called CLAVELLI masses M_ℓ and M_h can be calculated with $M_\ell < M_h$) the sign of the nonperturbative effects is positive, whereas for $(M_h^2 - M_\ell^2)/s$ and A_{EE} (the asymmetry of the energy-energy correlation, see below) the sign is negative. Various Monte Carlo hadronization models differ in the absolute value of Had (W), but seem to agree in the sign. The data of 3 groups are used (fig. 58a) to obtain $\alpha_s^{(1)}$ and $\alpha_s^{(2)}$ (fig. 58b) with the result

$$0.10 \leq \alpha_s \leq 0.14 \qquad \sqrt{s} = 30 \text{ GeV}$$

c) Energy-Energy-Correlations: Calling $x_i = E_i/\sqrt{s}$ the fractional energy of particle i in $e^+e^- \to i + j +$ anything the normalized energy-weighted angular distribution is defined as follows:

$$\frac{d\Sigma}{d\theta} \equiv \frac{1}{\sigma_{tot}} \sum_{i,j} \int x_i x_j \frac{\partial^3\sigma}{\partial x_i \partial x_j \partial\theta}\, dx_i dx_j$$

From this quantity an asymmetry can be derived:

$$A(\theta) \equiv \frac{d\Sigma(\pi-\theta)}{d\theta} - \frac{d\Sigma(\theta)}{d\theta}$$

The idea of forming the asymmetry consists in reducing the effects from hadronisation and in suppressing the contribution of 2-jet events which cluster near $\theta = 0$ and π. Three groups at PETRA (CELLO, JADE and TASSO)[102] have presented fully corrected asymmetries (fig. 59) for $\sqrt{s} \approx 34$ GeV. Within the quoted errors all data are consistent. When analysing the data in terms of QCD the three groups find different values for α_s depending on the hadronisation model used ranging from 0.11 to 0.16. The JADE group gets a good representation of their data with the LUND string model and $\alpha_s = 0.165 \pm 0.01 \pm 0.01$ (fig. 60a), however an unsatisfactory representation when using the independent jet fragmentation model (fig. 60b). It is clear

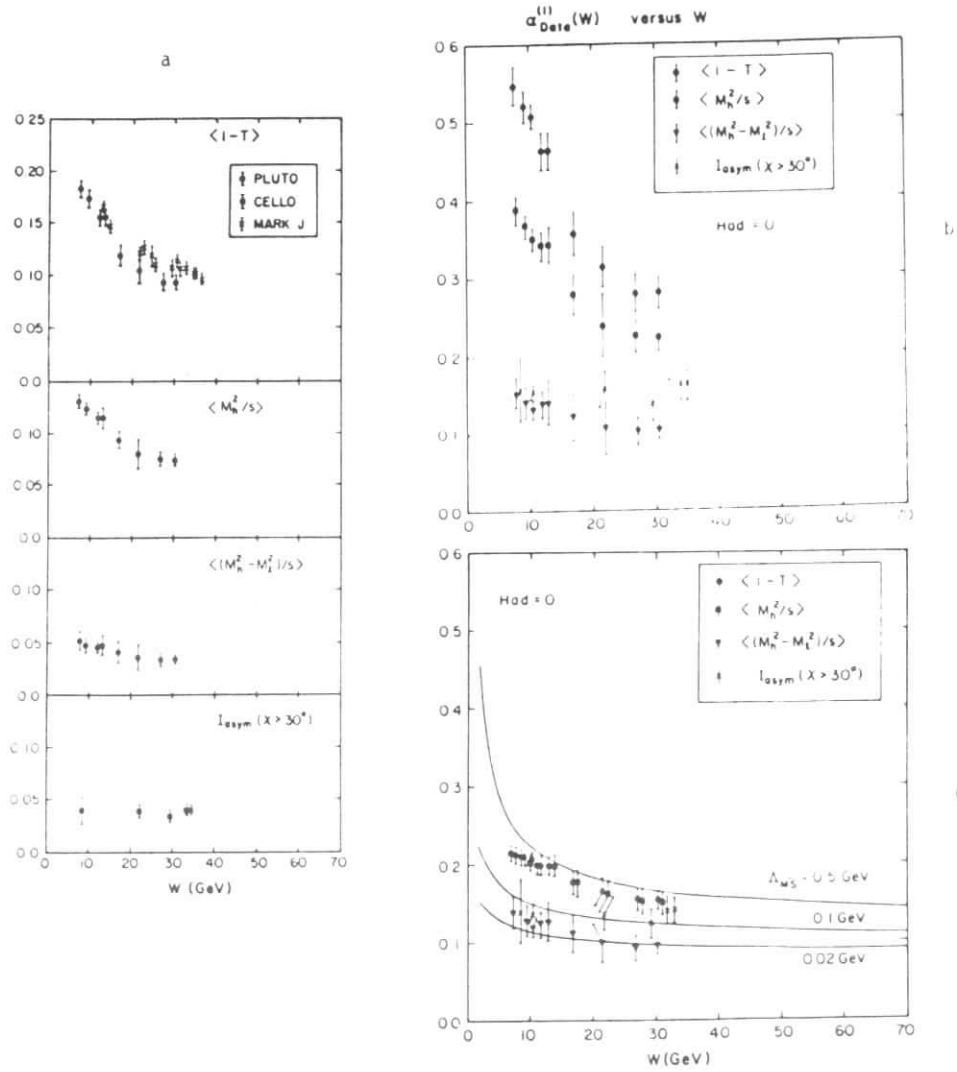

Fig. 58: a) Data on 4 quantities vs c.m. energy W - input for analysis of R.D. FIELD (ref. 101)

b) Interpretation in 1st approximation ($\alpha_s^{(1)}$)

c) Interpretation in 2nd approximation ($\alpha_s^{(2)}$)

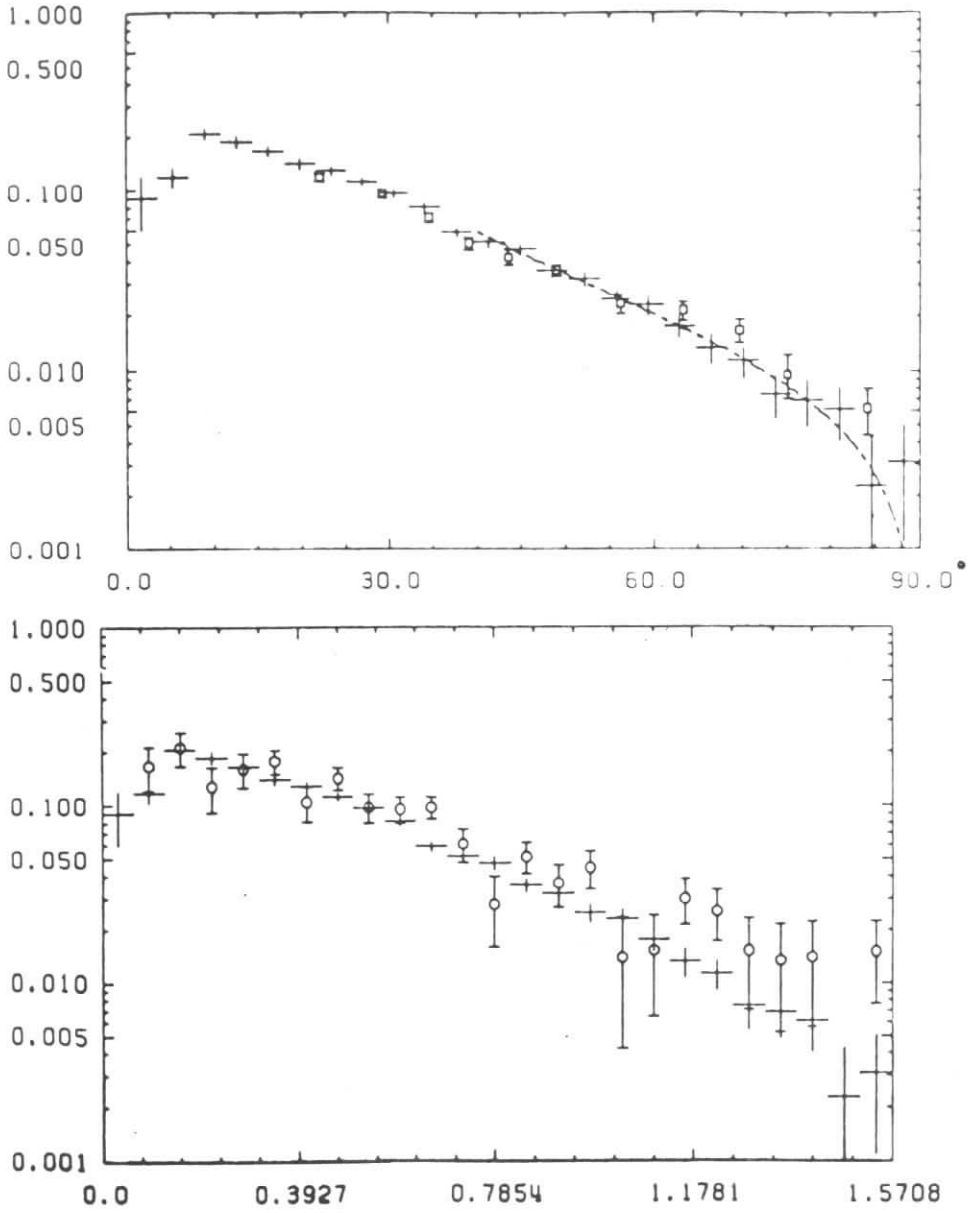

Fig. 59: Comparison on energy-energy correlations in e^+e^- → hadrons (ref. 103).
The data of all three groups are fully corrected.
Symbols: + JADE, □ TASSO, o CELLO.

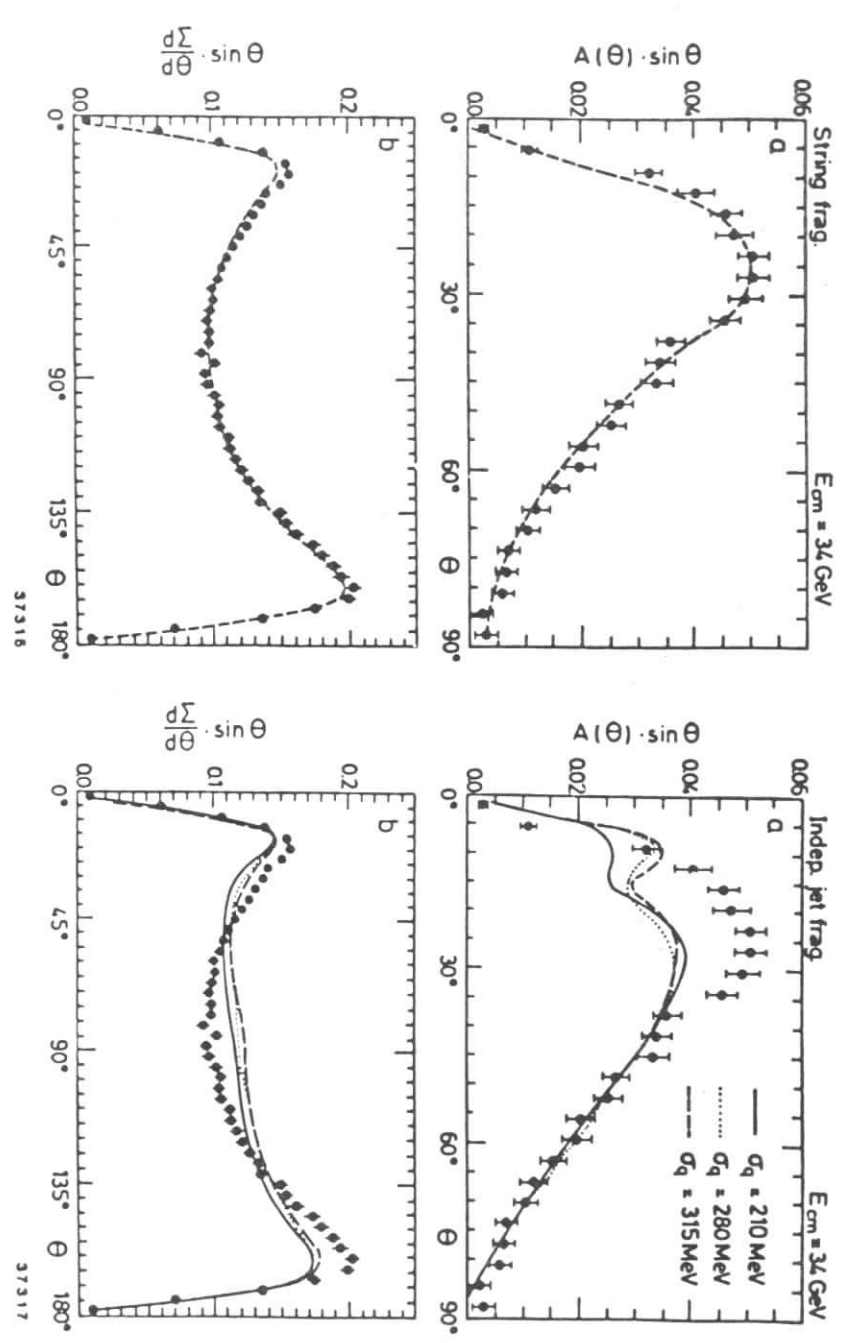

Fig. 60: JADE data (ref. 102b) on energy-energy correlations compared to two types of models.

that the extraction of α_s and its precision are not limited by statistics and quality of the experiments.

OUTLOOK

50 years after FERMI's theory of weak interactions the Standard Model of electroweak interaction based on SU(2) x U(1) and of strong interactions based on SU(3) provides a framework of all the elementary particle phenomenology. This is an important achievement as it constitutes a solid basis for future developments. It is, however, clear that even crucial aspects of the Standard Model are yet untested. Experiments aiming at tests at the 1-loop leval are underway. Tests of the nonabelian structure of electroweak interactions require very high energies. The HIGGS sector, and thus the nature of electroweak symmetry breaking is essentially unexplored.
The tests of QCD are qualitatively successful, but crucial quantitative tests are still missing.
The Standard Model summarizes known facts and is a source of new fundamental questions ensuring an exciting future.

ACKNOWLEDGEMENT

It is a pleasure to thank Cecilia Jarlskog and the organizers for the invitation to give lectures at such a nice place. In preparing the lectures I appreciated many discussions and contributions of material. In particular I wish to thank F. Dydak, J. Dowell, G. Ecker, F. Eisele, W. Geist, A. Petersen, R. Petronzio, H. Pietschmann, S. Rudaz and H. Wenninger. Special thanks to Mrs. Platz for the careful typing of the manuscript.

APPENDICE

Some definitions and relations are collected here (cf ref. 104).

1. The Interaction Lagrangians

$$L^{\gamma} = g \sin\theta \; J^{em}_{\lambda} A^{\lambda}$$

$$L^{W} = \frac{g}{2\sqrt{2}} \left(J^{CC}_{\lambda} W^{\lambda} + hc.\right)$$

$$L^{Z} = \frac{g}{4\cos\theta} J^{NC}_{\lambda} Z^{\lambda}$$

Identify $e = g \sin\theta$

2. Current x Current Form

$$L^{weak} = \frac{G}{\sqrt{2}} \left(J^{CC}_{\lambda} (J^{CC}_{\lambda})^{+} + \frac{\rho}{2} J^{NC}_{\lambda} J^{NC}_{\lambda}\right) \quad \text{for} \quad Q^2 \ll m_W^2, m_Z^2$$

$$\text{Identify} \quad \frac{G}{\sqrt{2}} = \frac{g^2}{8m_W^2} = \frac{1}{2v^2} \qquad \rho = \frac{m_W^2}{m_Z^2 \cos^2\theta}$$

The masses of $W^{\pm}$, Z are related to the HIGGS expectation value $\langle 0 | \phi | 0 \rangle = \frac{1}{\sqrt{2}} v$

$$m_W = \frac{gv}{2} \quad \text{and} \quad m_Z = \frac{gv}{2\cos\theta} = \frac{m_W}{\cos\theta}$$

3. The Currents

$$J^{em}_{\lambda} = \sum_f Q_f \bar{\psi}_f \gamma_{\lambda} \psi_f \qquad Q_f = \text{electric charge of fermion f in units of e} > 0$$

$$J^{CC}_{\lambda} = \sum_{\ell} \bar{\psi}_{\nu_\ell} \gamma_{\lambda} (1 + \gamma_5) \psi_{\ell} + \sum_{q,q'} \bar{\psi}_q \gamma_{\lambda} (1 + \gamma_5) U_{qq'} \psi_{q'}$$

$\ell = (e, \mu, \tau)$ $q = (u, c, t)$ $q' = (d, s, b)$

U = unitary quark flavor mixing matrix

$$J_\lambda^{NC} = \sum_f \bar{\psi}_f \gamma_\lambda (g_V^f + g_A^f \gamma_5)\psi_f \equiv 2 \sum_f \bar{\psi}_f \gamma_\lambda (\varepsilon_L^f (1 + \gamma_5) + \varepsilon_R^f (1 - \gamma_5))\psi_f$$

$g_{V,A}^f$ V,A weak coupling constants

$\varepsilon_{L,R}^f$ chiral weak coupling constants

Sometimes the shorthand notation

$$f_L \equiv \varepsilon_L^f \qquad f_R \equiv \varepsilon_R^f$$

for the left- resp. righthanded weak coupling of a fermion with flavor f is used. Often V and A couplings v_f and a_f are introduced instead of $g_{V,A}^f$. The relation is:

$$v_f \equiv \frac{1}{2} g_V^f = f_L + f_R \equiv \varepsilon_L^f + \varepsilon_R^f$$

$$a_f \equiv \frac{1}{2} g_A^f = f_L - f_R \equiv \varepsilon_L^f - \varepsilon_R^f$$

There is a third type of notation which proved particularly useful when investigating the isospin structure of the weak neutral quark current of the first generation:

$$J_\lambda^{iso} = \alpha(\bar{\psi}_u \gamma_\lambda \psi_u - \bar{\psi}_d \gamma_\lambda \psi_d) + \beta(\bar{\psi}_u \gamma_\lambda \gamma_5 \psi_u - \psi_d \gamma_\lambda \gamma_5 \psi_d)$$

IV - V IV - A

$$+ \gamma(\bar{\psi}_u \gamma_\lambda \psi_u + \bar{\psi}_d \gamma_\lambda \psi_d) + \delta(\bar{\psi}_u \gamma_\lambda \gamma_5 \psi_u + \bar{\psi}_d \gamma_\lambda \gamma_5 \psi_d)$$

IS - V IS - A

$$\equiv \bar{\psi}_u \gamma_\lambda (u_L(1+\gamma_5) + u_R(1-\gamma_5))\psi_u + \bar{\psi}_d \gamma_\lambda (d_L(1+\gamma_5) + d_R(1-\gamma_5))\psi_d$$

The isovector-vector (IV - V), isovector-axialvector (IV - A), isoscalar-vector (IS - V) and isoscalar-axialvector (IS - A) pieces are marked. The relations between α, β, γ, δ and $u_{L,R}$, $d_{L,R}$ follow from the above identity:

$$u_L = \frac{1}{4}(\alpha+\beta+\gamma+\delta) \qquad \alpha = u_L + u_R - d_L - d_R = 1 - 2\sin^2\theta$$

$$u_R = \frac{1}{4}(\alpha-\beta+\gamma-\delta) \qquad \beta = u_L - u_R - d_L + d_R = 1$$

$$d_L = \frac{1}{4}(-\alpha-\beta+\gamma+\delta) \qquad \gamma = u_L + u_R + d_L + d_R = -\frac{2}{3}\sin^2\theta$$

$$d_R = \frac{1}{4}(-\alpha+\beta+\gamma-\delta) \qquad \delta = u_L - u_R + d_L - d_R = 0$$

Note that β and δ do not depend upon $\sin^2\theta$.
In the following table the chiral $Zf\bar{f}$ couplings are listed for the fermions of the first generation together with their predicted value assuming $\sin^2\theta = 0.22$.

PARTICLE	$T_3 - Q\sin^2\theta$	$\sin^2\theta = 0.22$
ν_L	$+\frac{1}{2}$	0.500
e_L	$-\frac{1}{2} + \sin^2\theta$	-0.280
u_L	$+\frac{1}{2} - \frac{2}{3}\sin^2\theta$	0.353
d_L	$-\frac{1}{2} + \frac{1}{3}\sin^2\theta$	-0.427
ν_R	0	0.000
e_R	$\sin^2\theta$	0.220
u_R	$-\frac{2}{3}\sin^2\theta$	-0.147
d_R	$\frac{1}{3}\sin^2\theta$	0.073

LITERATURE

1) C. Jarlskog, Introduction to Gauge Theories, Lectures at this School.

2) R. Petronzio, Theoretical Aspects of QCD, Lectures at this School.

3) J. Dowell, Physics at the $\bar{p}p$ Collider, Lectures at this School.

4) G. Barbiellini, Experimental Tests of Gauge Theories, CERN Summer School 1982.
D. Perkins, Experimental Status of Gauge Theories, CERN Summer School 1981.

5) H. Pietschmann, Elementary Introduction to Gauge Theories, Acta Physica Austriaca, Suppl. XIX (1978) 5 - 46.
E. Paschos: Introduction to Electroweak Theory, Maria Laach School 1981, DESY Preprint 82-49.
K. Mess and B. Wiik, Recent Results in e^+e^- and ℓh Interactions, DESY Preprint 82-11.
L. Jauneau, Introduction to new Physics, Kupari Lectures 1982, Orsay Preprint LAL 82/34.
G. Ecker, Introduction to Gauge Theories of Electroweak Interactions, Acta Physica Austriaca, Suppl. XXIV (1982) 3-62.

6) H. Fritzsch, Composite Quarks and Leptons and their Flavor Mixing, Max Planck Institut MPI-PAE/PTh 31/84.

7) G. Myatt, Contribution to the Workshop on SPS Fixed Target Physics 1982, CERN 83-02, Yellow Reports Vol. I and II.

8) C. Rubbia, LUND Conference, June 1984.

9) D.A. Ross and M. Veltman, NP B 95 (1975) 135.

10) D. Haidt, Summary Talk on Neutrino Physics at the SPS Fixed-Target Workshop loc.cit.

11) C. Llewellyn-Smith, Contribution to the SPS Fixed-Target Workshop, loc. cit.

12) D.H. Perkins, Rapporteur's Talk, Batavia 1972.

13) C. Albright, Phys. Rev. D2 (1970) 1883.

14) W. Lerche et al., NP 142 (1978) 65-76.
M. Pohl et al., NC lett. 24 (1979) 540.

15) Proposal for the First ν Experiment in GARGAMELLE, CERN TCC/70-12 (1970).

16) M. Bourquin et al., Tests of the CABIBBO Model, Z. Phys. C21 (1983) 27.

17) S. Glashow, J. Iliopoulos, L. Maiani, PR D2 (1970) 1285.

18) S. Glashow, NP 22 (1961) 579.
S. Weinberg, PRL (1967) 1264.
A. Salam, 1968 in Elementary Particle Theory: Relativistic Groups and Analyticity (Nobel Symposium No. 8), edited by N. Svartholm, Almquist and Wiksell, Stockholm.

19) G. t'Hooft, NP B33 (1971) 173; NP B35 (1971) 167.

20) 300 GeV Working Group, Proceedings of the 2nd Tirrenia Study Week 1972, CERN/ECFA/72/4 Vol II.

21) F.J. Hasert et al., Phys. Lett. 46B (1973) 121.

22) F.J. Hasert et al., Phys. Lett. 46B (1973) 138.

23) D. Haidt, Rückblick auf die Entdeckung der neutralen Strome, Phys. Blätter 31 (1975) 654.

24) F.W. Fry and D. Haidt, CERN-Yellow Report / 75-1 (1975).

25) A. Benvenuti et al., PRL 32 (1974) 800.
B. Aubert et al., PRL 32 (1974) 1454 and 1457.
S.J. Barish et al., PRL 33 (1974) 448.
B.C. Barish et al., PRL 34 (1975) 538.

26) F.J. Hasert et al., NP B73 (1974) 1.

27) E. Williams and P. Olsen, PRL 42 (1979) 1575.

28) K.L. Giovanetti et al., PR D29 (1984) 343.

29) F. Bergsma et al., PL 117B (1983) 272.

30) W. Marciano and A. Sirlin, PR D22 (1980) 2695.
A. Sirlin, PR D22 (1980) 571.
W. Marciano, Electroweak Interaction Parameters, BNL - 34728 (1984).

31) W. Krenz, private communication (May 1984), TH Aachen.

32) J. Blietschau et al. (GARGAMELLE), NP B144 (1976) 189.
H. Faissner et al. (AC-PD), PRL 41 (1978) 213.
M. Jonker et al. (CHARM), PL 105B (1981) 242.

33) H. Faissner et al., (AC-PD), PRL 41 (1978) 213.
A.M. Cnops et al., PRL 41 (1978) 357.
N. Armenise et al. (GARGAMELLE-SPS), PL 86 B (1979) 225.
R.H. Heisterberg et al., PRL 44 (1980) 635.
F. Bergsma et al. (CHARM), PL 117B (1982) 272.
L.A. Ahrens et al., PRL (1983) 1514.

34) F. Bergsma et al., Proposal CERN/SPSC/83-24 (1983).

35) B. Naroska, in Proceedings of the 1983 International Symposium on Lepton and Photon Interactions at High Energies, edited by D.G. Cassel and D.L. Kreinick, Newman Laboratory for Nuclear Studies, Cornell University, Ithaca, New York.

36) C. Bowdery, Private Communication, DESY.

37) K.L. Giovanetti et al., PR D29 (1984) 343.

38) J. Carr et al., LBL-16889 (1983).

39) W. Bartl et al. (SINDRUM) SIN Preprint PR-84-01.

40) N. Armenise et al., PL 84B (1979) 137.
M. Jonker et al., PL 93B (1980) 203.

41) M. Perl, The Tau Lepton, Ann. Rev. of Nucl. and Part. Science, Vol. 30 (1980) 299.
G. Flügge, The New Heavy Lepton τ, Z. Physik C1 (1979) 121-138.

42) G.F. Feldman et al. (MARK II), PRL 48 (1982) 106.
W.T. Ford et al. (MAC), PRL 49 (1982) 106.
H.J. Behrend et al. (CELLO), NP B211 (1983) 369.
J.A. Jaros et al. (MARK II), PRL 51 (1983) 955.
M. Althoff et al. (TASSO), DESY 84-17 (1984)

43) W. Bartel et al. (JADE), Z. Physik C19 (1983) 197.

44) S. Yamada, Proc. of the Lepton/Photon Conference, CORNELL, 1983.

45) W. Bartel et al. (JADE), PL 123B (1983) 353.

46) F. Dydak, private communication, CERN.

47) H. Wenninger, private communication, CERN.

48) J.E. Kim, P. Langacker, M. Levine and H.H. Williams, A Theoretical and Experimental review of the Weak Neutral Current, Rev. Mod. Phys. 53 (1981) 211.

49) D. Rein and L.M. Sehgal, Ann. Phys. 133 (1981) 79.
G.L. Fogli, NP B207 (1982) 322.

50) D. Allasia et al. (BEBC-WA25), PL 133B (1983) 129.

51) C. Geweniger, Proc. of HEP 1983, Brighton.

52) CHARM 81: M. Jonger et al., PL 99B (1981) 265.
CFRR : P. Reutens et al., UR 891 (1984).
CDHS 83 : Ref. 51, New Value Ref. 54.
BEBC D83: Ref. 50
BEBC TST 84: J. Moreels et al., PL 138B (1984) 230

53) W. Marciano, PR D29 (1984).
B.D. Paschos, PRL 52 (1984) 1192.

54) C. Geweniger, Proc. of the 1984 Neutrino Conference, Nordkirchen.

55) F. Dydak et al., Proposal to Measure $\sin^2\theta$ in Semileptonic νFe Interactions with High Precision, CERN/SPSC/83-49.

56) J.V. Allaby et al., Proposal to Measure the Ratio σ_ν (NC)/σ_ν (CC) with High Precision, CERN/SPSC/84-1 (1984).

57) W. Krenz et al. (GARGAMELLE), NP B135 (1978) 45.

58) J. Horstkotte et al., PR D25 (1982) 2743.

59) H. Faissner et al., PL 125B (1983) 230.

60) W. Bartel et al. (JADE), PL 129 (1983) 145.
B. Adeva et al. (MARK J), Phys. Rep. 109 (1984).
M. Althoff et al. (TASSO), PL 138 (1984) 441.

61) B. Naroska, Proc. of 1983 Symposium of Lepton Photon Interactions.

62) C.J. Prescott et al., PL 77B (1978) 347, ibid 84B (1979) 524.

63) A. Argento et al., PL 120B (1983) 245.

64) E.D. Commins and P.H. Bucksbau, The Parity Nonconserving eN Interaction, Ann. Rev. Nucl. Part. Sci. 30 (1980) 1-52.

65) M.A. Bouchiat, J. Guëna and L. Pottier, PL 134B (1984) 463.

66) F. Eisele, Proc. of the Int. High Energy Physics Conference PARIS, J. Phys. 43 (1982), Suppl. 12, C3.

67) H. Abramowicz et al. (CDHS), ZP C15 (1982) 19.
D. Allasia et al. (BEBC), PL 135B (1984) 231.

68) F. Dydak, Int. Symposium of Lepton/Photon Interaction, Cornell, 1983.

69) H. Deden et al., PL 58B (1975) 361.
P. Bosetti et al., PRL 38 (1977) 1248.

70) J. Blietschau et al. (BEBC), PL 86B (1979) 108.

71) V. Barger, Proc. of the Int. High Energy Physics Conference, PARIS, J. Phys. 43 (1982), Suppl. 12, C3.

72) J.G. de Groot et al. (CDHS), Z. Phys. C1 (1979) 143.
H. Abramowicz et al. (CDHS), Z. Phys. C12 (1982) 225.

73) D. Haidt, Invited Talk at 1977 Int. Symposium on Lepton and Photon Interactions at High Energies, Hamburg 1977, p. 329.

74) F. Reines and C.L. Cowan, PR 90 (1953) 492 and 113 (1959) 273.

75) A Proposal to the Department of Energy, LOS ALAMOS, National Laboratory, New Mexico (Dec. 1982): High Intensity Los Alamos Neutrino Source.

76) M. Kobayashi and K. Maskawa, Prog. Theor. Phys. 49 (1973) 652.

77) L. Maiani, Proceedings of the Int. Symp. on Lepton and Photon Interaction at High Energies, Hamburg 1977, p. 867.

78) L. Wolfenstein, PRL 51 (1983) 1945.

79) Ling-Lie Chao, Phys. Rep.
K. Kleinknecht, The Present Knowledge of Weak Quark Mixing Angles in the b-quark Scheme, Dortmund Preprint UNIDO 84/279 (1984).
S. Stone, Weak Decays of Heavy Quarks, Proc. 1983 Int. Lepton/Photon Symposium, Cornell University, p. 203.

80) W. Bartel et al. (JADE), PL 114B (1982) 71.

81) N.S. Lockyer et al. (MARK II), PRL 51 (1983) 1316.

82) E. Fernandez et al. (MAC), PRL 51 (1983) 1022.

83) S. Yamada, Proc. of the Lepton/Photon Conference, CORNELL 1983.

84) R.T. Giles et al. (CLEO), CLNS-84-611 (1984).

85) S. Stone, Weak Decays of Heavy Quarks, Proc. of 1983, Int. Lepton/Photon Symposium, Cornell, p. 203.

86) C. Klopfenstein et al. (CUSB), PL 130B (1983) 444,
A. Chen et al. (CLEO), PRL 52 (1984) 1084.

87) J. Green et al. (CLEO), PRL 51 (1983) 347.

88) H. Fritzsch, The Development of Quantum Chromodynamics, MPI-PAE/PTh/3-84 (Jan. 1984).
P. Söding and G. Wolf, Ann. Rev. Nucl. Part. Sci. 31 (1981) 231.

89) R. Brandelik et al. (TASSO), PL 97B (1980) 453.
W. Bartel et al. (JADE), PL 91B (1980) 142.
J.J. Aubert et al. (EMC), PL 95B (1980) 306.

90) D. Drijard et al. (CDHW), PL 121B (1983) 433.
A. Breakstone et al. (ABCDHW), PL 135B (1984) 510.

91) W. Bartel et al. (JADE), Z. Phys. C21 (1983) 37-52.
D. Haidt, Proc. of the 1981 Int. Lepton/Photon Conference, Bonn 1981, 558.

92) G. Altarelli and G. Parisi, N. Phys. B126 (1979) 298.

93) F. Dydak, Proc. of 1983 HEP Conference, Brighton.

94) W.A. Bardeen, A. Buras, D. Duke and T. Muta, PR D18 (1978) 3958.

95) H. Abramowics et al. (CDHS), Z. Phys. C13 (1982) 199-204.

96) D. Haidt, Proc. of the 1982 Int. High Energy Phys. Conference, Paris.

97) H. Abramowicz et al. (CDHS), Z. Phys. C12 (1982) 289.

98) D.H. Perkins, Experimental Tests of QCD, Oxford Preprint 37/81 (1981).

99) J. Drees and H. Montgomery, Muon Scattering, Ann. Rev. Nucl. Part. Sci. 33 (1983) 383-452.

100) G. Wolf, The Determination of α_s in e^+e^- Annihilation, DESY 83-96.

101) R.D. Field, Proc. of the 1983 Lepton/Photon Conference, CORNELL.

102) H.J. Behrend et al. (CELLO), DESY 83-127.
W. Bartel et al. (JADE), DESY 84-50 (1984).
M. Althoff et al. (TASSO), DESY 84-57 (1984).

103) A. Petersen, private communication, DESY.

104) Weak Interactions - Formulae, Results and Deviations, Springer Verlag, 1983.